

Functional Characterization of Four *Xanthomonas euvesicatoria* Type III Effectors

Zhibo Wang

Dissertation submitted to the faculty of the Virginia Polytechnic Institute and State University in partial fulfillment of the requirements for the degree of

Doctor of Philosophy
In
School of Plant and Environmental Sciences

Bingyu Zhao (Committee Chair)
John M. McDowell
Aureliano Bombarely Gomez
Jianyong Li

February 10th, 2020
Blacksburg, VA

Keywords: *Xanthomonas euvesicatoria*, *Nicotiana benthamiana*, Type III effector, XopQ, XopX, XopN, Xe-avrRxo1

Functional Characterization of Four *Xanthomonas euvesicatoria* Type III Effectors

Zhibo Wang

ABSTRACT

Pepper and tomato, as two common, popular, and important vegetables grown worldwide, provide human beings with high quality fruit of flavor and aroma, and a high concentration of vitamins and antioxidants. Pepper and tomato production is frequently affected by various pathogens, including nematodes, fungi, and bacteria. Among those phytopathogens, *Xanthomonas euvesicatoria* (*Xe*) causes a severe bacterial spot (BS) disease on pepper and tomato. The BS disease could cause a loss of approximately 10% of the total crop yield in the world. Breeding tomato and pepper cultivars with improved BS disease resistance is one of the most important breeding goals. A better understanding of the virulence mechanism of *Xe* could help breeders design new strategies for resistance breeding. In this dissertation, we characterized the virulence and avirulence functions of four *Xe* Type Three Secretion Effectors (T3Es): *Xe*-XopQ, *Xe*-XopX, *Xe*-XopN, and *Xe*-avrRxol1.

Xe-XopQ is a *Xe* T3E that functions as a determinant of host specificity. Here, we further explored the virulent and avirulent functions of *Xe*-XopQ. We identified another T3E *Xe*-XopX that could interact with XopQ and subsequently elicit the hypersensitive response in *N. benthamiana* in the *Agrobacterium*-mediated transient assay and *Xe*-mediated disease assay. The interaction is confirmed by bimolecular fluorescence complementation, co-immunoprecipitation and split luciferase assay. Intriguingly, we also revealed that XopX also interacts with multiple *Xe* T3Es including AvrBS2, XopN, XopB, and XopD in the co-IP assay. The virulent and avirulent functions of XopQ and AvrBS2 are compromised in the absence of *Xe*-XopX. Since XopX is conserved in diverse *Xanthomonas* spp., we speculate that *Xe*-XopX may have a general role required for the pathogenesis of *Xe*.

Xe-XopN has been reported to be a T3E with virulence function via targeting host defense-related proteins, including atypical receptor-like kinase named TARK1 and a 14-3-3 protein to suppress the PAMPs (pathogen-associated molecular patterns) triggered immunity upon *Xe* colonization of tomato. In this study, we revealed additional virulence

mechanisms of *Xe*-XopN, where *Xe*-XopN, is required for triggering the water-soaking symptom on *Nicotiana benthamiana* and pepper plants infected with *Xe*.

In addition, we identified that XopN interacts with a transcription factor, NbVOZ, and represses the expression of *NPR1*, a key component of the basal defense. Therefore, XopN has a role in maintaining a water-affluent environment for better replication of *Xe*, and it can also interact with NbVOZ1/2 to regulate plant immunity.

AvrRxo1, a T3E of *Xanthomonas oryzae* pv. *oryzicola* (*Xoc*), was previously identified to function as a NAD kinase. Here, we characterized a *Xe* T3E, *Xe* avrRxo1, that is a functional homologue of AvrRxo1, which is required for the full virulence of *Xe* to colonize the pepper and *N. benthamiana* plants. Overexpression of AvrRxo1 in bacterial or plant cells is toxic. Our group previously demonstrated AvrRxo1-ORF2 functions as an antitoxin that binds to AvrRxo1 to suppress its toxicity. In this study, we identified *Xe*4429 as the homologue of AvrRxo1-ORF2, which could interact with *Xe*-avrRxo1 to suppress its toxicity. We also revealed that *Xe*4429 could bind to the promoter of *Xe*-avrRxo1 and suppress its transcription. Therefore, we found *Xe*4429 encodes protein functions as an antitoxin and a transcription repressor in *Xe* bacterial cells.

GENERAL AUDIENCE ABSTRACT

Peppers and tomatoes are two of the most important vegetables grown worldwide, providing humans with high quality of flavor and aroma, vitamins, and antioxidants. The pepper and tomato production is frequently threatened by various pathogens, including nematodes, fungi, and bacteria. Among those phytopathogens, *Xanthomonas euvesicatoria* (Xe) causes a severe bacterial spot (BS) disease on peppers and tomatoes. The BS disease can be easily identified due to the appearance of the dark, irregular, water-soaked areas on the leaf, which can cause approximately 10% loss of the total yield of peppers and tomatoes. Breeding tomato and pepper cultivars with improved BS disease resistance is one of the most critical breeding goals. A better understanding of the virulence mechanism of Xe could help breeders to design new strategies for resistance breeding. In my seminar, I will discuss the virulence and avirulence functions of Xe type three secretion (T3S) effectors: Xe XopN, Xe XopQ, and Xe XopX. In my study, I identified Xe XopN is a key factor that regulates the development of the water-soaking symptom on pepper plants infected with Xe. In addition, we revealed Xe XopN interacts with a transcription factor NbVOZ to regulate the expression of NbNPR1 and PR1 genes expression, which may also contribute to the development of water-soaking phenotype. In addition, I identified that Xe XopN could interact with a transcription factor, NbVOZ, and represses the expression of NbNPR1, a key component of the basal defense, and the pathogenesis-related gene PR1. Therefore, Xe XopN has a role in regulating a water-affluent environment to promote bacterial proliferation in the infected plant tissue. Xe XopQ is a Xe T3S effector that functions as a determinant of host specificity. In my study, I identified another T3S effector Xe XopX that could interact with Xe XopQ to trigger the defense response in *Nicotiana benthamiana*. I also confirmed Xe XopQ physically interacts with Xe XopX inside of plant cells by using bimolecular fluorescence complementation, co-immunoprecipitation and split luciferase assay. Intriguingly, Xe XopX could also interact with multiple Xe T3Es including AvrBS2 in a co-IP assay. The virulence and avirulent functions of Xe XopQ and AvrBS2 are compromised in the absence of Xe XopX.

ACKNOWLEDGEMENTS

First and foremost, I would like to thank my parents for their love and encouragement throughout my graduate school career. They were always extremely supportive and able to provide inspiration when the rigors of research and thesis writing seemed too much to handle. I love you all!

I would like to express my sincere appreciation for my advisor, Dr. Bingyu Zhao, for his mentorship and advice during my graduate studies. I feel grateful to have the opportunity to work in his lab. Under his guidance, I systematically learned plant science and molecular biology techniques. And far beyond the knowledge and experimental skills, I was trained to be a capable scientist who is an independent researcher, and at the same time, also a compatible cooperater. In addition to being a research mentor, Dr. Bingyu Zhao has also been a life mentor. I will always remember his suggestions on magnanimity, responsibility and optimism. Dr. Bingyu Zhao has also been a great friend. I will never forget his Christmas chocolate and Spring Festival parties every year, especially the delicious traditional Chinese dumplings. And I am grateful to all the members of Dr. Bingyu Zhao's Lab. I would like to thank Dr. Jiamin Miao for teaching me many experimental skills. And I would like to thank Kerri Mills who helped me with English writing and proof reading. I also would like to thank my committee members: Dr. Jianyong Li, Dr. Boris Vinatzer and Dr. John McDowell. They were the best advisory committee and their advice and encouragement was very helpful for my research and even the whole career. I would like to thank Dr. Aureliano Bombarely, who helped me with bioinformatics skills. I would like to thank Dr. Jianyong Li for helping with the protein experiments. The Plant Pathology class taught by Dr. Bingyu Zhao and Dr. John McDowell, led me, as an almost outsider into the molecular plant pathology world.

I would like to specifically thank my former advisor, Dr. Yanping Guo, who initiated my scientific training. Many of my good habits for scientific research including the spirit of suspicion, perfection and enterprise, arose from his foresight and guidance.

I feel lucky and grateful to have pursued my PhD degree in the TPS program, previous Horticulture Department and School of Plant and Environmental Sciences, where I had been offered a supportive, constructive and very professional research environment. I

would like to express my appreciation to the Heads of Horticulture Department, Dr. J. Roger Harris and Dr. Richard Veilleux, as well as the Director of School of Plant and Environmental Sciences, Dr. Michael Evans, who provided my Teaching Assistance opportunity and other financial supports.

ATTRIBUTIONS

List of co-authors

Bingyu Zhao, Department of Horticulture, Virginia Tech
Jianyong Li, Department of Biochemistry, Virginia Tech
Changhe Zhou, Department of Horticulture, Virginia Tech
Jiamin Miao, Department of Horticulture, Virginia Tech
Qi Li, Department of Horticulture, Virginia Tech
Kunru Wang, Department of Horticulture, Virginia Tech
Zhibo Wang, Department of Horticulture, Virginia Tech

Contributions of co-authors

Chapter II

Bingyu Zhao and Zhibo Wang conceived and designed the experiments. Bingyu Zhao will be the corresponding author while Zhibo Wang will be the first author. Zhibo Wang contributed to the execution of experiments, data analysis and paper writing. Jianyong Li helped process protein experiments and he will be the co-author.

Chapter III

Bingyu Zhao and Zhibo Wang conceived and designed the experiments. Bingyu Zhao will be the corresponding author while Zhibo Wang will be the first author. Zhibo Wang contributed to the execution of experiments, data analysis and paper writing.

Chapter IV

Bingyu Zhao conceived and designed the experiments and will be the corresponding author. Zhibo Wang contributed to most experiments, data analysis and paper writing. He will be the first author. Jiaming Miao, Qi Li, and Kunru Wang processed the generation of expression constructs and *Xanthomonas euvesicatoria* isogenic mutants. Jianyong Li helped process protein experiments. Changhe Zhou processed the Nanoluc reporter assay. They will be co-authors.

TABLE OF CONTENTS

Chapter 1 Literature Review	1
Summary.....	1
Part 1: Effector-triggered susceptibility	1
Part 2: Effector triggered immunity	12
References	24
Chapter 2 <i>Xanthomonas euvesicatoria</i> type III effector XopQ interacts with another effector, XopX, to elicit the defense response in <i>Nicotiana benthamiana</i>	34
Summary.....	34
Introduction.....	34
Results	37
Discussion.....	42
Methods and materials	44
Supplementary information.....	63
References	68
Chapter 3 <i>Xanthomonas euvesicatoria</i> type III effector XopN interacts with transcription factor <i>NbVOZ</i> to promote an aqueous environment and enhance bacterial proliferation.....	71
Summary.....	71
Introduction.....	71
Results	73
Discussion.....	79
Methods and materials	82
Supplementary information.....	98
References	103
Chapter 4 <i>Xanthomonas euvesicatoria</i> Gene <i>Xe4429</i> Encodes an Antitoxin and also Functions as a Transcription Repressor	106
Summary.....	106
Introduction.....	106
Results and discussions	108
Methods and materials	113

Supplementary information	127
References	129

LIST OF FIGURES

Chapter 1

- Figure 1- 1 A zigzag model illustrates the quantitative output of the plant immune system.
..... 20

Chapter 2

- Figure 2- 1 XopQ and its homologues in diverse bacterial pathogens triggered NbEDS1-
dependent nonhost disease resistance in *N. benthamiana*. 52
- Figure 2- 2 Co-expression of XopQ and XopX elicited programmed cell death in *N.*
benthamiana in *Agrobacterium*-mediated transient assays. 53
- Figure 2- 3 Mutant *Xe* or *Xcc* strains lacking either XopQ or XopX failed to trigger
programmed cell death in *N. benthamiana*. 55
- Figure 2- 4 XopX displayed a virulent function in the presence of XopQ, while XopX
displayed an avirulent function in the absence of XopQ. 56
- Figure 2- 5 Mutations in the predicted active site of *Xe*-XopQ affected avirulence in *N.*
benthamiana. 57
- Figure 2- 6 The core domain of XopX physically interacted with multiple T3Es within
plant cells. 59
- Figure 2- 7 Impairment of *XopX* partially eliminated the virulence function of AvrBS2. 61
- Figure 2- 8 Impairment of *XopX* partially eliminated the avirulent function of AvrBS2 in
BS2 pepper. 62
- Figure S2- 1 Transient expression of NbEDS1 restored the ability of *N. benthamiana* to
recognize *Xe* and induced cell death. 63
- Figure S2- 2 *XopX* is conserved in *Xanthomonas* and its cooccurrence with a core set
T3Es. 64
- Figure S2- 3 *In planta* growth of *Xe* Δ *XopQ* in transgenic *N. benthamiana* inducibly
expressing XopX. 65

Chapter 3

- Figure 3- 1 The amplification of *Xe* increases with elevated humidity in both tobacco and
pepper. 89
- Figure 3- 2 XopN is required for developing of the water-soaking phenotype in the *Xe*
infected tobacco and pepper plants , but this function can be impacted by high
humidity. 90
- Figure 3- 3 Transient expression of XopN induces water-soaking symptoms in both
tobacco and pepper. 92
- Figure 3- 4 Different water-soaking phenotypes in presence or absence of XopN is not
caused by the variation of bacterial populations in the infected plant leaves. 93
- Figure 3- 5 XopN may up regulate stomatal aperture. 94
- Figure 3- 6 A nonpathogenic *Xe* strain, *Xe* Δ *HrcV*, can trigger weak water soaking with
the co-expression of XopN and can be introduced by water soaking induced by
XopN. 95

Figure 3- 7 XopN can regulate <i>NbNPR1</i> expression through its interaction with <i>NbVOZ1</i> and <i>NbVOZ2</i>	97
Figure S3- 1 Transient expression of XopN can trigger water-soaking cell death only localized at cytosol.....	98
Figure S3- 2 The localization of XopN can be changed upon co-expression with <i>NbVOZ1</i> and <i>NbVOZ2</i>	99
Figure S3- 3 Type 2 secretion system (T2SS) and glycerol uptake facilitator (glpF) are also involved in instigating water-soaking symptoms.	100
 Chapter 4	
Figure 4- 1 <i>Xe4428</i> is a homologue of <i>Xoc-avrRxo1</i> that can trigger the <i>Rxo1</i> -mediated defense response in <i>N. benthamiana</i>	119
Figure 4- 2 <i>Xe4428</i> possesses a remarkable virulence function that can enhance <i>X. euvesicatoria</i> proliferation on both pepper and tobacco.	120
Figure 4- 3 Expression of <i>Xe-avrRxo1</i> in <i>Xe</i> could increase the stomatal conductance in pepper leaves.....	121
Figure 4- 4 Expression of <i>AvrRxo1-ORF1</i> (<i>Xe4428</i>) is toxic to <i>Xe</i> and <i>E. coli</i> , and its toxicity can be suppressed by <i>AvrRxo1-ORF2</i> (<i>Xe4429</i>).....	122
Figure 4- 5 Purified <i>Xe-avrRxo1-ORF2</i> (<i>Xe4429</i>) protein binds to the promoter of <i>Xe-avrRxo1</i> (<i>Xe4428</i>).	123
Figure 4- 6 Nanoluc reporter assay to test the transcription activity driven by <i>Xe-avrRxo1</i> promoter <i>in vitro</i>	124
Figure 4- 7 Nanoluc reporter assay to test the transcription activity driven by <i>Xe-avrRxo1</i> promoter <i>in vivo</i>	126

LIST OF TABLES

Chapter 1

Table 1- 1 Biochemical and biological functions of T3 effectors in *Xanthomonas* 21

Table 1- 2 Cloned R genes for resistance to *Xanthomonas* species 23

Chapter 2

Table S2- 1 Sequences of primers utilized in this investigation 66

Chapter 3

Table S3- 1 Sequences of primers utilized in this chapter 101

Chapter 4

Table S4- 1 Sequences of primers utilized in this chapter 128

Chapter 1 Literature Review

Type III Secretion Effector: A Coin with Two-sides in the molecular plant-microbe interactions

Summary

During the co-evolution of plants and diverse phytopathogens, plants have evolved a sophisticated immune system with two-branched molecular mechanisms to protect their health and reproduction. The first branch of immune response recognizes the molecule patterns conserved in different classes of microbes, including the non-pathogens. The second branch of immune response recognizes specific pathogen virulence factors, either directly or indirectly. Almost all gram-negative bacterial pathogens possess the type III secretion system (T3S) that can inject a collection of bacterial effectors inside plant cells. These type three effectors (T3E) are required for the full bacterial pathogenesis. Many T3Es function as double-edged swords. For example, the T3Es can suppress plant immunity and promote bacterial proliferation on host plants that have no corresponding disease resistance (*R*) genes. On the other hand, if particular plant genotype carries specific *R* genes that can recognize the corresponding T3E, a robust and quick immune response usually manifests with a localized programmed cell death or hypersensitive response (HR) at the pathogen infection sites. Characterization of every individual T3E for their molecular functions will allow us to understand the plant's immune system and may breed new crop cultivars to achieve sustainable production of food, vegetable, fiber, and biofuels. In my dissertation, I mainly studied the virulence functions of *Xanthomonas euvesicatoria* (*Xe*) type three effectors. Therefore, this review will highlight the recent progress on the effector-triggered immunity (ETI) and the effector-triggered susceptibility (ETS) in plant and microbe interactions, with a focus on *Xe* T3Es.

Part 1: Effector-triggered susceptibility

The increasing world population challenges the security of the global food supply. Global climate change has made this food crisis issue even worse in the past decades. Protecting crops from different plant pathogens has a critical role in meeting the growing demand for food quality and quantity [1]. Roughly, direct yield losses caused by pathogens, including viruses, bacteria, fungi, oomycetes, nematodes, and various insects are about 20-40% of global agricultural productivity [2].

Unlike animals, crops are not able to escape from the danger of pathogens via adequate movement [3-5]. On the one hand, as engaged in an everlasting biotic threat in the field, plants have established a sophisticated immune system to monitor and restrict the amplification of microbial. On the other hand, phytopathogens also evolve constantly to escape or suppress plant immunity to colonize plants. Recent studies revealed the complicated plant-pathogen interactions from the perspective of both organisms. It is of particular importance for agricultural practice to apply new knowledge and novel biotechnological approaches for crop protection. In the first part of the review, I will review phytopathogen infection strategies involving different T3Es that have been reported recently, in aiming to understand the ‘enemies’ of crops.

Classic ‘zigzag’ model of plant immunity

During the past two decades, scientists developed several profound working models to explain the molecular interactions between plants and phytopathogens. Here, in order to introduce T3Es and explain what roles they play in the replications of microbial and plant immunity, the classic ‘zigzag’ model is cited to illustrate the plant immune system (Figure 1-1) [6]. There are four phases in this model. Owing to perceived various kinds of microbial, transmembrane pattern recognition receptors (PRRs) are utilized to respond to pathogen-associated molecular patterns (PAMPs), which are conserved among diverse microbial and have evolved slowly [7]. In phase 1, the recognitions of conserved PAMPs by PRRs result in a PAMP-triggered immunity (PTI) that can limit further colonization. PTI is a moderate response, and usually, no

obvious symptom can be overserved. In phase 2, successful pathogens can employ effectors to interfere with PTI, resulting in the effector-triggered susceptibility (ETS). In phase 3, plants deploy specific nucleotide binding-leucine rich repeat (NLR) protein to recognize a given effector delivered by the phytopathogen, and the related immunity is named as effector-triggered immunity (ETI) [3]. ETI serves an accelerated and amplified PTI immunity response, protecting plants from the infection of phytopathogens by processing a suicide hypersensitive cell death response (HR) at the infected site. In phase 4, natural selection, on one hand, directs phytopathogens to escape ETI through secreting additional effectors to suppress ETI, shedding alternation of the recognized effector primary sequence or structure. On the other hand, natural selection addresses the evolution of new R proteins to recognize the diversified effectors and trigger ETI again. The two aspects above tangle together along with the co-evolution between plant hosts and phytopathogens.

PTI: the first layer of plant immunity

As the first layer of plant immunity, PTI conditions the basal and broad disease resistance to diverse phytopathogens [8]. One of the typical elicitors of PTI is the bacterial flagella, which is necessary for bacterial motility and pathogenicity in plants. Because of the importance of flagella, it is conserved in diverse bacterial species. The flagella functions as a PAMP that triggers defense responses in various plant species [9]. A synthetic 22-amino-acid peptide (flg22) from a conserved flagella domain has been used as the synthetic elicitor of PTI [7, 10, 11]. An Arabidopsis leucine-rich repeat (LRR)-receptor kinase FLS2 has been identified in a genetic screen by using flg22 [12]. FLS2 can be internalized by binding flg22, in which a receptor-mediated endocytic process is required [7, 13]. Mutant of *fls2* exhibits enhanced susceptibility to spray application of pathogenic *Pseudomonas syringae* pv. *tomato* (*Pst*) *DC3000*, but not to straight infiltration of *Pst* *DC3000* into the leaf apoplast, implying that FLS2 mainly acts against early pathogen invasion [11, 14].

Bacterial elongation factor Tu (EF-Tu) activates similar defense responses like flg22 [15-17].

It can be recognized by an Arabidopsis LRR-kinase designated as EFR [17]. The mutant of *efr* allows higher efficiency of transient transformation with *Agrobacterium*, suggesting that PTI also limits *Agrobacterium* pathogenicity. Treatment with a conserved EF-Tu peptide, elf18, induces expression of a gene-set nearly identical to that induced by flg22 [17]. Furthermore, EFR transcription can be induced by flg22. Besides, both FLS2 and EFR belong to an atypical kinase family that might function similarly in the plant immune system. Thus, a common set of signaling pathways are shared by plant responses to different PAMPs. This convergence makes it possible for T3Es to target a limited number of genes and compromise PTI. By contrast, mutations in genes required for NLR function have no impact on responses of plants to flg22 [11]. Hence, NLR-dependent signaling and PAMP-mediated signaling own partially distinct components.

The molecules that can induce PTI are usually essential or critical for microbial growth, which can not be easily eliminated by the microbes, but variations exist in PAMPs in different microbes that can trigger a different response on different plant species. For instance, flagella of *Xanthomonas campestris* pv. *campestris* (*Xcc*) and *Agrobacterium tumefaciens* are less effective than that of *Pst DC3000* in triggering FLS2-mediated PTI in Arabidopsis [10]. Ef-Tu from *Pst DC3000* is much less active in eliciting PTI in Arabidopsis than Ef-Tu from *Agrobacterium*[16]. In terms of plant species, Arabidopsis accession Ws-0 carries a point mutation in FLS2, terminating its response to flg22 [9]. Individual plant species are not capable of recognizing all potential PAMPs [7]. Other unknown PAMPs and corresponding PRRs must exist. Twenty-eight of over 200 LRR-kinases in *Arabidopsis col-0* are induced within a treatment of flg22 for 30 min [11, 18]. Moreover, *Agrobacterium* extracts elicit PTI on a *fls2/efr-1* double mutant [17]. Following the current model, additional uncovered PRRs or LRR kinases should be stimulated transcriptionally by engagement of appropriate PAMPs [19, 20]. Conversely, the irrelevance between PAMPs and PRRs will lead to natural selection.

Suppression of PTI via Effectors

One of the most critical functions for a collection of effectors in phytopathogens is to suppress PTI [8]. Although eukaryotic pathogens including oomycetes and fungi, deliver effectors to plants as well as bacterial pathogens, effectors of oomycetes and fungi are still poorly understood, so this review focuses on discussing plant cellular processes targeted by bacterial type III effectors. Plant disease-associated bacteria deliver 15–40 effectors into host cells using the type III secretion system (T3S). A *Pst DC3000* strain mutated in the T3S triggers a faster and stronger transcriptional re-programming in hosts compared to the wild-type strain [21-24]. It can tell that the T3Es are necessary for colonization of bacterial pathogen in a manner mimicking or inhibiting eukaryotic cellular functions [25-28].

Here, I listed several classic cases of T3Es and their biochemical functions in regulating plant immunity [8, 29]. Two independent T3E effectors from *Pst DC3000*, AvrPto and AvrPtoB contribute to bacterial virulence by inhibiting upstream of MAPKKK, which is an early step in PTI [30]. AvrPtoB has two critical domains where the N terminus contributes to virulence function, while the C terminus blocks host cell death [31, 32]. A domain from the AvrPtoB C terminus forms an active E3 ligase and directs host protein degradation [33]. Another two unrelated T3Es from *Pst DC3000*, HopM, and AvrE, both target ARF-GEF protein, which is involved in host cell vesicle transport [28]. The redundant function of these two effectors suggests the importance of manipulating host vesicle transport in the successful bacterial colonization [34]. The *Yersinia* effector YopJ and its homologue in the avrRxv effector family have been reported to inhibit the turnover of MAP kinase cascades by acetylation of a MEK protein at its phosphorylation-regulated residues [35]. Although great achievements about the T3Es and their functions have been reached during the past two decades, the targets and biochemical activities of many bacterial type III effectors still await to be unraveled by plant pathologists.

Virulence and disease symptoms associated with T3Es in Xanthomonas

All *Xanthomonas* strains own a T3S system, which is well studied and shows a critical function

in facilitating a favorable environment for the living and replication of *Xanthomonas*. It is common for the T3Es in a particular *Xanthomonas* strain to share redundancy of function [36]. However, regardless of being functional in suppressing elicitor-triggered immunity or promoting infection via modifying plant innate metabolism, an increasing number of T3 effectors of *Xanthomonas* have been characterized with aspects of enhanced virulence and development of disease symptom (Table 1-1).

As one of the first identified T3Es, AvrBs2 has been indicated to contribute to virulence as a result of its ability to support increased numbers of bacteria within host tissue [37, 38]. Four T3 effectors of *Xe*, AvrBs1-4, were all found to have contributions to pathogen fitness to varying extents in the field tests [39].

The TAL effector family consist of a large number of closely related T3Es, and many members of this family have a critical impact on virulence and disease symptom [40]. For example, two TAL effectors within a high homology, PthA from *Xanthomonas axonopodis* pv. *citri* (*Xac*) and pthXo1 from *Xanthomonas oryzae* pv. *oryzae* (*Xoo*) have a positive effect on the ability of the pathogens to spread as well as to elicit disease symptoms [41]. The phenotype can also be observed in plant expression of the gene. Besides, one benefit of TAL effectors to bacteria may be an establishment of an aqueous apoplastic environment in the infected sites of leaf tissues. A period of high atmospheric relative humidity after rainfall, has repeatedly been shown to promote disease outbreaks in crops, implying that the availability of water is imperative for pathogenesis. The TAL effectors of *Xanthomonas campestris* pv. *malvacearum* (*Xcm*) and *Xoo* are associated with the increased appearance of water soaking, suggesting TAL effector can alter the water status in the apoplast for better colonization of bacterial pathogens in plants. As a consequence, a high water availability in the apoplast can in turn direct the success of potentially pathogenic microbes.

Another function of TAL effectors might be the promotion of bacteria release from infected tissue to uninfected tissue. *Xcm*-avrB6 and *Xe*-avrBS3 have been reported to increase populations of bacteria in the uninfected areas of cotton and pepper leaves, respectively [42,

43]. The lesions, chlorotic and desiccated leaf tissues are severely limited in the absence of the above mentioned two major TAL effectors in field tests [44-46], suggesting that enhanced release could have a fitness benefit for *Xanthomonas* colonization in a more spreading scale [39]. The function of *Xanthomonas* TAL effector can be interfered by R protein [47]. For example, the R gene xa13 specifically recognizes and subsequently interferes with the function of the TAL effector PthXo1, implying a practical application providing resistance against rice bacterial blight disease [41].

Chlorosis is a prevalent symptom in plants infected by *Xanthomonas*, in which a conserved T3E, early chlorosis factor (ECF), also named as XopAA, is reported to contribute this category of symptom [48]. ECF was identified by a complementation approach, in particular, the presence of ECF render *Xanthomonas* strains a greater ability to induce chlorosis but ECF did not show a detectable influence on bacterial populations. XopD and XopN of *Xe* have both been shown to contribute to virulence and disease symptoms in tomato. Plants infected with *Xe* strains impaired of XopD present a more significant leaf tissue necrosis, indicating that XopD can suppress innate plant immunity [45]. XopN is a T3E gene widely distributed in *Xanthomonas*. *Xe* Strains without XopN possess a smaller bacterial population and less necrosis and senescence in the plants after infection [46]. Impairment of the XopN homologue in *Xcc* also results in reduced disease in radish [49]. Other candidate T3 effectors have been characterized to impact virulence and disease symptoms, including XopJ or AvrXv4 [50], XopX [51], XopAE or HpaF [52] and XopAH or AvrXccC [53].

Biochemical functions of type three effectors in Xanthomonas

After reviewing the virulence function and symptom induced by *Xanthomonas* T3Es, here we will go further to discuss putative structural motifs and biochemical activities of some *Xanthomonas* T3Es underlying the previously mentioned virulence mechanism (Table 1-1). Structural motifs of 15 *Xanthomonas* T3Es have been linked to the function of those effectors. Twelve of the 15 indicate they may have enzymatic activities. Recent progress on specific

functions of individual T3 effectors in *Xanthomonas* gives an insight into how *Xanthomonas* effectors interact with host plants via altering plant innate metabolism. In the part of the present review, we focus on highlighting the biological functions of five *Xanthomonas* T3Es.

AvrBs3

The AvrBs3 group is a large family that consists of closely related TAL T3 effectors of *Xanthomonas*. Structurally, the N-terminal and C-terminal portions of TAL effectors are highly conserved. The conserved C-terminal portion of TAL effectors contains a strong nuclear localization signal (NLS) motif, as well as a robust acidic transcription activation domain (AD). Both of them are associated with biological effects such as pathogen virulence, inducement of host disease symptoms and facilitating pathogen spread [54-58]. A variety of TAL effectors are associated with biological effects, including virulence of the pathogen and disease symptoms. The most distinguishing feature of overall TAL effectors is their particular repetitive region containing varying numbers of near-identical repeats of 34 or 35 amino acids, which are able to determine DNA binding specificity. Thus, different TAL effectors bind to unique DNA elements in diverse host genomes. TAL effectors can function as transcription factors that bind to specific DNA elements of targeted host genes and regulate their transcriptions in the host nucleus [59].

As a typical TAL, AvrBs3 has 17.5 repeats and encodes a basic helix-loop-helix transcription factor. It has been reported that, specifically, it binds to the DNA sequence in several genes such as *upa20* (up-regulated by AvrBs3 20), which is responsible for the hypertrophy of the host cells. The same sequence is also found in the promoter of the resistant gene, BS3, resulting in the expression of BS3 in the presence of AvrBs3 [60]. Changes in the TAL effector binding domain can eliminate the response to TAL effector.

TAL effector, *pthXo6* in *Xoo*, has been shown to promote virulence upon the infection of *Xoo* to rice. *PthXo6* can upregulate the expression of a rice gene *OsTFX1*, encoding a plant transcription factor in bZip family [61]. A mutant in the DNA binding domain of *pthXo6* led

to a reduction of virulence, indicating the importance of DNA binding domain for the complete function of pthXo6. In turn, the ectopic overexpression of *OsTFXI* in rice restores the virulence function of pthXo6 [61]. As a member in bZip transcription factor family, *OsTFXI* might induce or repress multiple genes that are involved in host immunity. All strains of *Xoo* were proved to be capable to induce the expression of OsTFX1, supporting that *OsTFXI* is essential for the bacterial fitness of *Xoo* and its infection to rice. Furthermore, it might be a result of natural selection and long co-evolution between *Xoo* strains and rice. However, transgenic plants ectopic overexpressing of OsTFX1 did not cause any phenotypic abnormalities, implying post-translational regulating mechanism may exist upon infection of *Xoo* to rice [61].

XopD

XopD is a conserved T3E in diverse *Xanthomonas* strains, and it has multiple functions in the infection of *Xanthomonas* to various hosts (Table 1-1). Apart from the ability to suppress defense gene expression, the most significant function of XopD is its small ubiquitin-like modifier (SUMO) activity. It has a SUMO protease domain and is also a member of the C48 protease family and has been proven to be able to release SUMO from SUMO-modified plant proteins [62, 63]. The SUMOylation of host proteins regulates stress and developmental responses by subtly managing protein stability [64-66]. Specific alterations to the predicted catalytic sites of XopD also caused compromised virulence consistent with delayed necrosis [45].

XopD is localized at the nucleus and has a DNA binding activity [45, 62]. Sequence analysis revealed that the helix-loop-helix region of XopD at amino acids 113–131 is the key domain for its binding ability. The site-directed mutation on V118 of XopD reduced its contribution to virulence along with delayed development of necrosis in the infected tissues. It suggests the DNA binding domain in XopD protein is required for its complete functions. Two ethylene response factor-associated amphiphilic repression (EAR) motifs [L/FDLNL/F(x)P] were also characterized in XopD at amino acids 244–249 and 284–289. EAR motifs are found in host

transcription factors that repress salicylic acid- and jasmine acid-induced defense gene transcription *in planta*, but the exact mechanism remains unknown. Mutations in the EAR motifs led to a reduction in virulence and delayed necrosis, but did not influence the localization and catalytic activity of XopD.

Therefore, the functions of XopD can be split into two aspects. The first one is transcriptional regulation, that is directed to related defense or senescence transcription factors, either through DNA binding or the EAR motifs or both; the second one is post-translational modification, that is addressed to destabilize host defense proteins by way of deSUMOylation, which is the catalytic activity of XopD [45, 66].

XopJ

The T3Es in XopJ family are present in diverse phytopathogenic bacteria [67]. Since a high identity from the C55 group of cysteine protease, members in this family have been proposed to regulate the stability and activity of host proteins via SUMOylation (Table 1-1). For example, AvrXv4 likely functions as SUMO protease. Additionally, other members of the XopJ group are also found to function as transacetylases [50].

YopJ, the first identified member in this large family, has been previously revealed to target on trans-acetylating threonine and serine residues in several mitogen-activated kinases (MAPs). It can prevent the phosphorylation of MAP kinase, which is an important behavior to initiate innate immunity signal transduction in response to the attack of phytopathogens [68]. XopJ is also shown to interfere with the host callose deposition, which is a common PTI signaling event [69]. The myristoylation motif at the N-terminus can partially determine the localization of XopJ and it is usually targeting the protein at the host cell membranes [69, 70]. However, the direct host targets of XopJ have not been identified.

Another important member of this family is the AvrBsT in *Xcc*. Like YopJ, AvrBsT also possesses a transacetylase activity, but it fails to trigger resistant response in most ecotypes of *Arabidopsis* because its biochemical activity can be inhibited by the carboxylesterase activity

of SOBER (suppressor of AvrBsT elicited resistance1) [71]. Consistently, accession Pi-0 carrying a null mutation in SOBER shows a strong HR in an AvrBsT-dependent manner.

AvrRxv is another member belonging to the XopJ group. Previous reports suggest that the C-terminus and N-terminus of AvrRxv collaborate to execute its biochemical function that is required for the pathogenesis of *Xcc*. XopJ can induce HR in the tomato cultivar Hawaii 7998, which depends on several conserved catalytic residues at the C-terminal of XopJ [67, 72]. Interestingly, the ability of AvrRxv to elicit an HR remained after the replacement with the C-terminal domain of YopP. As the C-terminal domain of YopP has previously been characterized as a trans-acetylate MAP kinase, implying the putative transacetylase activity of AvrRxv. Besides, AvrRxv binds a tomato 14-3-3 protein mediated by the N-terminal segment of AvrRxv (1–141 amino acids) [67]. The 14-3-3 proteins have been extensively studied to function as chaperons in a variety of cellular complexes, like MAP kinase-related signal transduction pathways. AvrRxv fulfills its transacetylase activity and represses host innate immunity by binding to 14-3-3 protein that is engaged in the MAP kinase signal transduction pathway.

XopN

XopN has been characterized to interact with a variety of proteins including OsVOZ and OsXNP in rice and an atypical (phosphorylation-deficient) receptor-like kinase named TARK1, as well as 14-3-3 proteins, such as TFT1, TFT3, TFT5 and TFT6 in tomato (Table 1-1) [46, 73-75]. TARK1, similar to other RLK proteins, presents two membrane-spanning regions including an LRR domain outside the cell and a nonfunctional kinase domain in the cytoplasm. The interaction with TARK1 has been shown to require an “LXXLL” sequence in the cytoplasmic portion of TARK1. Intriguingly, an “LXXLL” motif in the N-terminal portion of XopN is also required for its interaction with TARK1. A site mutation in XopN lost the ability to bind to TARK1, which resulted in a reduction in its virulence effect but not its suppression of callose deposition [46]. Therefore, the crosstalk between TARK1 and XopN contributes to the virulence effects of XopN during *Xe* infection to tomato. Furthermore, suppression of

TARK1 expression in tomato also caused a partial suppression of XopN-mediated susceptibility [46]. These evidences comprehensively demonstrate that XopN interferes with TARK1-dependent signaling events in tomatoes invaded by *Xe*. However, as an atypical kinase without intrinsic catalytic activity, the mechanism of TARK1 engaged in host defense response is unknown yet, which may be distinct from signal transduction pathways mediated by other RLKs [76]. Also, the involvement of XopN was shown to interact with 14-3-3 proteins which are known to be involved in diverse signal pathways in plants and animals. It is perhaps a consequence of several anti-parallel α -helical repeats and HEAT (huntingtin, elongation factor 3, PR65/A, TOR1) repeats in XopN [44].

XopAC and XopAH

Two T3Es of *Xanthomonas*, XopAC, and XopAH, are taken together to be reviewed as a result of their sequences related to the Fido domain, which is derived from the fic [filamentation induced by cyclic adenosine monophosphate (cAMP)] and doc (death on curing) domains [77]. A fido domain is present in the T3E from the animal pathogen *Vibrio parahaemolyticus*, which was recently found to cause host cell cytotoxicity and can covalently modify Rho GTPases with adenosine monophosphate moieties (Table 1-1). This modification has been named as an AMPylation reaction and the central motif sequence in this domain is HPF_x(D/E)GN(G/K)R, in which histidine facilitates AMPylation. This modification has been proposed to alter signaling functions of the target proteins, similar to ribosylation, acetylation and phosphorylation modifications [78, 79]. Structural comparisons showed T3 effector AvrB of *P. syringae*, XopAC of *Xcc* and XopAH of *Xcc* all contain Fido-domain-like segments [80]. Although they do not have the histidine residue, other amino acid residues structurally related to histidine have been proposed to provide the same function [77].

Part 2: Effector triggered immunity

The gene-for-gene model

Over 50 years ago, H.H. Flor, working on flax and the flax rust fungus, gave a genetic definition for the interaction between plants and phytopathogens, which presented as the gene-for-gene hypothesis/model [55, 81-83]. In this hypothesis, plant resistance is activated when a specific Avr (avirulence) protein from the pathogen is recognized by a specific R (resistance) protein from the plant. A receptor-ligand model was used to interpret the biochemical nature of the gene-for-gene hypothesis. As explained in this model, plants can activate defense mechanisms upon R-protein-mediated recognition of pathogen-delivered Avr products. A ‘matched set’ of R and Avr alleles is necessary for the induction of resistance. If the two components do not ‘fit’ then resistance is not activated, and the plant is susceptible to the pathogen infection.

When pathogens infect plants that are lacking corresponding R proteins, the Avr products might function as virulence factors, which can repress plant immunity by reprogramming host transcriptome and altering the cellular metabolisms to favorite pathogen proliferation. The Avr products can directly or indirectly interact with plant pathogenesis targets. In order to suppress the pathogen infection, plants evolved a collection of R proteins to monitor and recognize the Avr products. The R-protein-mediated recognition of Avr products activates the plant defense responses, which are frequently indicated by an outburst of superoxide and nitric oxide, calcium fluxes and results in localized cell death. Pathogens can evade the R protein-mediated recognition when the Avr proteins are lost or mutated. Both pathogens and plants have therefore continually evolved in this battle to secure their survival and propagation.

Direct NLR-Effector Interactions

The core concept in the gene-for-gene model is that the crosstalk in a match pair of proteins, one from the host plants and another one from the phytopathogens, leads to the disease resistance. After half a century of research, the miracle of how a specific Avr (avirulence) protein and a specific R (resistance) protein interact with each has been gradually unraveled. On the one hand, the typical plant R protein usually presents in a nucleotide-binding/leucine-rich-repeat (NLR) scheme. On the other hand, the Avr protein is named as the effector, which

is usually delivered by type three secretion system in bacterial pathogen. In general, in terms of their recognition, an NLR protein is held in an ADP-bound “OFF” state when there is no infection of phytopathogens or a particular pathogen effector is absent. For instance, the activation of flax L6 protein and its recognition of flax rust (*Melampsora lini*) effector, AvrL567, requires the assistance of the Toll-like interleukin-1 receptor (TIR) domain at N-terminal. NLR protein turns to ‘ON’ state after recognizing a pathogen effector. NLR protein functions as a receptor and ligand to recognize a pathogen effector, a series of conformational changes complex causes the exchange of ADP to ATP at its nucleotide-binding (NB) domain. Eventually, the interaction between NLR protein and pathogen effector initiates ETI signaling events and plant cell death at the infection site.

Yeast two-hybrid and other *in vitro* interaction assays support the function of several direct NLR-effector interactions in plant resistance [36, 84-88]. A reverse genetic screen identified an NLR protein, Roq1, with a TIR domain, that can recognize XopQ to trigger the immune response of *N. benthamiana* [90]. Impairment of the LRR domain in Roq1 eliminates its ability to recognize XopQ and also abolish the subsequent cell death as well as *Xe* disease resistance in *N. benthamiana*. NLR mutational and domain swap experiments in the other R protein pairs also confirm the determinant role of variable LRR domains in the recognizing of specific pathogen effectors, where the mechanism remains unclear [88, 89].

Indirect NLR Surveillance of Effector Activities

Compared with the high diversity of direct NLR-effector recognitions, indirect NLR recognition of various pathogen effectors converges to a limited set of host proteins that are involved in the resistance signaling network. Beneficially, this strategy might help NLR mediated recognition catch up with the rapid pathogen evolution. Heretofore, there are two sub-models that have been developed to explain the indirect NLR surveillance system.

One indirect recognition model is named a guard model [3, 6, 91]. In this model, the receptor serves as a guard binding to a host protein which can be modified by a pathogen effector. Hence,

the host immunity can be initiated when the targeted host protein is modified. For instance, two Arabidopsis plasma membrane NLRs, RPS2 (resistance to *Pseudomonas syringae* 2) and RPM1 (resistance to *Pseudomonas syringae* pv. *maculicola* 1) constitutively guard a host protein, RIN4 (RPM1-interacting protein 4) [92-94]. RIN4 can be interfered by diverse *P. syringae* effectors AvrRpm1, AvrB and AvrRpt2 through divergent modifications [92-94]. For example, the isomerization of RIN4 induced by AvrB-initiated phosphorylation can be perceived by RPM1 to activate the immune response [95, 96]. In the absence of RPS2 and RPM1, RIN4 is targeted for manipulation by above bacterial effectors owing to downregulating basal resistance response activities [97-99].

Another indirect recognition model is named as a decoy model. In this model, the host factor with no resistance activity protects structurally related basal defense components from pathogen effectors' targeting and modification. This kind of host factor is defined as decoy, which can trap foreign effectors and thereby trigger ETI [100, 101]. For instance, tomato NLR Prf (Pseudomonas resistance and fenthion sensitivity) confers resistance to AvrPto from *P. syringae*. Prf is held in a locked form as a consequence of its binding to protein kinase Pto [102, 103]. Like PBS-1, the role of Pto in basal immunity has not been reported yet. However, the kinase domain of Pto is essential for resembling the complex consisting of FLS2, EFR and their coreceptor BAK1 (BRI1-associated receptor kinase 1), which are all targeted by AvrPto during infection [104, 105]. Besides, the Arabidopsis plasma membrane NLR RPS5 is another R protein that fits the decoy model. PRS5 is in an off state as a result of the interaction with the intact protein kinase PBS1 (AvrPphB susceptible 1) via its N-terminal CC domain, whereas PRS5 switches to an ON state after PBS1 is cleaved by the effector AvrPphB [106]. Several PBS1-like kinases have been proven critical in the plant surveillance mechanism, such as the soluble kinase BIK1 (Botrytis-induced kinase 1), which is a key component of PRR signaling in PTI [106-108]. In order to escape the immune system, *P. syringae* deploys AvrPphB, a key virulence effector, to cleave PBS1-like kinases including BIK1 [109]. Although PBS1 has no obvious basal resistance function, it can initiate RPS5 after cleavage, indicating the decoy

model has been applied to counter immunity and trigger susceptibility [106]. Hence, in theory, a family of structure-related host defense proteins or a complex of host defense components can be shielded by a single molecular decoy associated with one or more R proteins.

Effector recognizes specific promoter DNA sequence of host genes

Different from the recognition at the protein level, another kind of effector recognition occurs with the host DNAs. A specific class of transcription activator-like (TAL) effectors in *Xanthomonas* and *Ralstonia* bacterial species can be straightforwardly delivered to plant nuclei, where they bind to the promoters of host defense-related genes to regulate their expressions and enhance susceptibility [110, 111]. TAL effector has a unique series of amino acid repeats that can specifically bind to the promoter elements of their host targets to reprogramme the defense-related transcriptional network [112, 113].

In order to counter TAL, rice, and pepper plants have naturally developed corresponding R (resistance) genes, whose promoters can bind to TAL and initiate their expressions. Typical immune responses, including an outburst of superoxide and nitric oxide, calcium fluxes and HR, can be induced to stop pathogens from further spreading when those R genes are expressed driven by TALs [114, 115].

There is no conserved feature for the products of these R genes. In pepper, the binding of *Xe* TAL effector AvrBs3 to the resistance gene, BS3, can activate a homolog of a flavin-dependent monooxygenase enzyme and subsequent HR at the infection sites [116]. In addition, the *Xe* TAL effector AvrBs4 can induce the expression of the resistant gene, Bs4c-R, to elicit HR in pepper. In tomato, the TAL effector activates a TIR-NLR protein, Bs4, and results in disease resistance [115, 117]. In rice, the recognition between resistant gene *Xa10* gene and *Xoo* TAL effector AvrXa10 induces endoplasmic reticulum Ca²⁺ release and subsequent HR [118]. Another *Xoo* TAL effector, AvrXa27, can upregulate the expression of the rice resistance gene *Xa27*, whose protein can be secreted outside the plant cell to the apoplast and block the further bacterial growth there [114, 119].

As shown above, in order to preserve intracellular immunity, different plant species have evolved various mechanisms to defend against TAL, implying a high diversity on the TALs and the novelty of this pathogenicity. It is still not known whether NLRs are involved in the binding of the TAL effector to corresponding R genes. TAL effector-induced resistance occurring on host DNA provides the new possibility for innovative defense adaptations in plant defense pathways.

Necessary ETI signaling components, NDR1 and EDS1

Activation of the NLR signaling pathway requires the assistance of other components. Two central regulators for the NLR signaling transduction have been identified via the genetic screening. One component is the plasma membrane-anchored integrin-like protein NDR1 (non-race-specific disease resistance 1) while another one is the nucleocytoplasmic lipase-like protein EDS1 (enhanced disease susceptibility 1) [120-122]. As mentioned above, NLRs can be divided into two classes depending on the structure on the N-terminal TIR domain or coiled-coil (CC) domain. The corresponding NLRs are named as CC-NLR and TIR-NLR, respectively. In the plant immunity, NDR1 and EDS1 are recruited by CC-NLR and TIR-NLR sensor receptors to elicit ETI [122]. Moreover, EDS1 signals in all TIR-NLR-related defense events, including SA accumulation, HR and defense transcriptional reprogramming [122-124]. By contrast, NDR1 plays an essential role in the SA biosynthetic pathway, elicited by several CC-NLRs [125].

The mechanisms underlying the functions of NDR1 and EDS1 proteins in ETI are different. Arabidopsis NDR1 anchors RIN4 (guarded by the CC-NLRs RPS2 and RPM1) at the plasma membrane [120, 121]. This interaction was also found to be substantial for soybean CC-NLR resistance [126-128]. By contrast, Arabidopsis EDS1 forms nuclear signaling complexes with SAG101 (senescence-associated gene 101) and soluble nucleocytoplasmic with PAD4 (phytoalexin-deficient 4), respectively [129, 130]. Crystal structure analysis has shown that PAD4 and SAG101 compete for the same EDS1 interface. It is consistent with the fact that

PAD4-EDS1 and SAG101-EDS1 complexes have distinct immunity functions in ETI, which might be a mechanism of counterbalancing [130, 131]. Although EDS1 does not show a catalytic mechanism for TIR-NLR or basal resistance signaling, it resembles a plant lipase-like molecular switch as a consequence of its structural similarity to the lipase enzyme at N-terminal [131, 132]. Intriguingly, EDS1 was found to associate with Arabidopsis TIR-NLR receptor RPS4 and *P. syringae* effector AvrRps4 (recognized by the Arabidopsis RRS1/RPS4 TIR-NLR pair), implying the function of EDS1 in the recognition between R protein and T3E [133-135]. Thus, EDS1 seems to serve as a molecular hub not only for TIR-NLR effector activation but also for downstream defense pathways.

The cognate R genes recognize Xanthomonas T3Es

After discussing types of interactions between R proteins and T3Es, and the related signal transduction pathways, we would like to give a specific review on cognate R genes to T3Es in terms of *Xanthomonas* bacteria. Since *Xanthomonas* is one of the most important bacterial pathogens that causes a significant yield loss on the production of assorted vegetables, fruits, and crops, including *Solanaceae*, *Poaceae*, *Brassicaceae*, and *Rosaceae* for human beings. The ultimate goal for understanding the T3E function is to translate the knowledge to the breeding of durable and broad resistance [136]. Aim at this resistant breeding goal, during the past two decades, a variety of R genes against *Xanthomonas* species and their T3E have been cloned and characterized (Table 1-2). Most of them belong to the two largest and well-studied classes of R genes, RLK and NLR. *Bs2*, *Bs4*, *Xa1*, and *Rxo1* encode proteins in the NLR family while *Xa21* and *Xa26* are the members of the RLK class.

In addition to the major classes of R genes, studies of *Xoo*-caused disease in rice have identified a variety of novel R genes, particularly against TAL effectors, indicating that the battle continues in the host nucleus [29]. The host transcriptional machinery can be altered under the attack of *Xanthomonas*, in which XopD and the various TAL effectors play a critical role in regulating the expression of host genes. Under selective pressure, owing to termination of the

infection, hosts have to develop alternative strategies to abrogate the function of TAL effectors. *Xa27* and *Bs3* have been both reported to have the function of repressing self-inflicted cell damage and host lesion. Although they do not have a high similarity on the primary sequence and subcellular localizations, the mechanism underlying their function in plant immunity and resistance seems analogous. More concisely, *Xa27* and *BS3* can modify the gene-promoter combinations, which are the targets of TAL effectors. In addition, the discoveries of another two recessive resistance genes, *xa5* and *xa13*, provide new insights to host adaptations for resistance against *Xoo* and its TAL effectors [41, 137-139]. *Xa5* and *xa13* interfere with TAL effector function via different mechanisms. Specifically, *Xa13* interferes with *PthXo1* and blocks its action as a TAL effector. By contrast, *Xa5* serves as a component in the transcription complex that can interfere with the general TAL effector target on the host transcription machinery [41].

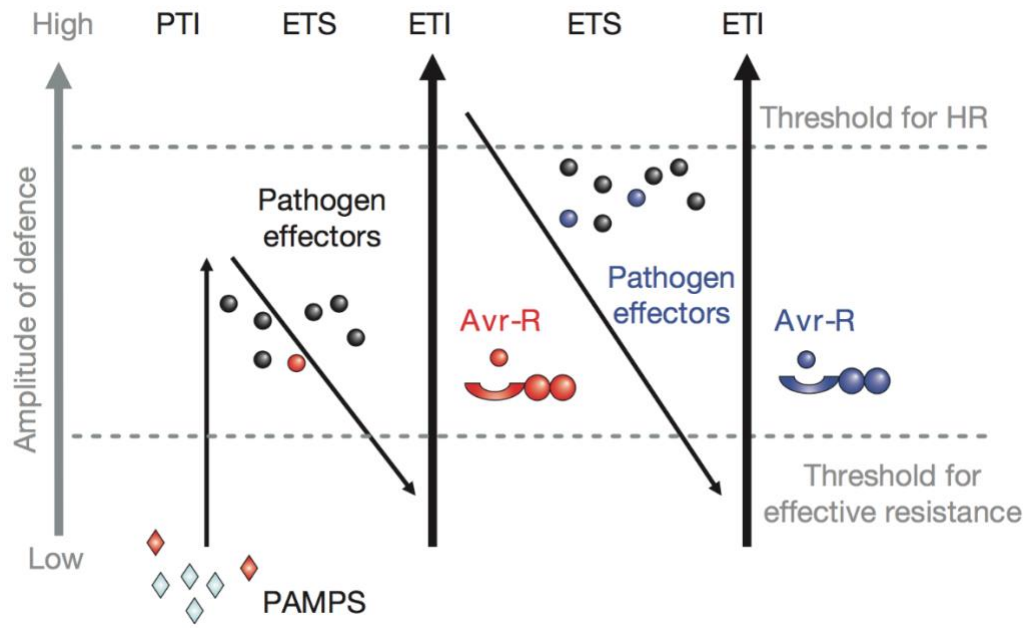


Figure 1- 1 A zigzag model illustrates the quantitative output of the plant immune system [6].

Table 1- 1 Biochemical and biological functions of T3 effectors in *Xanthomonas*

T3E (group)	Biochemical and biological functions	Host target(s)	References
AvrBs2	Glycerolphosphoryl diester phosphodiesterase		Kearney and Staskawicz, 1990; Swords et al., 1996
AvrBs3/PthA	Site-specific DNA binding; nuclear localization; transcription activation domain	Os8N3(Os); OsTFX1; upa20 (Ca)	Zhu et al.,1998; Yang et al., 2006; Romer et al., 2007; Sugio et al.,2007; Kay et al.,2007;
XopC	Haloacid dehalogenase hydrolase and phosphoribosyl transferase domain		Noel et al., 2003
XopD	Cysteine SUMO C48 protease; DNA binding; nuclear localization; EAR motif		Noel et al., 2002; Hotson et al., 2003; Chosed et al., 2007; Kimet al., 2008;
XopE (HopX)	Transglutaminase family		da Silva et al., 2002; Nimchuk et al., 2007; Thieme et al., 2007
XopG (HopH1 and HopAP1)	M27 zinc protease (clostridial toxin)		DaSilva et al., 2002; Ochiai et al., 2005; Salzberg et al., 2008
XopJ (HopJ1) [AvrBsT, AvrXv4, AvrRxv]	Acetyltransferase, C55 cysteine ubiquitin-like protease	14-3-3 protein (Sl)	Noel et al., 2003; Roden et al., 2004b; Thieme et al., 2007; Whalen et al., 2008; Bartetzko et al., 2009;
XopH (HopAO1)	Tyrosine phosphatase		Bretz et al., 2003; Espinosa et al., 2003
XopN (HopAU1)	ARM/HEAT repeat	VOZ2 and XNP (Os), TARK1, 14-3-3 proteins	Roden et al., 2004a; Kim et al., 2009; Taylor et al., 2012; Cheong et al., 2013;

		including TFT1, TFT3, TFT5 and TFT6,	
XopQ (HopQ)	Nucleoside hydrolase	14-3-3 protein TFT4 (Nb, Ca and Sl); 14-3- 3 proteins including TFT1 and TFT5 (At); MAPKKKa/ MEK2/SIPK (Nb)	Wei et al., 2007; Li et al., 2013; Teper et al., 2014
XopAA (HopAE1)	Colicin Ia C8 and C9 domains; ECF		Morales et al., 2005
XopAC	FIDO domain (AMPylation) PF02661; LRR, VHR		Xu et al., 2008; Kinch et al., 2009
XopAH	FIDO domain (AMPylation) PF02661		Wang et al., 2007; Kinch et al., 2009
XopAI (HopO1)	VIP2; ADP- ribosyltransferase		Silva et al., 2002
XopAJ [AvrRxo1]	Thiol protease, ATP/GTP binding, phosphorylation of NAD to 3'-NADP		Zhao et al., 2004; Shidore et al., 2017

The note for the name of T3E (group): Analogue T3Es from *Pseudomonas syringae* in a certain T3E group are shown in parentheses while those from *Xanthomonas* in the same group are present in square brackets.

Abbreviations for Biochemical and biological functions: ARM/HEAT, armadillo/Huntington, elongation factor 3, PR65/A, TOR domain; EAR, ethylene receptor factor-associated amphiphilic repression; ECF, early chlorosis factor; FIDO, fic, doc, AvrB domain; LRR, leucine-rich repeat; SUMO, small ubiquitin modifier protein; VHR, vascular hypersensitivity in *Arabidopsis landrace Col-0*.

Abbreviations for host targets: (Ca), pepper; (Os), rice; TARK, tomato atypical receptor kinase; (Sl), tomato; (Nb) *Nicotiana Benthamiana* (tobacco); *Arabidopsis thaliana* (At).

Table 1- 2 Cloned R genes for resistance to *Xanthomonas* species

Gene	Plant	Type	Comments	Cognate T3 effector	Reference
Bs2	Pepper	NLR		AvrBs2	Tai et al., 1999
Bs3	Pepper	Inducible	Flavin oxygenase-related protein	AvrBs3	Romer et al., 2007
Bs3-E	Pepper	Inducible	Promoter deletion of Bs3	AvrBs3 Δ 16	Romer et al., 2009
Bs4	Tomato	NLR	Cytoplasm	AvrBs4	Schornack et al., 2004
Rxo1	Maize	NLR	Cytoplasm; Condition rice resistant ability to <i>Xoc</i>	AvrRxo1	Zhao et al., 2005
Xa1	Rice	NLR	Cytoplasm	Unknown	Yoshimura et al., 1998
xa13	Rice	Promoter mutants of Os8N3; nodulin 3 family	Membrane protein; unresponsive S gene to TAL effector PthXo1	PthXo1	Chu et al., 2006; Yang et al., 2006
Xa21	Rice	RLK	Extracellular receptor, broad resistance	None	Song et al., 1995

References

1. Strange, R.N. and P.R. Scott, *Plant disease: a threat to global food security*. Annu Rev Phytopathol, 2005. 43: p. 83-116.
2. Oerke, E.C., et al., *Thermal imaging of cucumber leaves affected by downy mildew and environmental conditions*. J Exp Bot, 2006. 57(9): p. 2121-32.
3. Dangl, J.L. and J.D. Jones, *Plant pathogens and integrated defence responses to infection*. Nature, 2001. 411(6839): p. 826-33.
4. Ausubel, F.M., *Are innate immune signaling pathways in plants and animals conserved?* Nat Immunol, 2005. 6(10): p. 973-9.
5. Chisholm, S.T., et al., *Host-microbe interactions: shaping the evolution of the plant immune response*. Cell, 2006. 124(4): p. 803-14.
6. Jones, J.D. and J.L. Dangl, *The plant immune system*. Nature, 2006. 444(7117): p. 323-9.
7. Zipfel, C. and G. Felix, *Plants and animals: a different taste for microbes?* Curr Opin Plant Biol, 2005. 8(4): p. 353-60.
8. Bigeard, J., J. Colcombet, and H. Hirt, *Signaling mechanisms in pattern-triggered immunity (PTI)*. Mol Plant, 2015. 8(4): p. 521-39.
9. Gomez-Gomez, L. and T. Boller, *Flagellin perception: a paradigm for innate immunity*. Trends Plant Sci, 2002. 7(6): p. 251-6.
10. Felix, G., et al., *Plants have a sensitive perception system for the most conserved domain of bacterial flagellin*. Plant J, 1999. 18(3): p. 265-76.
11. Zipfel, C., et al., *Bacterial disease resistance in Arabidopsis through flagellin perception*. Nature, 2004. 428(6984): p. 764-7.
12. Chinchilla, D., et al., *The Arabidopsis receptor kinase FLS2 binds flg22 and determines the specificity of flagellin perception*. Plant Cell, 2006. 18(2): p. 465-76.
13. Robatzek, S., D. Chinchilla, and T. Boller, *Ligand-induced endocytosis of the pattern recognition receptor FLS2 in Arabidopsis*. Genes Dev, 2006. 20(5): p. 537-42.
14. Sun, W., et al., *Within-species flagellin polymorphism in Xanthomonas campestris pv campestris and its impact on elicitation of Arabidopsis FLAGELLIN SENSING2-dependent defenses*. Plant Cell, 2006. 18(3): p. 764-79.
15. Felix, G. and T. Boller, *Molecular sensing of bacteria in plants. The highly conserved RNA-binding motif RNP-1 of bacterial cold shock proteins is recognized as an elicitor signal in tobacco*. J Biol Chem, 2003. 278(8): p. 6201-8.
16. Kunze, G., et al., *The N terminus of bacterial elongation factor Tu elicits innate immunity in Arabidopsis plants*. Plant Cell, 2004. 16(12): p. 3496-507.
17. Zipfel, C., et al., *Perception of the bacterial PAMP EF-Tu by the receptor EFR restricts Agrobacterium-mediated transformation*. Cell, 2006. 125(4): p. 749-60.

18. Shiu, S.H. and A.B. Bleeker, *Expansion of the receptor-like kinase/Pelle gene family and receptor-like proteins in Arabidopsis*. Plant Physiol, 2003. 132(2): p. 530-43.
19. Dardick, C. and P. Ronald, *Plant and animal pathogen recognition receptors signal through non-RD kinases*. PLoS Pathog, 2006. 2(1): p. e2.
20. Fritz-Laylin, L.K., et al., *Phylogenomic analysis of the receptor-like proteins of rice and Arabidopsis*. Plant Physiol, 2005. 138(2): p. 611-23.
21. Jakobek, J.L., J.A. Smith, and P.B. Lindgren, *Suppression of Bean Defense Responses by Pseudomonas syringae*. Plant Cell, 1993. 5(1): p. 57-63.
22. Thilmony, R., W. Underwood, and S.Y. He, *Genome-wide transcriptional analysis of the Arabidopsis thaliana interaction with the plant pathogen Pseudomonas syringae pv. tomato DC3000 and the human pathogen Escherichia coli O157:H7*. Plant J, 2006. 46(1): p. 34-53.
23. Tao, Y., et al., *Quantitative nature of Arabidopsis responses during compatible and incompatible interactions with the bacterial pathogen Pseudomonas syringae*. Plant Cell, 2003. 15(2): p. 317-30.
24. Truman, W., M.T. de Zabala, and M. Grant, *Type III effectors orchestrate a complex interplay between transcriptional networks to modify basal defence responses during pathogenesis and resistance*. Plant J, 2006. 46(1): p. 14-33.
25. Grant, S.R., et al., *Subterfuge and manipulation: type III effector proteins of phytopathogenic bacteria*. Annu Rev Microbiol, 2006. 60: p. 425-49.
26. Abramovitch, R.B., J.C. Anderson, and G.B. Martin, *Bacterial elicitation and evasion of plant innate immunity*. Nat Rev Mol Cell Biol, 2006. 7(8): p. 601-11.
27. Mudgett, M.B., *New insights to the function of phytopathogenic bacterial type III effectors in plants*. Annu Rev Plant Biol, 2005. 56: p. 509-31.
28. Nomura, K., M. Melotto, and S.Y. He, *Suppression of host defense in compatible plant-Pseudomonas syringae interactions*. Curr Opin Plant Biol, 2005. 8(4): p. 361-8.
29. White, F.F. and B. Yang, *Host and pathogen factors controlling the rice-Xanthomonas oryzae interaction*. Plant Physiol, 2009. 150(4): p. 1677-86.
30. He, P., et al., *Specific bacterial suppressors of MAMP signaling upstream of MAPKKK in Arabidopsis innate immunity*. Cell, 2006. 125(3): p. 563-75.
31. Abramovitch, R.B., et al., *Pseudomonas type III effector AvrPtoB induces plant disease susceptibility by inhibition of host programmed cell death*. EMBO J, 2003. 22(1): p. 60-9.
32. de Torres, M., et al., *Pseudomonas syringae effector AvrPtoB suppresses basal defence in Arabidopsis*. Plant J, 2006. 47(3): p. 368-82.
33. Janjusevic, R., et al., *A bacterial inhibitor of host programmed cell death defenses is an E3 ubiquitin ligase*. Science, 2006. 311(5758): p. 222-6.
34. DebRoy, S., et al., *A family of conserved bacterial effectors inhibits salicylic acid-mediated basal immunity and promotes disease necrosis in plants*. Proc Natl Acad Sci U S A, 2004. 101(26): p. 9927-32.
35. Mukherjee, S., et al., *Yersinia YopJ acetylates and inhibits kinase activation by blocking phosphorylation*. Science, 2006. 312(5777): p. 1211-4.
36. Castaneda, A., et al., *Mutagenesis of all eight avr genes in Xanthomonas campestris pv.*

- campestris* had no detected effect on pathogenicity, but one *avr* gene affected race specificity. *Mol Plant Microbe Interact*, 2005. 18(12): p. 1306-17.
37. Kearney, B. and B.J. Staskawicz, *Widespread distribution and fitness contribution of Xanthomonas campestris avirulence gene avrBs2*. *Nature*, 1990. 346(6282): p. 385-6.
 38. Gassmann, W., et al., *Molecular evolution of virulence in natural field strains of Xanthomonas campestris pv. vesicatoria*. *J Bacteriol*, 2000. 182(24): p. 7053-9.
 39. Wichmann, G. and J. Bergelson, *Effector genes of Xanthomonas axonopodis pv. vesicatoria promote transmission and enhance other fitness traits in the field*. *Genetics*, 2004. 166(2): p. 693-706.
 40. Yang, B. and F.F. White, *Diverse members of the AvrBs3/PthA family of type III effectors are major virulence determinants in bacterial blight disease of rice*. *Mol Plant Microbe Interact*, 2004. 17(11): p. 1192-200.
 41. Yang, B., A. Sugio, and F.F. White, *Os8N3 is a host disease-susceptibility gene for bacterial blight of rice*. *Proc Natl Acad Sci U S A*, 2006. 103(27): p. 10503-10508.
 42. Whisson, S.C., et al., *Phytophthora sojae avirulence genes Avr4 and Avr6 are located in a 24kb, recombination-rich region of genomic DNA*. *Fungal Genet Biol*, 2004. 41(1): p. 62-74.
 43. Marois, E., G. Van den Ackerveken, and U. Bonas, *The xanthomonas type III effector protein AvrBs3 modulates plant gene expression and induces cell hypertrophy in the susceptible host*. *Mol Plant Microbe Interact*, 2002. 15(7): p. 637-46.
 44. Roden, J.A., et al., *A genetic screen to isolate type III effectors translocated into pepper cells during Xanthomonas infection*. *Proc Natl Acad Sci U S A*, 2004. 101(47): p. 16624-9.
 45. Kim, J.G., et al., *XopD SUMO protease affects host transcription, promotes pathogen growth, and delays symptom development in xanthomonas-infected tomato leaves*. *Plant Cell*, 2008. 20(7): p. 1915-29.
 46. Kim, J.G., et al., *Xanthomonas T3E XopN Suppresses PAMP-Triggered Immunity and Interacts with a Tomato Atypical Receptor-Like Kinase and TFT1*. *Plant Cell*, 2009. 21(4): p. 1305-23.
 47. Lee, K.S., et al., *Inheritance of resistance to bacterial blight in 21 cultivars of rice*. *Phytopathology*, 2003. 93(2): p. 147-52.
 48. Morales, C.Q., et al., *Functional analysis of the early chlorosis factor gene*. *Mol Plant Microbe Interact*, 2005. 18(5): p. 477-86.
 49. Jiang, B.L., et al., *The type III secretion effector XopXccN of Xanthomonas campestris pv. campestris is required for full virulence*. *Res Microbiol*, 2008. 159(3): p. 216-20.
 50. Roden, J., et al., *Characterization of the Xanthomonas AvrXv4 effector, a SUMO protease translocated into plant cells*. *Mol Plant Microbe Interact*, 2004. 17(6): p. 633-43.
 51. Metz, M., et al., *The conserved Xanthomonas campestris pv. vesicatoria effector protein XopX is a virulence factor and suppresses host defense in Nicotiana benthamiana*. *Plant J*, 2005. 41(6): p. 801-14.
 52. Kim, J.G., et al., *Characterization of the Xanthomonas axonopodis pv. glycines Hrp pathogenicity island*. *J Bacteriol*, 2003. 185(10): p. 3155-66.
 53. Wang, L., X. Tang, and C. He, *The bifunctional effector AvrXccC of Xanthomonas*

campestris pv. *campestris* requires plasma membrane-anchoring for host recognition. Mol Plant Pathol, 2007. 8(4): p. 491-501.

54. Zhu, W., et al., *The C terminus of AvrXa10 can be replaced by the transcriptional activation domain of VP16 from the herpes simplex virus*. Plant Cell, 1999. 11(9): p. 1665-74.

55. Yang, Y. and D.W. Gabriel, *Xanthomonas avirulence/pathogenicity gene family encodes functional plant nuclear targeting signals*. Mol Plant Microbe Interact, 1995. 8(4): p. 627-31.

56. Yang, B., et al., *The virulence factor AvrXa7 of Xanthomonas oryzae pv. oryzae is a type III secretion pathway-dependent nuclear-localized double-stranded DNA-binding protein*. Proc Natl Acad Sci U S A, 2000. 97(17): p. 9807-12.

57. Van den Ackerveken, G., E. Marois, and U. Bonas, *Recognition of the bacterial avirulence protein AvrBs3 occurs inside the host plant cell*. Cell, 1996. 87(7): p. 1307-16.

58. Szurek, B., et al., *Eukaryotic features of the Xanthomonas type III effector AvrBs3: protein domains involved in transcriptional activation and the interaction with nuclear import receptors from pepper*. Plant J, 2001. 26(5): p. 523-34.

59. Kay, S., et al., *A bacterial effector acts as a plant transcription factor and induces a cell size regulator*. Science, 2007. 318(5850): p. 648-51.

60. Romer, P., et al., *Recognition of AvrBs3-like proteins is mediated by specific binding to promoters of matching pepper Bs3 alleles*. Plant Physiol, 2009. 150(4): p. 1697-712.

61. Sugio, A., et al., *Two type III effector genes of Xanthomonas oryzae pv. oryzae control the induction of the host genes OsTFIIAgamma1 and OsTFXI during bacterial blight of rice*. Proc Natl Acad Sci U S A, 2007. 104(25): p. 10720-5.

62. Hotson, A., et al., *Xanthomonas type III effector XopD targets SUMO-conjugated proteins in planta*. Mol Microbiol, 2003. 50(2): p. 377-89.

63. Chosed, R., et al., *Structural analysis of Xanthomonas XopD provides insights into substrate specificity of ubiquitin-like protein proteases*. J Biol Chem, 2007. 282(9): p. 6773-82.

64. Ulrich, H.D., *Preface. Ubiquitin, SUMO and the maintenance of genome stability*. DNA Repair (Amst), 2009. 8(4): p. 429.

65. Ulrich, H.D., *SUMO Protocols. Preface*. Methods Mol Biol, 2009. 497: p. v-vi.

66. Ulrich, H.D., *The SUMO system: an overview*. Methods Mol Biol, 2009. 497: p. 3-16.

67. Whalen, M., et al., *Identification of a host 14-3-3 Protein that Interacts with Xanthomonas effector AvrRxv*. Physiol Mol Plant Pathol, 2008. 72(1-3): p. 46-55.

68. Mukherjee, S., Y.H. Hao, and K. Orth, *A newly discovered post-translational modification—the acetylation of serine and threonine residues*. Trends Biochem Sci, 2007. 32(5): p. 210-6.

69. Bartetzko, V., et al., *The Xanthomonas campestris pv. vesicatoria type III effector protein XopJ inhibits protein secretion: evidence for interference with cell wall-associated defense responses*. Mol Plant Microbe Interact, 2009. 22(6): p. 655-64.

70. Thieme, F., et al., *New type III effectors from Xanthomonas campestris pv. vesicatoria trigger plant reactions dependent on a conserved N-myristoylation motif*. Mol Plant Microbe Interact, 2007. 20(10): p. 1250-61.

71. Orth, K., et al., *Disruption of signaling by Yersinia effector YopJ, a ubiquitin-like protein*

- protease. *Science*, 2000. 290(5496): p. 1594-7.
72. Whalen, M.C., et al., *Avirulence gene avrRxv from Xanthomonas campestris pv. vesicatoria specifies resistance on tomato line Hawaii 7998*. *Mol Plant Microbe Interact*, 1993. 6(5): p. 616-27.
73. Taylor, K.W., et al., *Tomato TFT1 is required for PAMP-triggered immunity and mutations that prevent T3E XopN from binding to TFT1 attenuate Xanthomonas virulence*. *PLoS Pathog*, 2012. 8(6): p. e1002768.
74. Cheong, H., et al., *Xanthomonas oryzae pv. oryzae type III effector XopN targets OsVOZ2 and a putative thiamine synthase as a virulence factor in rice*. *PLoS One*, 2013. 8(9): p. e73346.
75. Sinha, D., et al., *Cell wall degrading enzyme induced rice innate immune responses are suppressed by the type 3 secretion system effectors XopN, XopQ, XopX and XopZ of Xanthomonas oryzae pv. oryzae*. *PLoS One*, 2013. 8(9): p. e75867.
76. Castells, E. and J.M. Casacuberta, *Signalling through kinase-defective domains: the prevalence of atypical receptor-like kinases in plants*. *J Exp Bot*, 2007. 58(13): p. 3503-11.
77. Kinch, L.N., et al., *Fido, a novel AMPylation domain common to fic, doc, and AvrB*. *PLoS One*, 2009. 4(6): p. e5818.
78. Yarbrough, M.L. and K. Orth, *AMPylation is a new post-translational modification*. *Nat Chem Biol*, 2009. 5(6): p. 378-9.
79. Yarbrough, M.L., et al., *AMPylation of Rho GTPases by Vibrio VopS disrupts effector binding and downstream signaling*. *Science*, 2009. 323(5911): p. 269-72.
80. Xu, R.Q., et al., *AvrAC(Xcc8004), a type III effector with a leucine-rich repeat domain from Xanthomonas campestris pathovar campestris confers avirulence in vascular tissues of Arabidopsis thaliana ecotype Col-0*. *J Bacteriol*, 2008. 190(1): p. 343-55.
81. Lyon, J.A., *Entrez Gene: A Gene-Centered "Information Hub"*. *Journal of Electronic Resources in Medical Libraries*, 2007. 4(3): p. 53-78.
82. Keen, N.T., *Gene-for-gene complementarity in plant-pathogen interactions*. *Annu Rev Genet*, 1990. 24: p. 447-63.
83. Gabriel, D.W., A. Burges, and G.R. Lazo, *Gene-for-gene interactions of five cloned avirulence genes from Xanthomonas campestris pv. malvacearum with specific resistance genes in cotton*. *Proc Natl Acad Sci U S A*, 1986. 83(17): p. 6415-9.
84. Deslandes, L., et al., *Physical interaction between RRS1-R, a protein conferring resistance to bacterial wilt, and PopP2, a type III effector targeted to the plant nucleus*. *Proc Natl Acad Sci U S A*, 2003. 100(13): p. 8024-9.
85. Dodds, P.N., et al., *Direct protein interaction underlies gene-for-gene specificity and coevolution of the flax resistance genes and flax rust avirulence genes*. *Proc Natl Acad Sci U S A*, 2006. 103(23): p. 8888-93.
86. Jia, Y., et al., *Direct interaction of resistance gene and avirulence gene products confers rice blast resistance*. *EMBO J*, 2000. 19(15): p. 4004-14.
87. Kanzaki, H., et al., *Arms race co-evolution of Magnaporthe oryzae AVR-Pik and rice Pik genes driven by their physical interactions*. *Plant J*, 2012. 72(6): p. 894-907.
88. Ravensdale, M., et al., *Intramolecular interaction influences binding of the Flax L5 and*

- L6 resistance proteins to their AvrL567 ligands.* PLoS Pathog, 2012. 8(11): p. e1003004.
89. Krasileva, K.V., D. Dahlbeck, and B.J. Staskawicz, *Activation of an Arabidopsis resistance protein is specified by the in planta association of its leucine-rich repeat domain with the cognate oomycete effector.* Plant Cell, 2010. 22(7): p. 2444-58.
90. Schultink, A., et al., *Roq1 mediates recognition of the Xanthomonas and Pseudomonas effector proteins XopQ and HopQ1.* Plant J, 2017. 92(5): p. 787-795.
91. Van der Biezen, E.A. and J.D. Jones, *Plant disease-resistance proteins and the gene-for-gene concept.* Trends Biochem Sci, 1998. 23(12): p. 454-6.
92. Axtell, M.J. and B.J. Staskawicz, *Initiation of RPS2-specified disease resistance in Arabidopsis is coupled to the AvrRpt2-directed elimination of RIN4.* Cell, 2003. 112(3): p. 369-77.
93. Kim, M.G., et al., *Two Pseudomonas syringae type III effectors inhibit RIN4-regulated basal defense in Arabidopsis.* Cell, 2005. 121(5): p. 749-59.
94. Mackey, D., et al., *Arabidopsis RIN4 is a target of the type III virulence effector AvrRpt2 and modulates RPS2-mediated resistance.* Cell, 2003. 112(3): p. 379-89.
95. Li, M., et al., *Proline isomerization of the immune receptor-interacting protein RIN4 by a cyclophilin inhibits effector-triggered immunity in Arabidopsis.* Cell Host Microbe, 2014. 16(4): p. 473-83.
96. Chung, E.H., et al., *A plant phosphoswitch platform repeatedly targeted by type III effector proteins regulates the output of both tiers of plant immune receptors.* Cell Host Microbe, 2014. 16(4): p. 484-94.
97. Liu, J., et al., *RIN4 functions with plasma membrane H⁺-ATPases to regulate stomatal apertures during pathogen attack.* PLoS Biol, 2009. 7(6): p. e1000139.
98. Luo, Y., et al., *Proteolysis of a negative regulator of innate immunity is dependent on resistance genes in tomato and Nicotiana benthamiana and induced by multiple bacterial effectors.* Plant Cell, 2009. 21(8): p. 2458-72.
99. Wilton, M., et al., *The type III effector HopF2Pto targets Arabidopsis RIN4 protein to promote Pseudomonas syringae virulence.* Proc Natl Acad Sci U S A, 2010. 107(5): p. 2349-54.
100. van der Hoorn, R.A. and S. Kamoun, *From Guard to Decoy: a new model for perception of plant pathogen effectors.* Plant Cell, 2008. 20(8): p. 2009-17.
101. Collier, S.M. and P. Moffett, *NB-LRRs work a "bait and switch" on pathogens.* Trends Plant Sci, 2009. 14(10): p. 521-9.
102. Xing, W., et al., *The structural basis for activation of plant immunity by bacterial effector protein AvrPto.* Nature, 2007. 449(7159): p. 243-7.
103. Ntoukakis, V., et al., *The changing of the guard: the Pto/Prf receptor complex of tomato and pathogen recognition.* Curr Opin Plant Biol, 2014. 20: p. 69-74.
104. Shan, L., et al., *Bacterial effectors target the common signaling partner BAK1 to disrupt multiple MAMP receptor-signaling complexes and impede plant immunity.* Cell Host Microbe, 2008. 4(1): p. 17-27.
105. Xiang, T., et al., *Pseudomonas syringae effector AvrPto blocks innate immunity by*

- targeting receptor kinases. *Curr Biol*, 2008. 18(1): p. 74-80.
106. Zhang, J., et al., *Receptor-like cytoplasmic kinases integrate signaling from multiple plant immune receptors and are targeted by a Pseudomonas syringae effector*. *Cell Host Microbe*, 2010. 7(4): p. 290-301.
107. Li, L., et al., *The FLS2-associated kinase BIK1 directly phosphorylates the NADPH oxidase RbohD to control plant immunity*. *Cell Host Microbe*, 2014. 15(3): p. 329-38.
108. Kadota, Y., et al., *Direct regulation of the NADPH oxidase RBOHD by the PRR-associated kinase BIK1 during plant immunity*. *Mol Cell*, 2014. 54(1): p. 43-55.
109. Ade, J., et al., *Indirect activation of a plant nucleotide binding site-leucine-rich repeat protein by a bacterial protease*. *Proc Natl Acad Sci U S A*, 2007. 104(7): p. 2531-6.
110. Schornack, S., et al., *Engineering plant disease resistance based on TAL effectors*. *Annu Rev Phytopathol*, 2013. 51: p. 383-406.
111. Boch, J. and U. Bonas, *Xanthomonas AvrBs3 family-type III effectors: discovery and function*. *Annu Rev Phytopathol*, 2010. 48: p. 419-36.
112. Deng, D., et al., *Structural basis for sequence-specific recognition of DNA by TAL effectors*. *Science*, 2012. 335(6069): p. 720-3.
113. Mak, A.N., et al., *The crystal structure of TAL effector PthXo1 bound to its DNA target*. *Science*, 2012. 335(6069): p. 716-9.
114. Gu, K., et al., *R gene expression induced by a type-III effector triggers disease resistance in rice*. *Nature*, 2005. 435(7045): p. 1122-5.
115. Strauss, T., et al., *RNA-seq pinpoints a Xanthomonas TAL-effector activated resistance gene in a large-crop genome*. *Proc Natl Acad Sci U S A*, 2012. 109(47): p. 19480-5.
116. Romer, P., et al., *Plant pathogen recognition mediated by promoter activation of the pepper Bs3 resistance gene*. *Science*, 2007. 318(5850): p. 645-8.
117. Schornack, S., et al., *The tomato resistance protein Bs4 is a predicted non-nuclear TIR-NB-LRR protein that mediates defense responses to severely truncated derivatives of AvrBs4 and overexpressed AvrBs3*. *Plant J*, 2004. 37(1): p. 46-60.
118. Tian, D., et al., *The rice TAL effector-dependent resistance protein XA10 triggers cell death and calcium depletion in the endoplasmic reticulum*. *Plant Cell*, 2014. 26(1): p. 497-515.
119. Wu, L., et al., *XA27 depends on an amino-terminal signal-anchor-like sequence to localize to the apoplast for resistance to Xanthomonas oryzae pv oryzae*. *Plant Physiol*, 2008. 148(3): p. 1497-509.
120. Knepper, C., E.A. Savory, and B. Day, *The role of NDR1 in pathogen perception and plant defense signaling*. *Plant Signal Behav*, 2011. 6(8): p. 1114-6.
121. Day, B., D. Dahlbeck, and B.J. Staskawicz, *NDR1 interaction with RIN4 mediates the differential activation of multiple disease resistance pathways in Arabidopsis*. *Plant Cell*, 2006. 18(10): p. 2782-91.
122. Wiermer, M., B.J. Feys, and J.E. Parker, *Plant immunity: the EDS1 regulatory node*. *Curr Opin Plant Biol*, 2005. 8(4): p. 383-9.
123. Wirthmueller, L., et al., *Nuclear accumulation of the Arabidopsis immune receptor RPS4 is necessary for triggering EDS1-dependent defense*. *Curr Biol*, 2007. 17(23): p. 2023-

9.

124. Garcia, A.V., et al., *Balanced nuclear and cytoplasmic activities of EDS1 are required for a complete plant innate immune response*. PLoS Pathog, 2010. 6: p. e1000970.
125. Venugopal, S.C., et al., *Enhanced disease susceptibility 1 and salicylic acid act redundantly to regulate resistance gene-mediated signaling*. PLoS Genet, 2009. 5(7): p. e1000545.
126. Selote, D. and A. Kachroo, *RIN4-like proteins mediate resistance protein-derived soybean defense against Pseudomonas syringae*. Plant Signal Behav, 2010. 5(11): p. 1453-6.
127. Selote, D. and A. Kachroo, *RPG1-B-derived resistance to AvrB-expressing Pseudomonas syringae requires RIN4-like proteins in soybean*. Plant Physiol, 2010. 153(3): p. 1199-211.
128. Selote, D., et al., *Soybean NDR1-like proteins bind pathogen effectors and regulate resistance signaling*. New Phytol, 2014. 202(2): p. 485-98.
129. Feys, B.J., et al., *Arabidopsis SENESCENCE-ASSOCIATED GENE101 stabilizes and signals within an ENHANCED DISEASE SUSCEPTIBILITY1 complex in plant innate immunity*. Plant Cell, 2005. 17(9): p. 2601-13.
130. Rietz, S., et al., *Different roles of Enhanced Disease Susceptibility1 (EDS1) bound to and dissociated from Phytoalexin Deficient4 (PAD4) in Arabidopsis immunity*. New Phytol, 2011. 191(1): p. 107-19.
131. Wagner, S., et al., *Structural basis for signaling by exclusive EDS1 heteromeric complexes with SAG101 or PAD4 in plant innate immunity*. Cell Host Microbe, 2013. 14(6): p. 619-30.
132. Janssen, B.J. and K.C. Snowden, *Strigolactone and karrikin signal perception: receptors, enzymes, or both?* Front Plant Sci, 2012. 3: p. 296.
133. Heidrich, K., et al., *Arabidopsis EDS1 connects pathogen effector recognition to cell compartment-specific immune responses*. Science, 2011. 334(6061): p. 1401-4.
134. Kim, T.H., et al., *Natural variation in small molecule-induced TIR-NB-LRR signaling induces root growth arrest via EDS1- and PAD4-complexed R protein VICTR in Arabidopsis*. Plant Cell, 2012. 24(12): p. 5177-92.
135. Bhattacharjee, S., et al., *Pathogen effectors target Arabidopsis EDS1 and alter its interactions with immune regulators*. Science, 2011. 334(6061): p. 1405-8.
136. Boller, T. and S.Y. He, *Innate immunity in plants: an arms race between pattern recognition receptors in plants and effectors in microbial pathogens*. Science, 2009. 324(5928): p. 742-4.
137. Chu, Z., et al., *Promoter mutations of an essential gene for pollen development result in disease resistance in rice*. Genes Dev, 2006. 20(10): p. 1250-5.
138. Jiang, G.H., et al., *Testifying the rice bacterial blight resistance gene xa5 by genetic complementation and further analyzing xa5 (Xa5) in comparison with its homolog TFIIAgamma1*. Mol Genet Genomics, 2006. 275(4): p. 354-66.
139. Iyer, A.S. and S.R. McCouch, *The rice bacterial blight resistance gene xa5 encodes a novel form of disease resistance*. Mol Plant Microbe Interact, 2004. 17(12): p. 1348-54.

140. Wei, C.F., et al., *A Pseudomonas syringae pv. tomato DC3000 mutant lacking the type III effector HopQ1-1 is able to cause disease in the model plant Nicotiana benthamiana*. Plant J, 2007. 51(1): p. 32-46.
141. Schwartz, A.R., et al., *Phylogenomics of Xanthomonas field strains infecting pepper and tomato reveals diversity in effector repertoires and identifies determinants of host specificity*. Front Microbiol, 2015. 6: p. 535.
142. Adlung, N., et al., *Non-host Resistance Induced by the Xanthomonas Effector XopQ Is Widespread within the Genus Nicotiana and Functionally Depends on EDS1*. Front Plant Sci, 2016. 7: p. 1796.
143. Adlung, N. and U. Bonas, *Dissecting virulence function from recognition: cell death suppression in Nicotiana benthamiana by XopQ/HopQ1-family effectors relies on EDS1-dependent immunity*. Plant J, 2017. 91(3): p. 430-442.
144. Qi, T., et al., *NRG1 functions downstream of EDS1 to regulate TIR-NLR-mediated plant immunity in Nicotiana benthamiana*. Proc Natl Acad Sci U S A, 2018. 115(46): p. E10979-E10987.
145. Teper, D., et al., *Xanthomonas euvesicatoria type III effector XopQ interacts with tomato and pepper 14-3-3 isoforms to suppress effector-triggered immunity*. Plant J, 2014. 77(2): p. 297-309.
146. Li, W., Y.H. Chiang, and G. Coaker, *The HopQ1 effector's nucleoside hydrolase-like domain is required for bacterial virulence in arabidopsis and tomato, but not host recognition in tobacco*. PLoS One, 2013. 8(3): p. e59684.
147. Gupta, M.K., et al., *Mutations in the Predicted Active Site of Xanthomonas oryzae pv. oryzae XopQ Differentially Affect Virulence, Suppression of Host Innate Immunity, and Induction of the HR in a Nonhost Plant*. Mol Plant Microbe Interact, 2015. 28(2): p. 195-206.
148. Giska, F., et al., *Phosphorylation of HopQ1, a type III effector from Pseudomonas syringae, creates a binding site for host 14-3-3 proteins*. Plant Physiol, 2013. 161(4): p. 2049-61.
149. Yu, S., I. Hwang, and S. Rhee, *Crystal structure of the effector protein XOO4466 from Xanthomonas oryzae*. J Struct Biol, 2013. 184(2): p. 361-6.
150. Yu, S., I. Hwang, and S. Rhee, *The crystal structure of type III effector protein XopQ from Xanthomonas oryzae complexed with adenosine diphosphate ribose*. Proteins, 2014. 82(11): p. 2910-4.
151. Stork, W., J.G. Kim, and M.B. Mudgett, *Functional Analysis of Plant Defense Suppression and Activation by the Xanthomonas Core Type III Effector XopX*. Mol Plant Microbe Interact, 2015. 28(2): p. 180-94.
152. Teper, D., et al., *Five Xanthomonas type III effectors suppress cell death induced by components of immunity-associated MAP kinase cascades*. Plant Signal Behav, 2015. 10(10): p. e1064573.
153. Salomon, D., et al., *Expression of Xanthomonas campestris pv. vesicatoria type III effectors in yeast affects cell growth and viability*. Mol Plant Microbe Interact, 2011. 24(3): p. 305-14.

154. Lee, S.W. and P.C. Ronald, *Marker-exchange mutagenesis and complementation strategies for the Gram-negative bacteria Xanthomonas oryzae pv. oryzae*. *Methods Mol Biol*, 2007. 354: p. 11-8.
155. Melotto, M., et al., *Plant stomata function in innate immunity against bacterial invasion*. *Cell*, 2006. 126(5): p. 969-80.
156. Katagiri, F., R. Thilmony, and S.Y. He, *The Arabidopsis thaliana-pseudomonas syringae interaction*. *Arabidopsis Book*, 2002. 1: p. e0039.
157. Gookin, T.E. and S.M. Assmann, *Significant reduction of BiFC non-specific assembly facilitates in planta assessment of heterotrimeric G-protein interactors*. *Plant J*, 2014. 80(3): p. 553-67.
158. Rigoulot, S.B., et al., *Populus trichocarpa clade A PP2C protein phosphatases: their stress-induced expression patterns, interactions in core abscisic acid signaling, and potential for regulation of growth and development*. *Plant Mol Biol*, 2019. 100(3): p. 303-317.
159. Lang, Y., Z. Li, and H. Li, *Analysis of Protein-Protein Interactions by Split Luciferase Complementation Assay*. *Curr Protoc Toxicol*, 2019. 82(1): p. e90.
160. Kato, N. and J. Jones, *The split luciferase complementation assay*. *Methods Mol Biol*, 2010. 655: p. 359-76.

Chapter 2 *Xanthomonas euvesicatoria* type III effector XopQ interacts with another effector, XopX, to elicit the defense response in *Nicotiana benthamiana*

Summary

Xanthomonas euvesicatoria (*Xe*), a gram-negative bacterium, can infect pepper and tomato plants and causes bacterial leaf spot disease. In contrast, *Xe* is unable to infect the nonhost plant *Nicotiana benthamiana* (*N. benthamiana*; a relative of the tobacco plant). The nonhost resistance in *N. benthamiana* is conditioned by a disease resistant gene *NbRoq1* that recognizes a type III effector *Xe-XopQ* expressed by *Xe*. However, the *Agrobacterium*-mediated transient expression of *Xe-XopQ* alone in *N. benthamiana* failed to trigger programmed cell death (PCD). It was speculated that an unknown T3E is required for enhancing the PCD triggered by *Xe-XopQ/Roq1*. In this study, we identified that *Xe-XopX* is the T3E, which is required for triggering the strong PCD response from *Xe-XopQ/NbRoq1* in *N. benthamiana*. We confirmed that *Xe-XopQ* physically interacts with *Xe-XopX* *in vivo* by using bimolecular fluorescence complementation (BiFc), co-immunoprecipitation (co-IP), and split luciferase assays. Interestingly, we also discovered that the core domain of *Xe-XopX* interacts with multiple T3Es, including AvrBS2, AvrPphD1, Xe1298, XopB, XopN, *Xe-AvrRxo1*, and XopJ1 in plant cells. The deletion of *Xe-XopX* in *Xe* compromised the *NbRoq1/Xe-XopQ*-mediated disease resistance in *N. benthamiana* and the Bs2/AvrBs2-mediated disease resistance in pepper. Compared to the wild type *Xe* strain, the *XeΔXopX* mutant strain has a reduced growth ability on pepper plants lacking *BS2* and on *N. benthamiana* lacking *EDS1*. Therefore, we speculate that *Xe-XopX* confers avirulence function by helping the translocation of other type T3Es including *Xe-XopQ* and AvrBs2.

Introduction

Xanthomonas euvesicatoria (*Xe*) causes bacterial spot disease on cultivated pepper (*Capsicum annuum*) and tomato (*Solanum lycopersicum*) and are the most devastating to crops grown in warm, humid climates such as in southeastern Asia and the southeastern/midwestern United States [1]. As a model plant also in the *Solanaceae* family and genetically closely related to tomato and pepper, *N. benthamiana* could be a useful tool for research on the mechanisms underlying the interactions between *Xanthomonas* pathovars and hosts [2, 3]. However, *N. benthamiana* is not a natural host of *Xe*. Recently, a large-scale screening of 21 different *Xe* type three secretion (T3S) effectors among 86 *Solanaceae* lines revealed that XopQ is the key effector determining the host range for many *Nicotiana* species [4, 5]. Specifically, wild-type *Xe* induces a strong hypersensitive response (HR), while the deletion mutant *Xe*Δ*XopQ* grows to a high titer and produces the appearance of water soaking and disease lesions in *N. benthamiana* [4]. This new finding confers that it is feasible to take advantage of the abundant genetic resources and efficient transformation system of *N. benthamiana* for studying the biological and biochemical functions of type III effectors (T3Es) upon the infection of *Xe* to *N. benthamiana*.

Research indicates that *NbEDS1* is necessary for nonhost resistance against *Xe* and XopQ in *N. benthamiana*; this reported correlation implies that a Toll-like interleukin-1 receptor (TIR) domain-containing resistant (R) protein must present in many *Nicotiana* lines to specifically recognize XopQ [5, 6]. More recently, a resistant gene, *Recognition of XopQ* 1 (*Roq1*), has been identified from *N. benthamiana* using a reverse genetic screening approach [7]. Similar to many other typical disease-resistant proteins, *Roq1* has a nucleotide-binding leucine-rich repeat (NLR) domain, while the TIR domain determines its dependence on EDS1-mediated signal pathways in a plant's immunity response. *Roq1* and its orthologs mediate the recognition of XopQ alleles from various *Xanthomonas* species, as well as HopQ1 from *Pseudomonas* pathovars in the *Nicotiana* genus [8]. Another gene, *N. benthamiana* N requirement gene 1 (*NRG1*), is reported to mediate XopQ-triggered immunity through associating various EDS1 signaling events, such as (a) XopQ elicited HR by the recognition of *Roq1* and (b) XopQ-

induced transcriptional changes in *N. benthamiana* [9]. Thus, in the classic gene-for-gene model, a new member consisting of *Xe-XopQ*, *NbRoq1*, *NbNRG1*, and *NbEDS1* is characterized and might serve as a candidate that may dramatically improve disease resistance among crops, since *XopQ* has conserved homologues in diverse bacterial pathogens including pathovars of *Xanthomonas*, *Pseudomonas*, and *Acidovorax* [8].

However, the *Agrobacterium*-mediated transient expression of *Xe-XopQ* alone in *N. benthamiana* failed to trigger programmed cell death (PCD). It was speculated that an unknown component or mechanism is required for inducing PCD triggered by *Xe-XopQ/Roq1*. Intriguingly, *Xanthomonas campestris* pv. *campestris* (*Xcc*), the causal agent for black rot and the most important disease affecting Brassica vegetable crops worldwide, can cause neither a strong immunity response like HR nor disease symptoms in *N. benthamiana* with the presence of its own *Xcc-XopQ*. Another T3E, *XopX*, identified in *Xe* can condition *Xcc* strain 8004 to have the ability to cause HR in *N. benthamiana* [10]. Unexpectedly, the characterization of *XopX* reveals that there is no *XopX* activation involved in nonhost resistance [10, 11]. Thus, we hypothesize that *XopX* can interact with *XopQ* and the two T3Es together influence the immunity response in *N. benthamiana*.

In the present study, we confirmed *Xe-XopX* is required for triggering strong PCD by *Xe-XopQ/NbRoq1* in *N. benthamiana*. The physical interaction between *Xe-XopQ* and *Xe-XopX* *in vivo* is affirmed by bimolecular fluorescence complementation (BiFc), co-immunoprecipitation (co-IP), and split luciferase assay. Furthermore, we revealed that the core domain of *Xe-XopX* interacts with multiple T3Es, including *AvrBS2*, *AvrPphD1*, *Xe1298*, *XopB*, *XopN*, *Xe-AvrRxo1*, and *XopJ1* in plant cells. The deletion of *Xe-XopX* in *Xe* compromised the *NbRoq1/Xe-XopQ*-mediated disease resistance in *N. benthamiana* as well as the *Bs2/AvrBs2*-mediated disease resistance in pepper. By contrast, compared to the wild type *Xe* strain, the *Xe ΔXopX* mutant strain has reduced growth ability on pepper plants lacking *Bs2* and *N. benthamiana* lacking *EDS1*. Therefore, in considering these various findings, we speculate that *XopX* may contribute to bacterial virulence via helping the translocation of other

type T3Es, which facilitates an enhanced immunity response in *N. benthamiana* and pepper infected by a high titer inoculation of *Xe*.

Results

Deletion of XopQ and its homologues in diverse bacterial pathogens impart their ability to infect N. benthamiana

Bacterial spot disease (BS) caused by *Xe* is one of the most important bacterial diseases that threatens pepper production. However, pepper tends to be recalcitrant for tissue culture and transformation, which hinders the characterization of molecular interaction between *Xe* and pepper plants. The model plant *N. benthamiana* is genetically related to pepper, and they both belong to the *Solanaceae* family. One of the most significant advantages of analyzing *N. benthamiana* instead of pepper is that *N. benthamiana* can be easily transformed. However, *N. benthamiana* is not a natural host of *Xe*. In order to take advantage of the abundant genetic resources in *N. benthamiana* that enables the study of the biological and biochemical functions of the type III effectors (T3Es) of *Xe*, we developed a mutant *Xe* strain that is pathogenic on *N. benthamiana*. We performed marker-exchange mutagenesis to delete XopQ from *Xe*. We were successful in infecting *N. benthamiana* plants with the mutant strain *Xe* Δ *XopQ* (Figure 2-1 A and C). Furthermore, when *Xe-XopQ* homologues were eliminated from *Xcc* strain *Xcc8004*, Arabidopsis pathogen *Pseudomonas syringae* pv. *tomato* (*Pst*) *DC3000*, and the watermelon pathogen *Acidovorax citrulli* *AAC00-1*, all three bacteria phytopathogens become pathogenic in *N. benthamiana* (Figure 2-1 A and C). This outcome is consistent with previous research suggesting that XopQ plays a critical role in determining host specificity. The important function of *Xe-XopQ* and its homologues are dependent on *NbEDS1* (Figure 2-1 B). Wild-type strains of *Xe*, *Pst* *DC3000*, and *AAC00-1* all exhibited a significantly weaker response in *eds1* mutant of *N. benthamiana* compared with analogous findings for wild-type *N. benthamiana*. Consistently, the transient complementation of *NbEDS1* restored the XopQ/Roq1-mediated resistance response (Figure S2-1). Accordingly, we developed a host-microbe system

consisting of *Xe* mutant strains and *N. benthamiana* in order to investigate the virulence and avirulence mechanisms of *Xe* with respect to infection in selected plants in the *Solanaceae* plant family.

Co-expression of XopQ and XopX elicits a programmed cell death in N. benthamiana in Agrobacterium-mediated transient assay

Despite the fact that *Xe*, *Pst DC3000*, and *AAC00-1* containing *Xe*-XopQ or its homologues can cause strong cell death in *N. benthamiana*, this was not the case in *Agrobacterium*-mediated transient assays where we observed that all XopQ homologues only elicited a mild chlorotic response. Even when all the XopQ homologues were fused with the strong and constitutive CaMV35S promoter, strong cell death was not observed at 4 day post inoculation (dpi) (Figure 2-2 A). We hypothesize that XopQ alone was insufficient to trigger programmed cell death in *N. benthamiana*.

Another T3E in *Xe*, *Xe*-XopX, sparked our interest as a due to its ability to confer *Xcc*-eliciting cell death in *N. benthamiana* (conversely, *Xcc*, *per se*, does not trigger a hypersensitive response in *N. benthamiana*)[10]. We speculated that XopQ may require XopX to elicit a strong HR in *Agrobacterium*-mediated transient assays. Accordingly, we co-infiltrated XopQ and XopX to *N. benthamiana* and a very rapid hypersensitive response occurred (Figure 2-2 B). To confirm these findings, additional tests were conducted. We then inoculated *Xe*-XopX along with other XopQ homologues from *Pst DC3000*, *Xcc*, and *AAC00-1*; in response, cell death was observed in *N. benthamiana* in all cases at 3 dpi (Figure 2-2 B). This outcome demonstrates the function of XopQ as being determinant in the host range, depending on the function of XopX, which has not been previously reported.

Mutant Xe and Xcc strains with deletion of either XopQ or XopX was unable to trigger HR in N. benthamiana

As noted earlier, *N. benthamiana* exhibits strong cell death upon infection with wild-type *Xcc*

harboring *Xe-XopQ* or with the co-expression of *Xcc-XopQ* and *Xe-XopX* via-*Agrobacterium*-mediated transient assay. Therefore, we attempted to exclude the possibility that *Xe-XopX* alone would be sufficient to trigger cell death; thus, a mutant strain of *Xcc* Δ *XopQ* carrying a plasmid-borne *Xe-XopX*, was created using marker exchange and complementary approaches. The *Xcc* strain was inoculated into *N. benthamiana* and no cell death was observed (Figure 2-3 A). Taken together, we concluded that *Xcc* is capable of triggering cell death only when *Xcc-XopQ* and *Xe-XopX* are both present in the bacterial cells.

Compared with *Xcc*, *Xe* is able to trigger cell death in *N. benthamiana* when *XopQ* plays a dominant role in triggering the immune response. However, in the current study, *XopX* also appears to play a role in triggering an immune response. Accordingly, we investigated whether a single T3E, *XopQ* or *XopX* in *Xe*, would be sufficient to trigger a hypersensitive response in *N. benthamiana*. As shown in Figure 2-3 B, mutant *Xe* strains with deletions of either T3E, *XopQ* or *XopX*, were unable to trigger cell death in *N. benthamiana*. The double mutant *Xe XopQ-/XopX-* was similarly unable to trigger cell death with complementation of either *XopQ* or *XopX* (Figure 2-3 B). These results are consistent with findings from *Agrobacterium*-mediated transient assays, further substantiating that *XopQ* requires the presence of *XopX* to determine host specificity.

The virulent and avirulent functions of XopX varies with the presence or absence of XopQ

The evidence that emerged from this investigation confirms that *Xe-XopX* has an avirulent-like function, where the co-expression of *Xe-XopX* with *Xe-XopQ* or its homologs in *N. benthamiana* triggered HR-like cell death. However, previous reports suggest that *XopX* has a virulent function for bacterial pathogenesis, a finding that augments its functional complexity [10, 11]. The contradiction led us to hypothesize that *XopX* demonstrates a virulent role in the absence of *XopQ* or its homologues; whereas *XopX* is avirulent in the presence of *XopQ* or its homologues. To test this hypothesis, we developed two groups of growth curve assays with *Xe* strains inoculated in both *N. benthamiana* and pepper plants. In the first group, wild type *Xe*

has a reduced growth population-level in comparison to *Xe*Δ*XopX* in *N. benthamiana* (Figure 2-4 A). This outcome suggests that XopX has an avirulent function when paired with XopQ and a cognate *R* gene *NbRoq1* in *N. benthamiana*. As shown in Figure 2-4B, when the same pairs of strains, *Xe* and *Xe*Δ*XopX*, were inoculated on pepper plants that are without the *Roq1* gene, wild type *Xe* grew to a higher population level than that of *Xe*Δ*XopX* in pepper plants, which suggests that XopX has a virulent function. In another growth curve assay, *Xe*Δ*XopQ* grew to a higher population level than that of the *Xe*Δ*XopQ*Δ*XopX* in both tobacco and pepper (Figure 2-4 C and D), which again supports the idea that XopX has a virulent function in the absence of XopQ, even in the presence of the cognate *R* gene *NbRoq1*. These observations support our hypothesis that *Xe*-XopX plays a dual role in the host and pathogen interactions. XopQ and XopX are both conserved T3Es present in diverse bacterial phytopathogens and they also have high a high frequency of co-occurrence in different *Xanthomonas* species (Figure S2-2).

Essential residues of XopQ are required for its interaction with XopX

To understand the interaction between XopX and XopQ and their ability to induce an immune response in *N. benthamiana*, we reviewed prior findings on the biochemical and biological functioning of the two T3Es. Previous results show that XopQ has a putative nucleotide hydrolase (NH) catalytic site [12-15]. Here, we introduced mutations on the putative NH catalytic site of *Xe*-XopQ to investigate the essential amino acid residues required for its interplay with XopX to trigger the cell death phenotype in *N. benthamiana*.

In a disease assay conducted on *N. benthamiana*, *Xe*Δ*XopQ* (*pXopQ*-Y279A) was found to trigger a faster cell death than that of wild-type *Xe*; in contrast, *Xe*Δ*XopQ* (*pXopQ*-S65A), *Xe*Δ*XopQ* (*pXopQ*-D116A) and *Xe*Δ*XopQ* (*pXopQ*-DDD120_122_123AAA) induced similar symptoms as did *Xe*Δ*XopQ* (Figure 2-5 A). This outcome illustrates that the presence of D116, DDD120_122_123, and Y279 might all be required for XopQ to trigger *RopI*-mediated HR in *N. benthamiana*. Interestingly, the mutation at S65 could induce a stronger immune response,

suggesting that XopQ-S65A has improved protein stability or protein activity, which needs to be further investigated. In *Agrobacterium*-mediated transient assays, XopQ-D116A lost its ability to elicit cell death after being co-infiltrated with *Xe*-XopX in *N. benthamiana*, while other mutations including XopQ-S65A, XopQ-DDD120_122_123AAA, and XopQ-Y279A all mimicked the wild-type XopQ by triggering cell death in *N. benthamiana* (Figure 2-5 B). Thus, we conclude that D116 is the probable interaction site or catalytic site required for XopQ to fulfill its biological function.

The core domain of XopX physically interacts with multiple T3Es within plant cells

Since the co-infiltration of XopQ and XopX could trigger cell death in *N. benthamiana*, we tried to determine if the two effector proteins interact inside plant cells. To this end, we employed three methodologies including Co-immunoprecipitation (co-IP), bimolecular fluorescence complementation (BiFC), and split luciferase assays to validate the interactions between XopQ and XopX. As the full-length XopX was not expressed very well in our transient assay, we used a truncated version of XopX, designated as XopX₁₁₂₋₅₇₃ for all further assays. As shown in Figure 2-6A, B and C, XopQ indeed physically interacts with XopX₁₁₂₋₅₇₃ *in vivo*. The BiFC result also confirms that the interaction occurred in the cytosol and plasma membrane of the transformed plant cells (Figure 2-6 B). The strong XopQ-XopX interaction observed inside the plant cells prompted us to investigate whether XopX also interacts with other T3Es. Surprisingly, in our co-IP assay, XopX₁₁₂₋₅₇₃ was able to interact with AvrBS2, AvrPphD1, Xe1298, XopB, XopN, Xe4428 (a homologue of AvrRxo1) and XopJ effector proteins (Figure 2-6 A). This finding led us to speculate whether or not XopX might have a role in assisting other T3Es to fulfill their function of promoting *Xe* infection. To our knowledge, this is the first report showing that a T3E could interact with numerous other T3Es within plant cells. Additional studies, however, are needed to identify the key residue in XopX that interacts with other effectors, as well as to characterize the interaction mechanisms among those effectors.

The deletion of XopX compromises both the virulent and avirulent functions of AvrBS2

Since XopX₁₁₂₋₅₇₃ interacts with AvrBS2, the first identified virulent T3E in *Xe*, we decided to test the influence of XopX on the virulent and avirulent functions of AvrBS2. As shown in Figure 2-7 A, *Xe*Δ*XopQ*, the XopQ deletion mutant of *Xe*, grew much more efficiently than the double mutant strain *Xe*Δ*XopQ*Δ*avrBS2*. This finding is consistent with the fact that AvrBS2 plays a significant virulent role in enhancing *Xe* infection in pepper. We further investigate the virulence function of AvrBS2 in mutant *Xe* strains where both XopQ and XopX have been deleted. The *Xe* strain *Xe*Δ*XopQ*Δ*XopX* still grew to a higher population level than that of *Xe*Δ*XopQ*Δ*XopX*Δ*AvrBs2* (Figure 2-7 A and B); however, the difference between the two bacterial populations was reduced, and the two strains triggered similar disease symptoms (Figure 2-7 A and B). This discovery is consistent with an earlier report showing that AvrBS2 had a reduced virulence function in the absence of XopX at the early infection stage on susceptible pepper plants [10]. In addition, when *Xe* strains with or without XopX were inoculated on pepper plants carrying the Bs2 gene (ECW-R20), *Xe*Δ*XopX* triggered a weaker and slower HR than that of the wild type *Xe* strain (Figure 2-8A). The growth curve assay also confirmed that *Xe*Δ*XopX* grew to higher population levels than that of wild type *Xe* on ECW-R20 plants (Figure 2-8B). Therefore, the avirulence function of AvrBS2 was also partially compromised in the absence of XopX. Taken together, we speculate that XopX might facilitate the translocation of AvrBS2 and other T3Es at the early stages of *Xe* colonization, which needs to be further investigated in the future.

Discussion

In this study, we revealed that the *Xe* T3E XopX have functions by interacting with other T3Es inside of plant cells, which can modulate not only PTI, but also the ETI (effector-triggered immunity) and ETS (effector-triggered susceptibility), especially for XopQ and AvrBS2 [10, 11]. Although XopX could enable *Xcc* strain *Xcc* 8004 to trigger HR in *N*.

benthamiana, XopX alone delivered by bacteria is not able to elicit HR on *N. benthamiana* in the absence of XopQ, nor on BS2 pepper plants (ECW-R20) in the absence of AvrBS2. There is also no previous report of XopX-triggered nonhost resistance in any plant species. In the tomato and pepper plant disease assays, XopX is required for the full virulent functioning of *Xe* strain GM98-38 [10]. Transgenic *N. benthamiana* expressing XopX is viable and also shows more susceptibility to wild type *Xanthomonas* and *Pseudomonas* pathovars, but not to T3S mutant strain (Figure S2-3). Stock et al. (2015) suggest that the primary virulent role of XopX is associated with its ability to modulate PTI [16]. However, the authors also demonstrated that *Xe*-XopX could also promote the accumulation of pattern-triggered immunity (PTI) gene transcripts [11]. These results suggest XopX may have both virulent and avirulent functions [17]. Based on our new finding, we suggest that XopX might function as a helper T3E in the crosstalk between susceptible hosts and pathogenic bacterial pathogens. The virulent or avirulent function of XopX might depend on the interaction of other T3Es and the cognate plant R proteins that may only present in specific plant genotypes.

Given that XopX is cytotoxic when expressed in yeast, it is also likely that XopX targets a broadly conserved eukaryotic cell process in which other T3Es are also involved [18]. Since the T3Es that interact with XopX share very low sequence homology to each other, the interactions between these T3Es and XopX might be via the T3S signal translocation peptide at their N terminus, which may have a conserved secondary structure being recognized by XopX. Bioinformatic analysis also revealed that XopX has a novel methionine-rich domain that is nearly ubiquitous in *Xe* [11], which may enable it to form a flexible protein structure and interact with diverse proteins.

Although XopX is required for the full virulent and avirulent functions of at least two effectors, XopPQ and AvrBs2, the deletion of XopX can only delay, but not completely abolish, the AvrBS2-mediated cell death on BS2 pepper plants in our tested conditions. We therefore speculate that XopX is not part of the T3S system; instead it might function as a non-essential facilitator of the T3S translocation during *Xe* infection in hosts. XopX is conserved among

almost all *Xanthomonas* pathovars except *Xanthomonas axonopodis* pv. *anacardii*, the causal agent of cashew bacterial leaf spot disease in Brazil [19]. This cashew disease usually breaks out during the rainy season in tropical areas. We speculate that XopX could be essential for the colonization of *Xe* in specific environmental conditions, such as in times of cold temperatures or drought conditions. It also encourages *Xe* to compete with other phytopathogens for more nutrients and water in a commensal microbial community on the phyllosphere. Therefore, the exact function of XopX still needs to be further investigated.

XopQ and its homologues are also known to have a virulent function in host plants apart from their avirulent function to trigger disease resistance in nonhost plants. During the infection of *Xe* in Solanaceous plants, XopQ shows its ability to inhibit cell death induced by avirulent *Xe* in disease-resistant pepper, and also enhances the growth of *Xe* in resistant pepper and tomato [12, 15, 20, 21]. The structural and functional studies on XopQ and its homologues suggest that it might also function as nucleoside hydrolases [8, 12-15]. However, purified proteins of neither *Xoo*-XopQ nor *Xe*-XopQ exhibit any expected nucleoside hydrolase activity *in vivo* [14]. Furthermore, the AvrBs2 protein was predicted to be a glycerolphosphodiesterase (GDE) but GDE enzymatic activity could not be confirmed *in vivo* [22]. As the interactor of both XopQ and AvrBS2, it would be worthy to test whether or not XopX is required for XopQ and AvrBS2 to fulfill their predicted biochemical functions.

Methods and materials

Plant material and inoculation experiments

Seeds from *N. benthamiana* and *Capsicum annuum* (*C.annuum*, cultivar *ECW*) were germinated in soil at room temperature under a 8h/16h light/dark cycle at 25°C/20°C. After germination, the plants were grown under a 14h/10h light/dark cycle at 25°C/20°C. Ultimately, 6-week-old plants were used for experiments.

Bacterial growth

Escherichia coli (*E. coli*) *DH5α* and *Rho5* were grown on Luria agar medium at 37°C. *Agrobacterium tumefaciens* (*A. tumefaciens*) strain *GV2260* and *AAC00-1* were grown at 28°C on a Luria agar medium. Two *Xanthomonas* pathovars including *Xe* and *Xcc* were grown on NYGA medium while *Pst DC3000* was grown on PA medium at 28°C. The following concentrations of antibiotic selection were utilized in this study: 50 µg/ml kanamycin (Km), 100 µg/ml spectinomycin (Sp), and 30 µg/ml gentamycin (Gm). Note that *AAC00-1*, *Xcc*, *Xe*, *Pst* and *A. tumefaciens* strain *GV2260* are all intrinsically resistant to rifampicin (Rif) in concentrations of 100 µg/ml.

Phytopathogen strains and mutant strains generated by marker exchange approach

Four different phytopathogens were used in this study: *AAC00-1*, *Xcc*, *Xe*, and *Pst DC3000*. *XopQ* and three of its homologues (*Aave3626*, *Xcc-XopQ* and *HopQ*) were eliminated from the four named phytopathogens, respectively, using marker exchange [23]. A general marker exchange construct scheme is shown in the supplemental information. Kanamycin was used as the marker for selecting the mutant strain. Upstream and downstream sequences flanking *XopQ* and its homologues were amplified using genome DNAs of *AAC00-1*, *Xcc*, *Xe*, and *Pst DC3000* as a template. In terms of the primers we utilized, *Xe-XopQ* upstream was amplified with primers “*Xe-XopQ* upstream *SwaI* For” and “*Xe-XopQ* downstream *SwaI* Rev,” while *Xe-XopQ* downstream was amplified with primers “*Xe-XopQ* upstream *pmeI* For” and “*Xe-XopQ* downstream *pmeI* Rev.” For primers used to amplify the other three homologues of *XopQ*, they follow the above naming rule and can be found in the primer list in the supplemental table provided. The upstream sequence of *XopQ* was cloned to the PCR8 vector using Gibson assembly (New England Biolabs); the downstream sequence of *XopQ* was cloned to the construct during a final step - again using Gibson assembly. We refer to the latter as *PCR8-XopQ upstream-Kmr-XopQ downstream*, which was subcloned to vector *PLVC18L* via LR Gateway cloning (Invitrogen) to generate *PLVC18L-XopQ upstream-Kmr-XopQ downstream*. The plasmid DNA was transfected to *Rho5* for further conjugation. Note that *Rho5* already

carried the helper plasmid DNA.

Xe and *Rho5* carrying the construct were co-cultured for 4 hours in liquid medium with diaminopimelate (DAP), an important cell wall constituent. They were then placed on a nutrient broth medium for 48 hours for co-cultivation. The *Xe* Δ *XopQ* mutant was selected for by rifamycin and kanamycin in NYGA medium, plus. Other mutants of *AAC00-1*, *Xcc*, and *Pst DC3000* were created using the same protocol.

In order to eliminate another T3E gene (*XopX*) from the *Xe* Δ *XopQ* background, we needed to remove the selection marker introduced to *Xe* during the last step. The plasmid DNA of *pEDV6-flippase-Gmr-SacB/R* is able to recognize the flanking sequence of kanamycin and the gene is removed using flippase. After conjugating the above-named plasmid DNA to *Xe* Δ *XopN* (*Kmr*), the *Xe* clone carrying the vector was screened on selection medium containing gentamycin. We then tested the material to ensure that the kanamycin had been removed, but it remained sensitive to this antibiotic. Due to the fact that the *SacB/R* gene is toxic in the presence of sucrose, the supplementation of sucrose in the medium is typically used to eliminate the *pEDV6* construct. The *Xe* clone sensitive to both gentamycin and kanamycin can be used to neutralize another T3E. This process represents the typical procedure for fabricating mutant strains of phytopathogens impaired with multiple T3Es. Using this approach, we synthesized 5 mutants: *Xe* Δ *XopQ*, *Xe* Δ *XopQ* Δ /*XopX*, *AAC00-1* Δ *Aave3626*, *Xcc* Δ *XopQ*, and *PstDC3000* Δ *HopQ*, which we then applied to this project. All primers used for marker exchange can be found in supplemental table S2-1.

Gene cloning, site-directed mutagenesis, and plasmid construction

Four open reading frames (ORF) of *XopQ* and its homologues, along with the ORF of *Xe-XopX*, were cloned to *pEarley101* vector with a 35S promoter. Since we used the same procedure for cloning each, we show *Xe-XopQ* as the example, as follows. The *Xe-XopQ* ORF was amplified from the genome DNA of *Xe* using primers “*Xe-XopQ* ORF For” and “*Xe-XopQ* ORF Rev,” and then cloned into the *pDonr207* vector (donor vector) using BP Gateway cloning

(Invitrogen). The sequences for the other primers can be found in the supplementary table. The vector or *pDonr207-Xe-XopQ-ORF* was subcloned to a pEarley101 vector in *GV2260* using the LR Gateway cloning kit as previously described.

The vector *pDonr207-Xe-XopQ-ORF* was used to generate 4 mutants *Xe-XopQ-D116A*, *Xe-XopQ-DDD120_122_123AAA*, *Xe-XopQ-Y279A*, and *Xe-XopQ-S65A* by site-directed mutagenesis using primers “*Xe-XopQ-ORF-D116A For*” and “*Xe-XopQ-ORF-D116A Rev*,” and others listed in Table S2-1. The vector *pDonr207-Xe-XopQ-ORF-D116A* along with the other three XopQ mutants in the donor vectors, were subcloned into the pEarleyGate101 vector in *GV2260* using modified LR Gateway cloning approach as above.

Bacterial growth curve assay

Bacterial proliferation in inoculated *N. benthamiana* and *C. annuum* plants were measured by standard growth curve assays [24, 25]. The infiltration inoculation method was used in this study. In brief, the bacteria were cultivated on respective medium supplemented with appropriate antibiotics at 28 °C for 48 hours; the bacterial cells were suspended in 10 mM MgCl₂ and diluted to 1X10⁵ CFU/ml. The bacterial inoculum was infiltrated into the backside of the plant leaf using a blunt-end needleless syringe. The inoculated plants were maintained under 14 h light/10 h dark conditions at room temperature for 6 days; then the leaf discs (990 mm²) were randomly sampled from inoculated leaves at Day 0 and Day 6 for growth curve assay. The sampled leaf discs were ground in 990 µL of 10mM MgCl₂, and then vortexed for one minute before dilution and plated on respective media supplemented with proper selection antibiotics. The plates were cultivated at 28 °C until the bacterial colonies could be measured. The bacterial colony numbers were used to calculate the bacterial proliferation ratio (Log₁₀ CFU/cm²). All growth curves underwent three biological repeats with three technical replicates.

Agrobacterium-mediated transient assay, western blot, and co-immunoprecipitation

Agrobacterium infiltration, plant protein isolation, and co-IP were performed as previously described [26]. Different *Agrobacterium*-carrying constructs were infiltrated to the mesophyll tissues using blunt-end needleless syringes within a concentration of OD600 of 0.4. Leaf disks (1 cm²) were collected at 2 dpi and ground in a 100µl 1X Laemmli SDS-PAGE buffer. Then, 25 µl protein extract samples were loaded into a 10% SDS-PAGE gel. The protein samples were blotted to PVDF membrane and hybridized with appropriate antibodies [anti-HA-HRP (1: 2,000), anti-T7-3Flag (1: 2,000)]. The western blot signal was detected by using an ECL kit (Thermo Scientific, USA). Following western blot detection, the PVDF membrane was stained with 0.5 % Ponceau S solution to detect the Rubisco protein as the equal loading control. For co-IP, the Flag-tagged fusion protein was immunoprecipitated with anti-3Flag and the co-IP samples were detected with anti-HA-HRP. Prior to immunoprecipitation, 25µl of the samples were retained as the input control. The immunoprecipitated proteins and input controls were loaded onto a 10% SDS-PAGE gel, blotted to a nitrocellulose membrane, and probed with either anti-Flag followed by a secondary antibody or anti-HA-HRP.

Bimolecular fluorescence complementation (BiFC)

BiFC analyses were performed using source materials as previously described [27, 28], which features an optimized split-mVenus yellow fluorescent protein displaying a much-reduced background in planta. The vector pDOE-01 was acquired from the Arabidopsis Biological Resource Center, Stock no. CD3-1901.

The XopQ-ORF amplicon was amplified using *pDonr207-XopQ* as the template with primers “XopQ-ORF BiFC For” and “XopQ-ORF BiFC Rev” (Table S2-1). This amplicon was then cloned into pDOE01 MCS upstream of the N-terminal of mVenus (35S:X-NmVenus210) using a Gibson Assembly Kit (New England Biolabs). This vector also served as the negative control for BiFC experiments because the C-terminal YFP at MCS upstream remained isolated, but is still in-frame to allow for translation of the C-terminal YFP portion. A truncated amplicon of *XopX112-573* was amplified out using pEntry-XopX112-573 as the template with primers “XopX112-

573 BiFC For” and “XopX₁₁₂₋₅₇₃ BiFC Rev” (Table S2-1). This material was then cloned into the pDOE01-35S:X-CVenus210 portion of above parent vector harboring XopQ.

N. benthamiana leaves were infiltrated with *Agrobacterium GV2260* cultures within a concentration of OD₆₀₀ of 0.2 and incubated for 48 h post-inoculation. Imaging of BiFC results were performed using a Zeiss LSM880 fluorescent microscope with a 505–550-nm band-pass emission filter and a 488-nm argon laser.

Split Luciferase construct generation and assay

Xe-XopQ and truncated *Xe-XopX₁₁₂₋₅₇₃* in donor vectors generated above were subcloned to the luciferase expression vector via LR cloning. Specifically, *Xe-XopQ* was cloned to the vector harboring N-terminal luciferase (NLUC), while *Xe-XopX₁₁₂₋₅₇₃* was cloned to the vector harboring C-terminal luciferase (CLUC); both were then transfected into *Agrobacterium GV2260*. *GV2260* cultures carrying above two constructs were co-infiltrated to *N. benthamiana* leaves within OD₆₀₀ 0.4 (0.2 + 0.2). After 48 hours, luciferin (0.25 g/L) was infiltrated to the same spot carrying the *Agrobacterium* and incubated for an additional 10 min. The positive controls, NLUC-RAR and CLUC-SGT1, along with the negative control, NLUC-GUS and CLUC-GUS, were used to validate the efficacy of this approach. Prior to detecting the luciferase signal, *N. benthamiana* leaves were placed in the dark for 10 min owing to quenching auto-fluorescence signals. Chemical fluorescence signals were detected using the CCD camera of a Gel DocTM XR+ System (Bio-Rad).

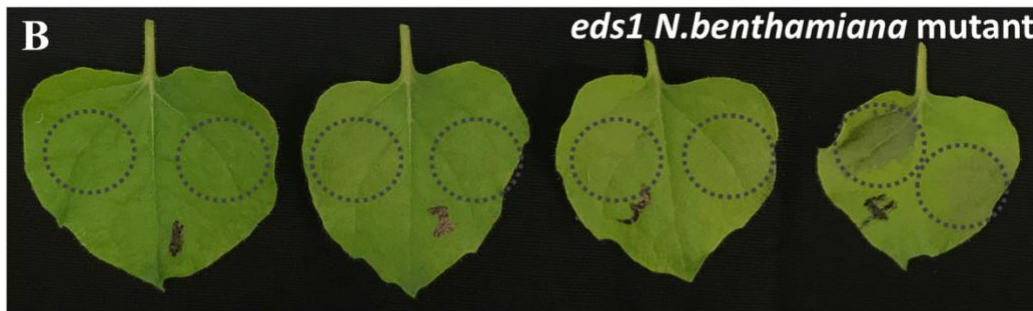
RNA isolation, RT-PCR and real-time PCR

For RT-PCR, total RNA was extracted from *N. benthamiana* leaf tissues using TRIzol Reagent (Invitrogen) according to the manufacturer’s instructions. DNA contamination was eliminated by treating total RNAs with UltraPure DNase I (Invitrogen). The integrity of the total RNA were verified by running products through a 0.8% agarose gel and quantified using a NanoDrop ND-1000 spectrophotometer (NanoDrop Technologies, Wilmington, DE). cDNA

synthesis was performed using the SuperScript III First-Strand System for RT-PCR kit (Invitrogen) with an oligo-dT primer. Real-time PCR was carried out on the cDNA, which was diluted 20 times, using the Quantitect SYBR Green PCR kit (Qiagen) and gene-specific primers in a LightCycler (Roche) according to the manufacturer's instruction. Gene-specific primers for real-time PCR were synthesized by IDT (Integrated DNA Technologies) and designated as “*NbActin* real-time PCR For,” “*NbActin* real-time PCR Rev,” etc. (Supplemental Table 2-1).

Trypan blue staining

The trypan blue staining assay was conducted according to prior reports [29, 30]. *N. benthamiana* leaves inoculated by *Agrobacteria* were boiled for approximately 1 min in 0.025% trypan blue staining solution (lactic acid:glycerol:water-saturated phenol:water=1:1:1:1) and were incubated overnight at room temperature. Then, samples were decolorized in a 0.25% (w/v) chloral hydrate destaining buffer for 24 hours.



Xe *Xe* Δ *XopQ* *Xcc* *Xcc* Δ *XopQ* *AAC* *AAC* Δ *Aave3626* *Pst DC3000* *Pst DC3000* Δ *HopQ*

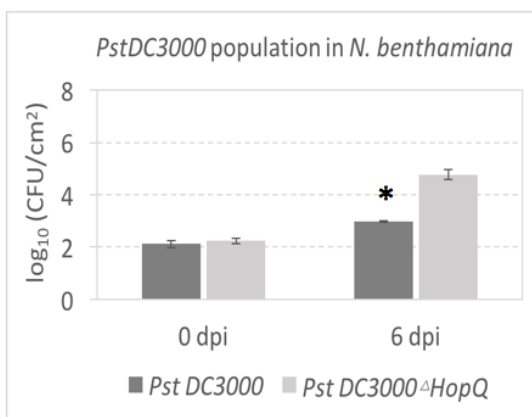
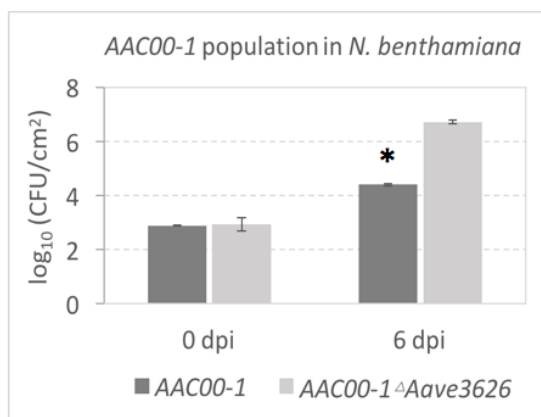
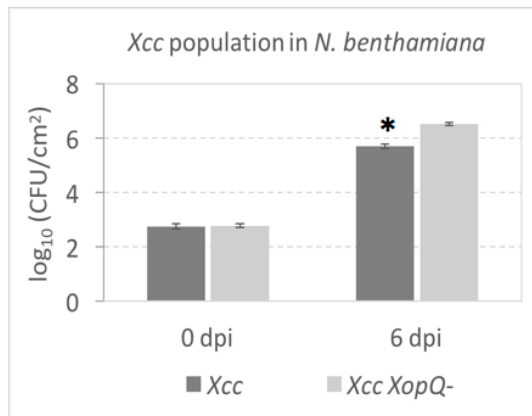
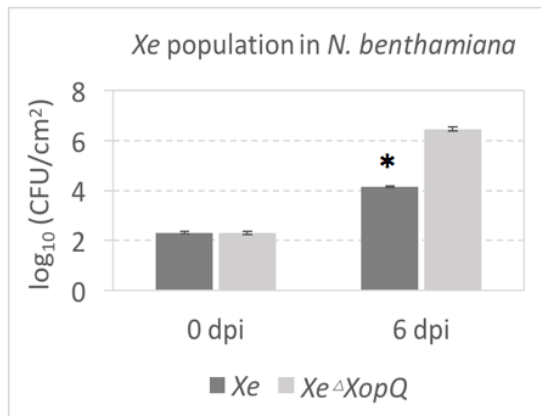


Figure 2- 1 XopQ and its homologues in diverse bacterial pathogens triggered NbEDS1-dependent nonhost disease resistance in *N. benthamiana*.

Four phytopathogens including *Xe*, *Xcc*, *AAC00-1*, *Pst DC3000*, and their XopQ knock-out mutants with a concentration of OD600 at 0.4 were inoculated to wild-type *N. benthamiana* (A) and *EDS1* mutant of *N. benthamiana* (B). Pictures were obtained 2 days post-inoculation. (C) *In planta* growth of these four bacterial pathogens and their XopQ deletion mutants measured at Days 0 and 6 in *N. benthamiana* leaves infiltrated with a starting inoculum of 1×10^5 CFU/mL. Star indicates a statistically significant difference. Experiments were replicated three times with comparable results.

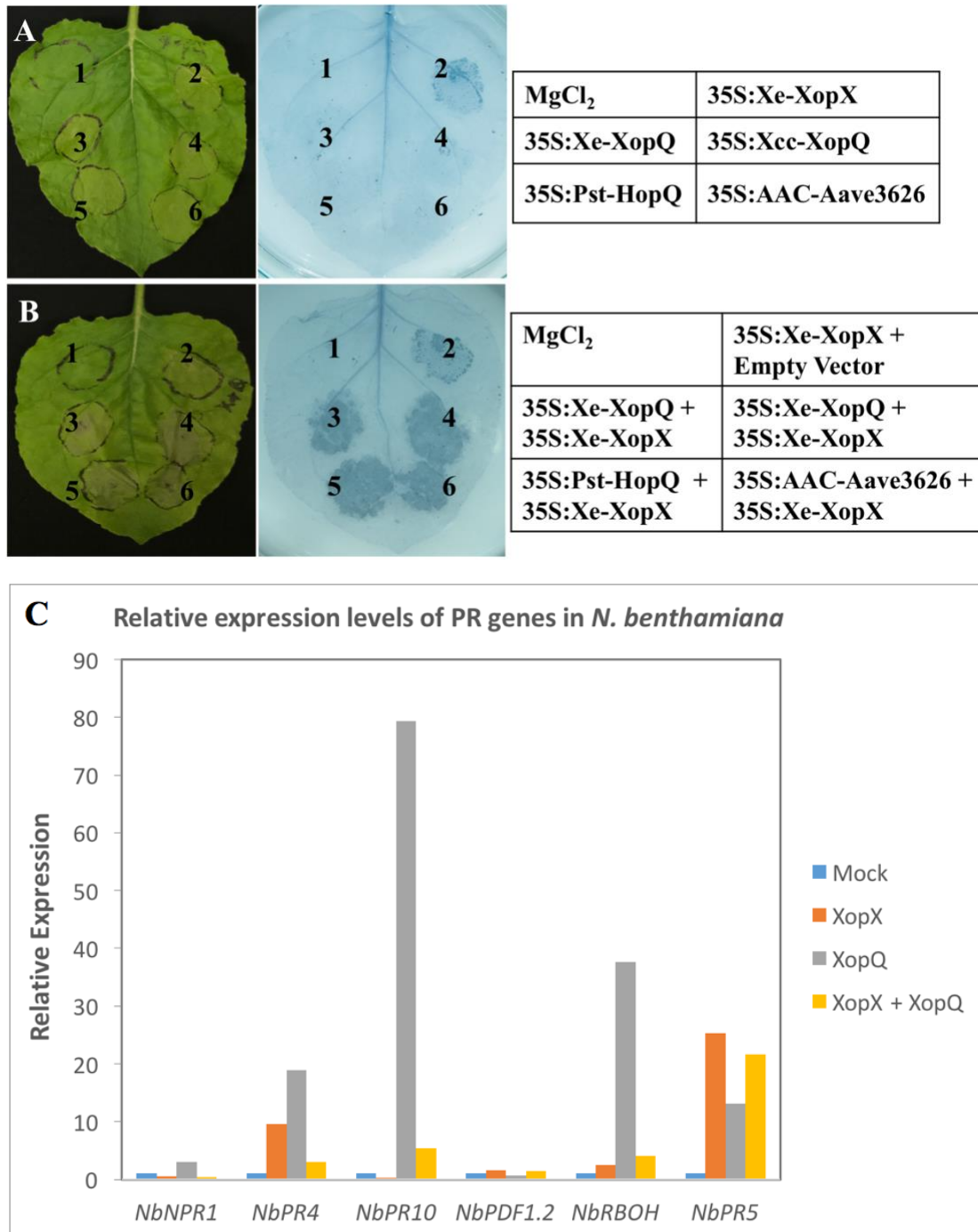


Figure 2- 2 Co-expression of XopQ and XopX elicited programmed cell death in *N. benthamiana* in *Agrobacterium*-mediated transient assays.

(A) XopX and XopQ homologues fused with a 35S overexpression promoter were individually

inoculated to wild-type *N. benthamiana* within a concentration of OD600 at 0.4. Picture was taken at 2 days post-inoculation. Trypan blue staining was subsequently processed using the same leaf. (B) Four XopQ homologues and *Xe-XopX* were co-inoculated to wild-type *N. benthamiana* within a concentration of OD600 at 0.4 + 0.4. Picture was taken at 2 days post-inoculation. Trypan blue staining was subsequently processed using the same leaf. (C) Real-time PCR was used to check expression levels of pathogenetic related genes in *N. benthamiana* treated with mock (MgCl₂), *Xe-XopQ* only, *Xe-XopX* only, and a combination of *Xe-XopQ* and *Xe-XopX*.

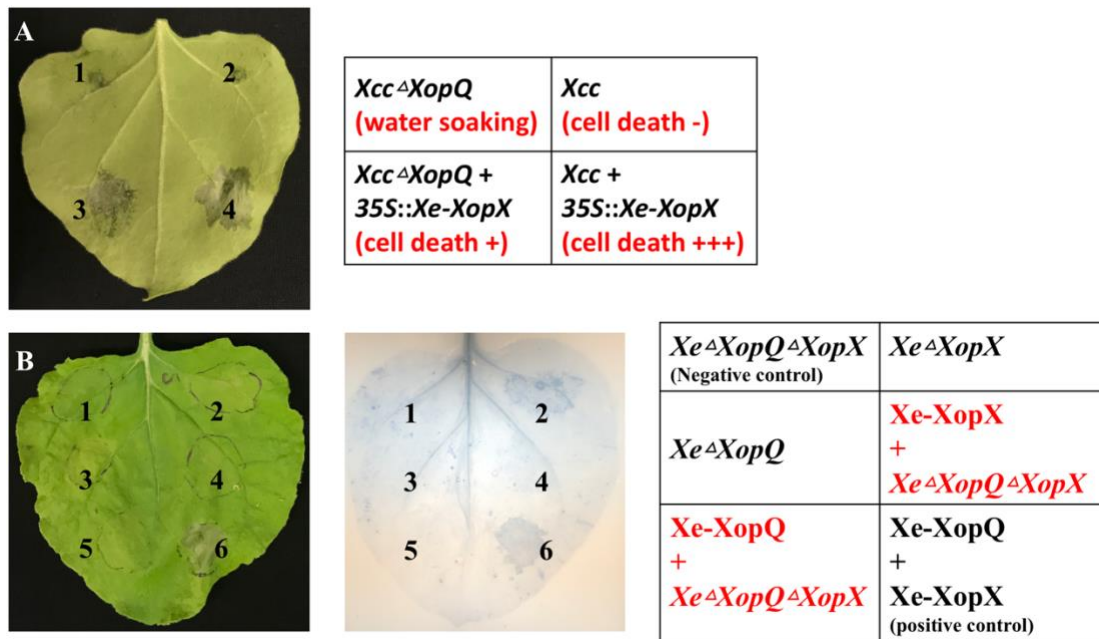


Figure 2- 3 Mutant *Xe* or *Xcc* strains lacking either *XopQ* or *XopX* failed to trigger programmed cell death in *N. benthamiana*.

(A) *N. benthamiana* leaf inoculated by *Xcc*, *Xcc* Δ *XopQ*, a combination of *Xcc* Δ *XopQ* and *Xe-XopX* (*Agrobacteria*), and a combination of *Xcc* and *Xe-XopX* (*Agrobacteria*) with a concentration of OD600 at 0.4 (single inoculation) , or at 0.4 (0.2 + 0.2) (co-inoculation). Picture was taken at 2 days post-inoculation. (B) *N. benthamiana* leaf inoculated by *Xe* Δ *XopQ* Δ *XopX*, *Xe* Δ *XopX*, *Xe* Δ *XopQ*, a combination of *Xe* Δ *XopQ* Δ *XopX* and *Xe-XopX* (*Agrobacteria*), a combination of *Xe* Δ *XopQ* Δ *XopX* and *Xe-XopQ* (*Agrobacteria*), and a combination of *Xe-XopQ* and *Xe-XopX* (*Agrobacteria*) with a concentration of OD600 at 0.4 (single inoculation) , or at 0.4 (0.2 + 0.2) (co-inoculation). Picture was taken at 2 days post-inoculation. Trypan blue staining was subsequently processed using the same leaf.

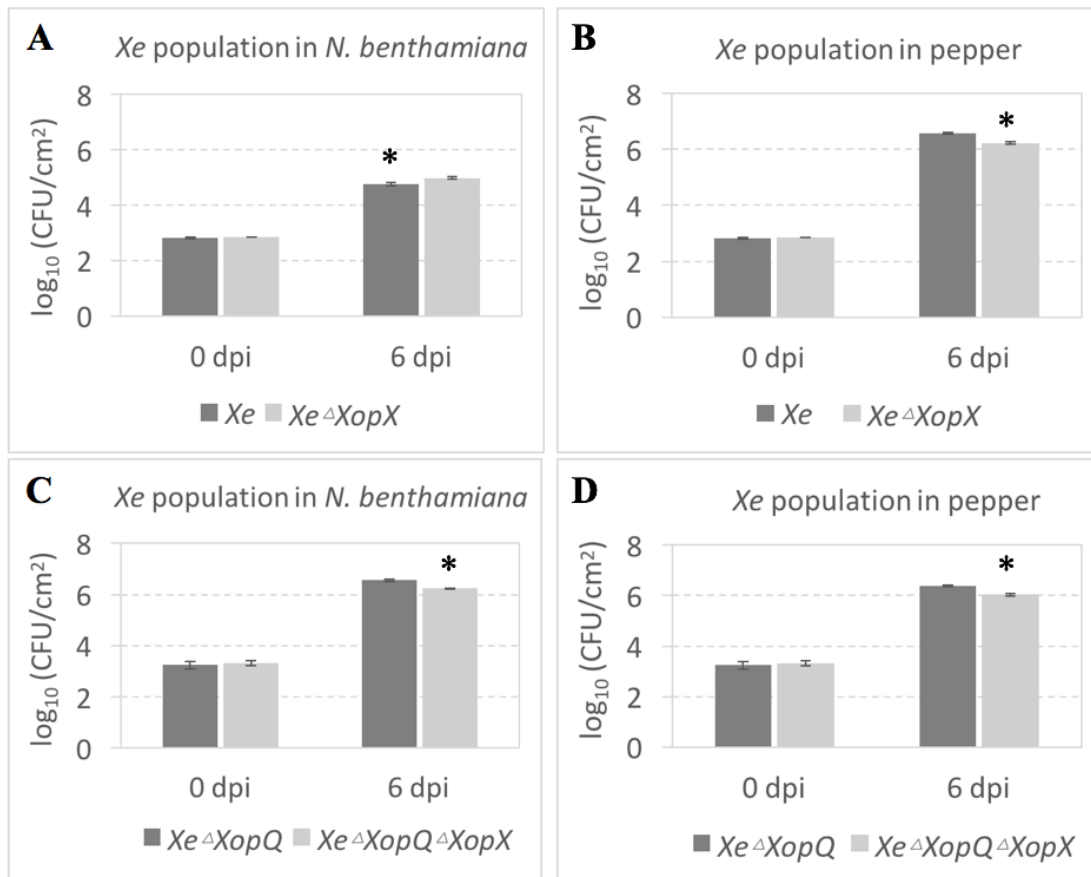


Figure 2- 4 XopX displayed a virulent function in the presence of XopQ, while XopX displayed an avirulent function in the absence of XopQ.

In planta growth comparing two pairs of *Xe* strains: *Xe* with *Xe*Δ*XopX* (A and C), and *Xe*Δ*XopQ* with *Xe*Δ*XopQ*Δ*XopX* (B and D) measured at Days 0 and 6 in *N. benthamiana* and pepper leaves infiltrated with a starting inoculum of 1×10^5 CFU/mL. Star indicates statistically significant differences. Experiments were replicated three times with comparable results.



MgCl₂	<i>Xe</i>
<i>Xe^ΔXopQ</i>	<i>Xe^ΔXopQ pXopQ</i>
<i>Xe^ΔXopQ pXopQ D116A</i>	<i>Xe^ΔXopQ pXopQ DDD120_122_123 AAA</i>
<i>Xe^ΔXopQ pXopQ S65A</i>	<i>Xe^ΔXopQ pXopQ Y279A</i>



MgCl₂	Xe-XopX + Xe-XopQ
Xe-XopX + Xe-XopQ D116A	Xe-XopX + Xe-XopQ DDD120_122_123AAA
Xe-XopX + Xe-XopQ S65A	Xe-XopX + Xe-XopQ Y279A

Figure 2- 5 Mutations in the predicted active site of *Xe-XopQ* affected avirulence in *N. benthamiana*.

(A) *N. benthamiana* leaf was inoculated by mock (MgCl₂) as a control, and 7 *Xe* strains including wild-type *Xe*, *Xe^ΔXopQ*, *Xe^ΔXopQ pXopQ*, *Xe^ΔXopQ pXopQ-D116A*, *Xe^ΔXopQ pXopQ-DDD120_122_123AAA*, *Xe^ΔXopQ pXopQ-S65A*, and *Xe^ΔXopQ pXopQ-Y279A* within a concentration at OD600 0.4. Picture was taken at 2 days post-inoculation. (B) *N. benthamiana* leaf was inoculated by mock (MgCl₂) as a control and five *Agrobacteria* combinations, including *Xe-XopX* along with *XopQ* and its four *XopQ* site mutations at a concentration of OD600 0.4 (0.2 +0.2). Picture was taken at 2 days post-inoculation.

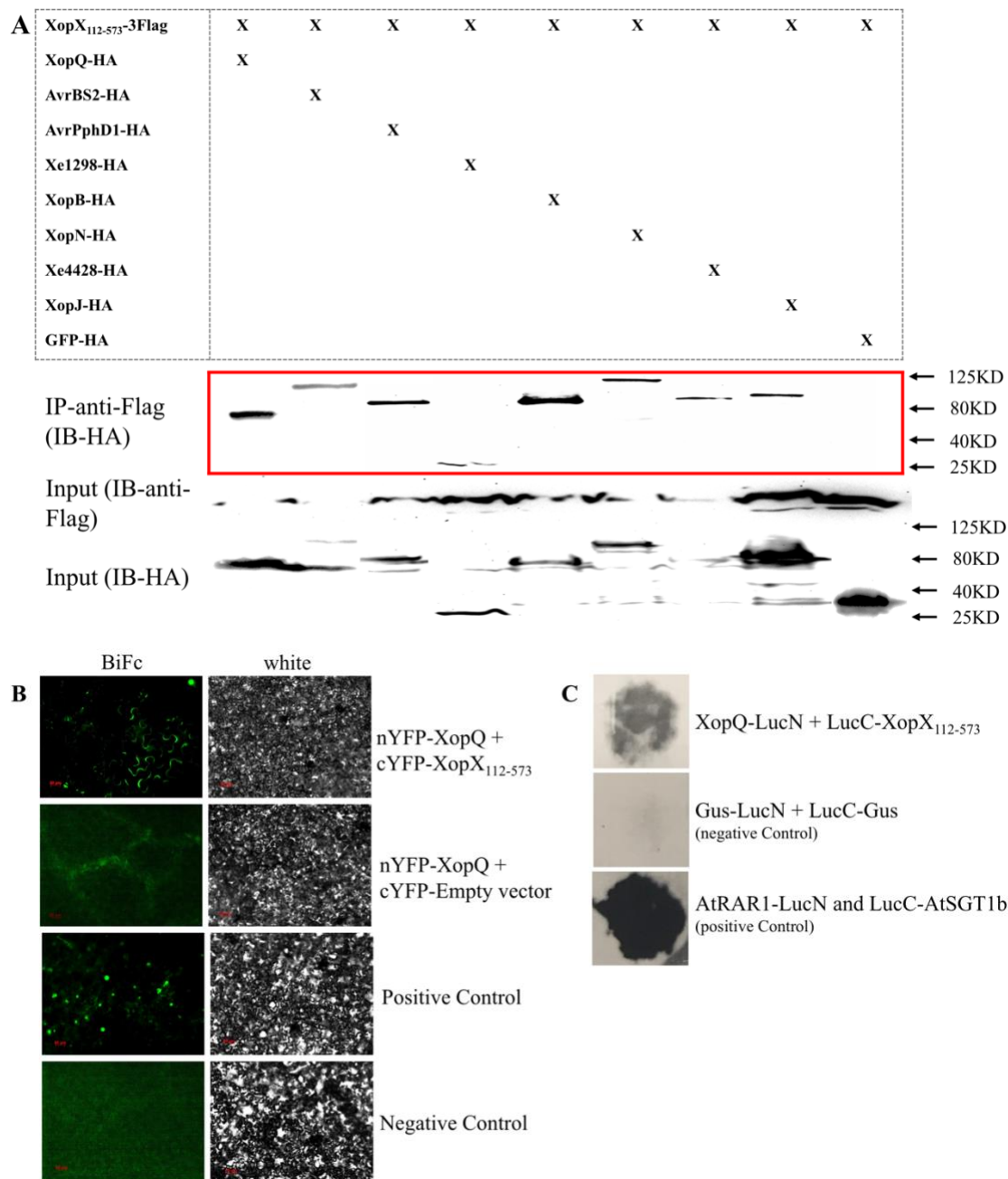


Figure 2- 6 The core domain of XopX physically interacted with multiple T3Es within plant cells.

(A) Co-immunoprecipitation of truncated XopX and multiple T3Es. *XopX*₁₁₂₋₅₇₃-3xFlag, was transiently co-expressed with XopQ, avrBS2, avrpphd1, Xe1298, XopB, XopN-GFP, avrRxo1-GFP, XopJ1-GFP, and GFP—all fused with a HA tag in *N. benthamiana* leaves. The proteins

pulled down by anti-3Flag beads were detected via western blotting using a-HA-HRP primary antibody. Two western blots of the input protein extracts (prior to precipitation) are shown in the middle and bottom. (B) Split luciferase assay results for XopQ with XopX and XopX₁₁₂₋₅₇₃. Negative control is a combination of GUS-LucN and LucC-GUS, while positive control is a combination of RAR1-LucN and LucC-SGT1. (C) BiFC results for XopQ with XopX₁₁₂₋₅₇₃. Negative control and positive control are from Dr. Eric Beers lab (507 Latham Hall, 220 Ag Quad Ln. Blacksburg, VA). Scale bars are 50 μ m in all panels.

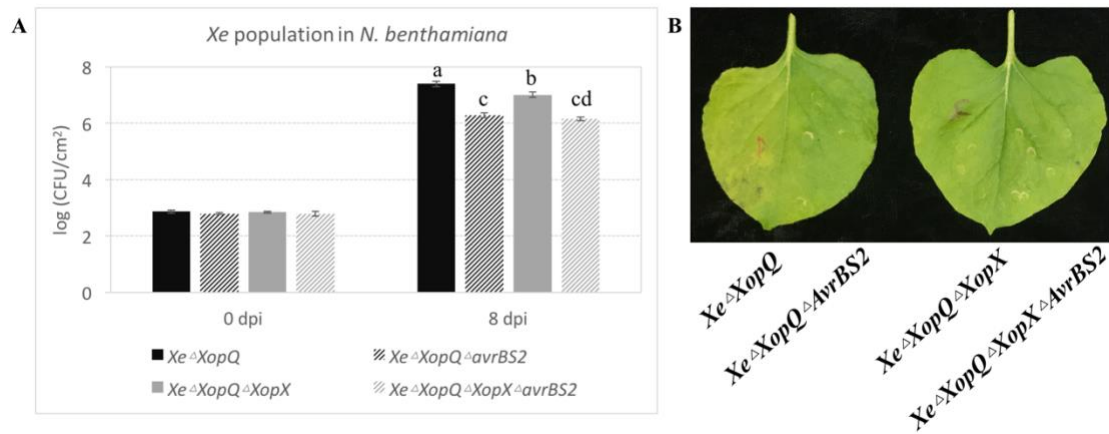


Figure 2- 7 Impairment of *XopX* partially eliminated the virulence function of *AvrBS2*.

(A) *In planta* growth comparing two pairs of *Xe* strains: *Xe*Δ*XopQ* with *Xe*Δ*XopQ*Δ*XopX*, and *Xe*Δ*XopQ*Δ*XopX* with *Xe*Δ*XopQ*Δ*XopX*Δ*avrBS2* at days 0 and 8 in *N. benthamiana* leaves infiltrated with a starting inoculum of 1×10^5 CFU/mL. The letters suggest statistically significant differences. (B) Corresponding disease symptoms from (A). Experiments were repeated three times with comparable results.

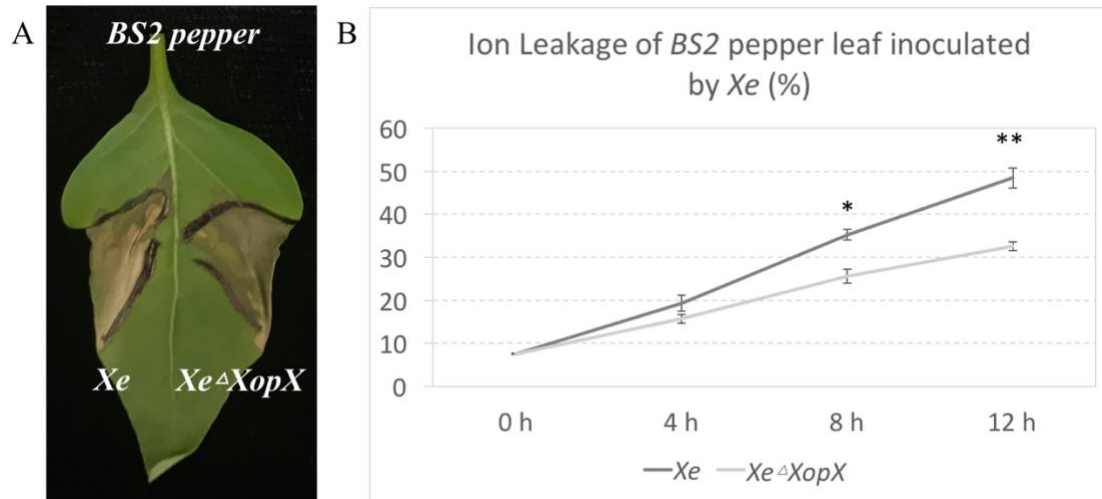


Figure 2- 8 Impairment of *XopX* partially eliminated the avirulent function of AvrBS2 in *BS2* pepper.

(A) *Xe* and *Xe Δ XopX* at OD600 0.4 were inoculated to *BS2* pepper to visualize cell death phenotypes. Pictures of the front side of the leaf (left) and the back side of the leaf (right) were obtained at 48 hpi. (B) Ion leakage of *N. benthamiana* leaves inoculated by *Xe* and *Xe Δ XopX* were measured at 4 time intervals: 0 h, 4 h, 8 h, and 12 h. Experiments were repeated three times with comparable results.

Supplementary information



Figure S2- 1 Transient expression of *NbEDS1* restored the ability of *N. benthamiana* to recognize *Xe* and induced cell death.

Four treatments including *Xe* Δ *XopQ* with a concentration of OD600 at 0.4 (A), Wild-type *Xe* at OD600 0.4 (B), the combination of 35S:*NbEDS1* with *Xe* at OD600 0.4 + 0.4 (C), and the combination of 35S:*NbEDS1* with *Xe* Δ *XopQ* at OD600 0.4 + 0.4 (D) were inoculated to *eds1* mutant of *N. benthamiana*.

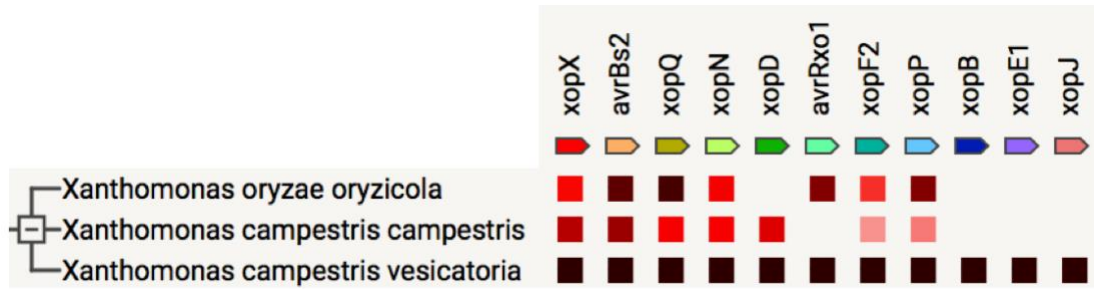


Figure S2- 2 *XopX* is conserved in *Xanthomonas* and its cooccurrence with a core set T3Es.

The information utilized in this figure was obtained from the software of String (Search Tool for the Retrieval of Interacting Genes/Proteins).

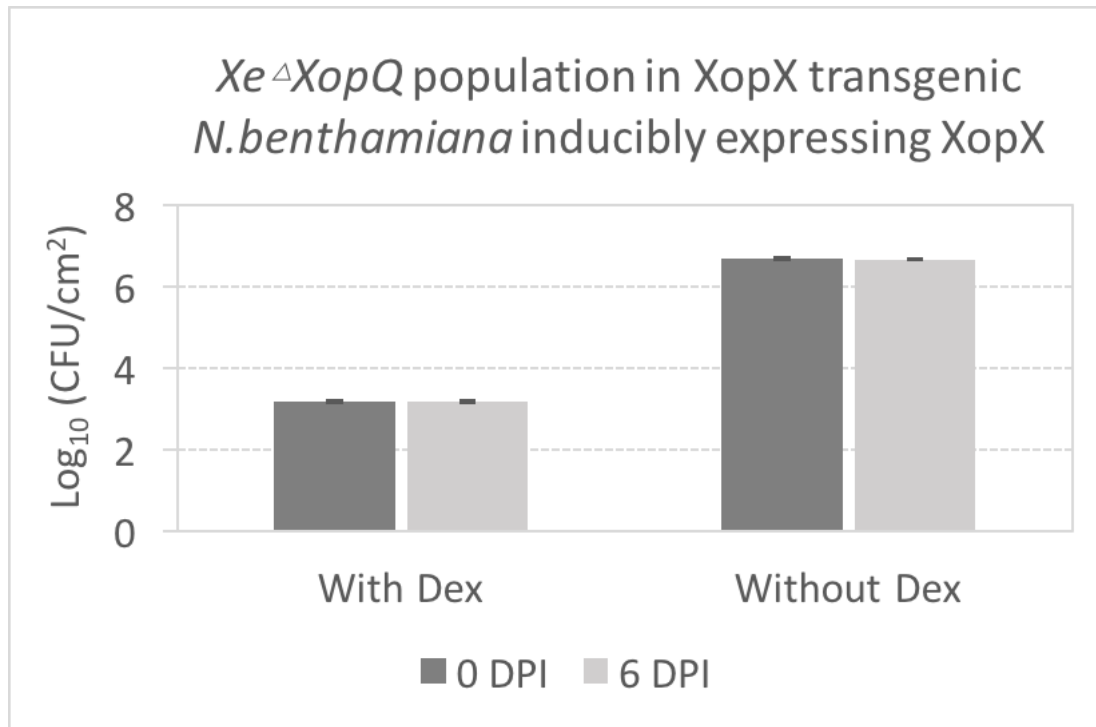


Figure S2- 3 *In planta* growth of *XeΔXopQ* in transgenic *N. benthamiana* inducibly expressing XopX.

The strain of *XeΔXopQ* was infiltrated to XopX transgenic *N. benthamiana* leaves infiltrated with a starting inoculum of 1×10^5 CFU/mL. The leaves were pre-treated with dexamethasone (DEX) and mock. The population of *XeΔXopQ* was measured at Days 0 and 6 post inoculation. Experiments were replicated three times with comparable results.

Table S2- 1 Sequences of primers utilized in this investigation

Name	Sequences
<i>Xe</i> -XopQ ORF For	aaaaagcaggcttgctagaatgcagcccaccgcaatccg
<i>Xe</i> -XopQ ORF Rev	agaaagctgggtagaattcgcgcccgcttgcccctcgt
<i>Xcc</i> -XopQ ORF For	aaagcaggcttgatgcccgaggcgctcatgcaacgt
<i>Xcc</i> -XopQ ORF Rev	caagaaagctgggtattgttcgtagcaagcggcgt
<i>Pst</i> DC3000-HopQ ORF For	aaaagcaggcttgatgcatcgtcctatcaccgcagg
<i>Pst</i> DC3000-HopQ ORF Rev	caagaaagctgggtaattcgggctaccgtcgactgg
<i>AAC001</i> -Aave3626 ORF For	aaaaagcaggctgggatccatgacatccattcctccatca
<i>AAC001</i> -Aave3626 ORF Rev	agaaagctgggtagaattcgtccccagcgcggtctggcga
<i>Xe</i> -XopQ upstream SwaI For	gcaggctccgaattcgccttatttcaggggcagcgaagtgcctgac
<i>Xe</i> -XopQ upstream SwaI Rev	aagcttaattggatccatttaacggattgcggtgggctgcat
<i>Xe</i> -XopQ upstream PmeI For	tggctaattcccatgctgtttacgagggcaacgcggcgctga
<i>Xe</i> -XopQ upstream PmeI Rev	actagtcgacttaattaagttgtttgacgctacgccatcctg
<i>Xe</i> -XopX upstream SwaI For	gcaggctccgaattcgccttatttggtccagttggaataggacatgt
<i>Xe</i> -XopX upstream SwaI Rev	aagcttaattggatccattgtttgctgtttcttgatcctcat
<i>Xe</i> -XopX upstream PmeI For	atggctaattcccatgctgtttgacggtagccgcccggctcat
<i>Xe</i> -XopX upstream PmeI Rev	actagtcgacttaattaagttgttcgaccgcggtacacctc
<i>Xcc</i> -XopQ upstream SwaI For	gcaggctccgaattcgccttatttaaccatcggacgatgcagacgcct
<i>Xcc</i> -XopQ upstream SwaI Rev	aagcttaattggatccattatgcagtggtggcgatgcctgat
<i>Xcc</i> -XopQ upstream PmeI For	atggctaattcccatgctgtttcaccgatcgtttcagacgc
<i>Xcc</i> -XopQ upstream PmeI Rev	actagtcgacttaattaagttgttcaacgaggggatcagc
<i>AAC001</i> -Aave3626 upstream SwaI For	gcaggctccgaattcgccttatttggtatcgtatcaggtatc
<i>AAC001</i> -Aave3626 upstream SwaI Rev	aagcttaattggatccattatggatgcatctttccatcctgc
<i>AAC001</i> -Aave3626 upstream PmeI For	atggctaattcccatgctgtttaagaccgcgctgggagctga
<i>AAC001</i> -Aave3626 upstream PmeI Rev	actagtcgacttaattaagttcttcgacctgccgttcggactc
<i>Xe</i> -AvrBS2 upstream SwaI For	gcaggctccgaattcgccttatttctgctgcagctgcggcctc
<i>Xe</i> -AvrBS2 upstream SwaI Rev	aagcttaattggatccattgatgacctgaaaacgcggcg
<i>Xe</i> -AvrBS2 upstream PmeI For	atggctaattcccatgctgtttgcaattcaggccagctccat
<i>Xe</i> -AvrBS2 upstream PmeI Rev	actagtcgacttaattaagtttacgcccggcgtatcgggcac
<i>Xe</i> -XopQ-ORF-S65A For	acggcaccgcccgcgcgagccttccccgcgattgacgcct
<i>Xe</i> -XopQ-ORF-S65A Rev	aggcgtcaatcgcgcgggcaaggcctgcgcgcccgggtccgt
<i>Xe</i> -XopQ-ORF-D116A For	acgctgctgttcaccgccccgaacaaggacc
<i>Xe</i> -XopQ-ORF-D116A Rev	gggtcctgttcggggcggtgaacagcagcgt
<i>Xe</i> -XopQ-ORF-DDD120_122_123AAA For	accgaccgaacaaggccccccgctgctgtgacctacacc
<i>Xe</i> -XopQ-ORF-DDD120_122_123AAA Rev	ggtgtaggtcacgacagcggcggggccttctgggtcgggt

<i>Xe-XopQ</i> -ORF-Y279A For	ccggacacgcgcgccccaacaacgccaccgac
<i>Xe-XopQ</i> -ORF-Y279A Rev	gtcggtgggcgtgttggcggcgcgcgtgtcgg
<i>NbActin</i> real-time PCR For	tgaagatcctcacagagcgtgg
<i>NbActin</i> real-time PCR Rev	ttgtatgtggctcgtggattc
<i>NbNPR1</i> real-time PCR For	atggataatagtaggactgcgtt
<i>NbNPR1</i> real-time PCR Rev	aatgtcatgaggcaaggctttatc
<i>NbPR4</i> real-time PCR For	gctttctgcgctacttggg
<i>NbPR4</i> real-time PCR Rev	gcccttcttattctaaacggc
<i>NbPR10</i> real-time PCR For	gttcgtataggggcaagtt
<i>NbPR10</i> real-time PCR Rev	ttaagcataggcttcaggatt
<i>NbPDF1.2</i> real-time PCR For	atggcaaaatctatgcgctt
<i>NbPDF1.2</i> real-time PCR Rev	gcaaggcctagtagacaacaac
<i>NbRBOH</i> real-time PCR For	tttctctgaggttggccagccaccaccta
<i>NbRBOH</i> real-time PCR Rev	gccttcatgttgtgacaatgtctttaaca
<i>NbPR5</i> real-time PCR For	gctggggtaaaccaccaaca
<i>NbPR5</i> real-time PCR Rev	actataggcatcaggacatct
<i>Xe-XopQ</i> -ORF BiFC For	accatggggcgcgccctaggaactagccaactttgtacaaaaagca
<i>Xe-XopQ</i> -ORF BiFC Rev	tgaccacctccggatcctcactagtaactttgtacaagaaagctgg
<i>Xe-XopX</i> ₁₁₂₋₅₇₃ BiFC For	ttacaattacaatggggtccctacgtacaactttgtacaaaaagca
<i>Xe-XopQ</i> ₁₁₂₋₅₇₃ BiFC Rev	aacctcggagctcacgtgactacgtactttgtacaagaaagctgg

References

1. Jones, J.B., et al., *Reclassification of the xanthomonads associated with bacterial spot disease of tomato and pepper*. Syst Appl Microbiol, 2004. 27(6): p. 755-62.
2. Schultink, A., et al., *Using forward genetics in Nicotiana benthamiana to uncover the immune signaling pathway mediating recognition of the Xanthomonas perforans effector XopJ4*. New Phytol, 2019. 221(2): p. 1001-1009.
3. Derevnina, L., S. Kamoun, and C.H. Wu, *Dude, where is my mutant? Nicotiana benthamiana meets forward genetics*. New Phytol, 2019. 221(2): p. 607-610.
4. Schwartz, A.R., et al., *Phylogenomics of Xanthomonas field strains infecting pepper and tomato reveals diversity in effector repertoires and identifies determinants of host specificity*. Front Microbiol, 2015. 6: p. 535.
5. Adlung, N., et al., *Non-host Resistance Induced by the Xanthomonas Effector XopQ Is Widespread within the Genus Nicotiana and Functionally Depends on EDS1*. Front Plant Sci, 2016. 7: p. 1796.
6. Adlung, N. and U. Bonas, *Dissecting virulence function from recognition: cell death suppression in Nicotiana benthamiana by XopQ/HopQ1-family effectors relies on EDS1-dependent immunity*. Plant J, 2017. 91(3): p. 430-442.
7. Schultink, A., et al., *Roq1 mediates recognition of the Xanthomonas and Pseudomonas effector proteins XopQ and HopQ1*. Plant J, 2017. 92(5): p. 787-795.
8. Wei, C.F., et al., *A Pseudomonas syringae pv. tomato DC3000 mutant lacking the type III effector HopQ1-1 is able to cause disease in the model plant Nicotiana benthamiana*. Plant J, 2007. 51(1): p. 32-46.
9. Qi, T., et al., *NRG1 functions downstream of EDS1 to regulate TIR-NLR-mediated plant immunity in Nicotiana benthamiana*. Proc Natl Acad Sci U S A, 2018. 115(46): p. E10979-E10987.
10. Metz, M., et al., *The conserved Xanthomonas campestris pv. vesicatoria effector protein XopX is a virulence factor and suppresses host defense in Nicotiana benthamiana*. Plant J, 2005. 41(6): p. 801-14.
11. Stork, W., J.G. Kim, and M.B. Mudgett, *Functional Analysis of Plant Defense Suppression and Activation by the Xanthomonas Core Type III Effector XopX*. Mol Plant Microbe Interact, 2015. 28(2): p. 180-94.
12. Li, W., Y.H. Chiang, and G. Coaker, *The HopQ1 effector's nucleoside hydrolase-like domain is required for bacterial virulence in arabidopsis and tomato, but not host recognition in tobacco*. PLoS One, 2013. 8(3): p. e59684.
13. Yu, S., I. Hwang, and S. Rhee, *Crystal structure of the effector protein XOO4466 from Xanthomonas oryzae*. J Struct Biol, 2013. 184(2): p. 361-6.
14. Yu, S., I. Hwang, and S. Rhee, *The crystal structure of type III effector protein XopQ from Xanthomonas oryzae complexed with adenosine diphosphate ribose*. Proteins, 2014. 82(11): p. 2910-4.
15. Gupta, M.K., et al., *Mutations in the Predicted Active Site of Xanthomonas oryzae pv.*

- oryzae XopQ Differentially Affect Virulence, Suppression of Host Innate Immunity, and Induction of the HR in a Nonhost Plant.* Mol Plant Microbe Interact, 2015. 28(2): p. 195-206.
16. Teper, D., et al., *Five Xanthomonas type III effectors suppress cell death induced by components of immunity-associated MAP kinase cascades.* Plant Signal Behav, 2015. 10(10): p. e1064573.
17. Sinha, D., et al., *Cell wall degrading enzyme induced rice innate immune responses are suppressed by the type 3 secretion system effectors XopN, XopQ, XopX and XopZ of Xanthomonas oryzae pv. oryzae.* PLoS One, 2013. 8(9): p. e75867.
18. Salomon, D., et al., *Expression of Xanthomonas campestris pv. vesicatoria type III effectors in yeast affects cell growth and viability.* Mol Plant Microbe Interact, 2011. 24(3): p. 305-14.
19. Hajri, A., et al., *A "repertoire for repertoire" hypothesis: repertoires of type three effectors are candidate determinants of host specificity in Xanthomonas.* PLoS One, 2009. 4(8): p. e6632.
20. Teper, D., et al., *Xanthomonas euvesicatoria type III effector XopQ interacts with tomato and pepper 14-3-3 isoforms to suppress effector-triggered immunity.* Plant J, 2014. 77(2): p. 297-309.
21. Giska, F., et al., *Phosphorylation of HopQ1, a type III effector from Pseudomonas syringae, creates a binding site for host 14-3-3 proteins.* Plant Physiol, 2013. 161(4): p. 2049-61.
22. Zhao, B., et al., *Computational and biochemical analysis of the Xanthomonas effector AvrBs2 and its role in the modulation of Xanthomonas type three effector delivery.* PLoS Pathog, 2011. 7(12): p. e1002408.
23. Lee, S.W. and P.C. Ronald, *Marker-exchange mutagenesis and complementation strategies for the Gram-negative bacteria Xanthomonas oryzae pv. oryzae.* Methods Mol Biol, 2007. 354: p. 11-8.
24. Melotto, M., et al., *Plant stomata function in innate immunity against bacterial invasion.* Cell, 2006. 126(5): p. 969-80.
25. Katagiri, F., R. Thilmony, and S.Y. He, *The Arabidopsis thaliana-pseudomonas syringae interaction.* Arabidopsis Book, 2002. 1: p. e0039.
26. Krasileva, K.V., D. Dahlbeck, and B.J. Staskawicz, *Activation of an Arabidopsis resistance protein is specified by the in planta association of its leucine-rich repeat domain with the cognate oomycete effector.* Plant Cell, 2010. 22(7): p. 2444-58.
27. Gookin, T.E. and S.M. Assmann, *Significant reduction of BiFC non-specific assembly facilitates in planta assessment of heterotrimeric G-protein interactors.* Plant J, 2014. 80(3): p. 553-67.
28. Rigoulot, S.B., et al., *Populus trichocarpa clade A PP2C protein phosphatases: their stress-induced expression patterns, interactions in core abscisic acid signaling, and potential for regulation of growth and development.* Plant Mol Biol, 2019. 100(3): p. 303-317.
29. Lang, Y., Z. Li, and H. Li, *Analysis of Protein-Protein Interactions by Split Luciferase Complementation Assay.* Curr Protoc Toxicol, 2019. 82(1): p. e90.

30. Kato, N. and J. Jones, *The split luciferase complementation assay*. Methods Mol Biol, 2010. 655: p. 359-76.

Chapter 3 *Xanthomonas euvesicatoria* type III effector XopN interacts with transcription factor *NbVOZ* to promote an aqueous environment and enhance bacterial proliferation

Summary

Bacterial spot (BS) disease is one of the most common and destructive diseases that infect both tomatoes and peppers. BS can be easily identified due to the appearance of dark, irregular, water-soaked areas on the leaf. While a number of studies have indicated that an aqueous environment is essential for bacterial proliferation, it remains unclear which component of *Xanthomonas euvesicatoria* (*Xe*) contributes principally to the water-soaked symptoms of BS in affected pepper and tomato plants. In this study, we report that a *Xe* type III secreted effector, *Xe*-XopN, is required for triggering the water-soaking symptom on *Nicotiana benthamiana* (*N. benthamiana*) and pepper plants infected with *Xe*. In addition, we revealed that XopN interacts with two members in a transcription factor, *NbVOZ*, and represses the expression of *NPRI*, a key component of basal defense. Therefore, XopN has a role in maintaining a water-affluent environment for better replication of *Xe*, and it can also interact with *NbVOZ1/2* to regulate plant immunity.

Introduction

Because of climate change and the demand for a more sustainable food supply, the concerns of various plant diseases that can severely threaten world crop production are becoming a more urgent problem than ever. In field conditions, plants can be infected by diverse microorganisms throughout their lifetimes. Certain genetically-adapted microorganisms have the ability to colonize and proliferate in host plants and cause disease problems. It is well known that the environment plays a crucial role in the battle between host plants and phytopathogens [1-3]. The classic concept of the “disease triangle” demonstrates that disease can only occur under specific environmental conditions. Notably, among environmental factors involving water

availability such as drought conditions and heavy rainfall events are well known to have a significant impact on the occurrence and/or proliferation of plant disease [4]. Specifically, under drought conditions plants are usually more resistant to disease in comparison to plants exposed to high humidity. These findings reinforce the notion that global water wars that support human life may also be reflected in the important battle between plants and pathogens. Recent longitudinal studies show that pathogenic bacteria develop virulent proteins to promote an aqueous apoplast, which supports the successful colonization of pathogenic microbes [5]. For example, *Xanthomonas gardneri* (*X. gardneri*) recruits a transcription activator-like (TAL) effector (TALE), AvrHah1 to induce water-soaked lesions in fruits and leaves of infected tomato plants. With the function of AvrHah1, water can be drawn into the apoplast of the infected area by *X. gardneri*. The pull of water can facilitate the entry of additional bacteria and consequently causes more severe disease. Two T3S (Type III Secretion) effectors in *Pseudomonas syringae*, HopM1 and AvrE, have been also reported to be responsible for the establishment of the aqueous apoplast [1, 6-8].

Bacterial spot (BS) disease caused by *Xanthomonas euvesicatoria* (*Xe*), is a primary concern for producers of bell peppers and tomatoes [9]. *Xe*, as a phyllosphere bacterial pathogen, proliferates mainly into the air-filled apoplast, which is connected directly to open air through epidermal pores called stomata. The water status within the apoplast could, therefore, be influenced by localized humidity levels during pathogen infection. In pepper and tomato fields, phyllosphere bacterial disease outbreaks typically occur after rainfall and/or during periods of high humidity, consistent with the “disease triangle” dogma in plant pathology. In addition, one of the earliest and most common symptoms of phyllosphere bacterial disease is the appearance of so-called “water-soaked” lesions in infected tissues. Although a highly recognizable feature of BS, it remains unclear the degree to which water soaking plays an active role in pathogen pathogenesis. Thus far, no molecular components have been identified as regulators of water-soaking symptoms in either *Xe* or its host plant candidate.

NPR1 is a well-studied master regulator for the expression of pathogenesis-related (PR) genes including PR1, PR2, and PR5 in plant response to various biotic challenges [10-14]. NPR1 also serves as a bridge connecting the expressions of PR genes and salicylic acid (SA) levels for triggering systemic acquired resistance (SAR), which is a very important plant immune system providing a broad-spectrum resistance effectively against a wide range of phytopathogens [15, 16]. Despite an extensive study on the role of NPR1 in plant immunity, few studies report the mechanism of transcriptional regulation on NPR1, and in particular whether and how the T3E influences NPR1 expression.

In this study, we identified XopN, a type three secretion (T3S) effector, as a functional contributor to the development of water-soaking in infected plant tissues. Furthermore, our results showed that both a glycerol uptake facilitator (glpF) and the type two secretion system of *Xe* are also partially responsible for the development of the water-soaking phenotype. We also demonstrated that XopN plays a role in suppressing the expression of NPR1 (nonexpressor of PR1) perhaps via the modification of the vascular one zinc transcription factor (VOZ) in *Nicotiana benthamiana* (*N. benthamiana*).

Results

*Increased humidity promotes the bacterial proliferation of *Xe* in infected tobacco and pepper plants*

To investigate if and how humidity impacts pathogen proliferation in plants infected with *Xe*, we setup disease assays under four different relative humidity (RH) levels: 40%, 60%, 80% and 90% RH, to mimick humidity levels in crop fields after different rainfall amounts. We monitored the growing populations of wild type *Xe* and various *Xe* isogenic strains, which were inoculated on *N. benthamiana* and pepper plants. As shown in Figure 3-1 A and C, *Xe* infected on *N. benthamiana* and pepper plants have increased population levels in response to increased humidity levels. However, the increased humidity did not appear to boost the proliferation of *Xe* Δ *HrcV* (a mutant with an impaired type III secretion system) (Figure 3-1). The *Xe*

inoculated *N. benthamiana* and pepper plant leaves developed more obvious water-soaking symptoms when the plants were incubated under higher humidity (90 % RH) compared to those that were incubated under lower relative humidity (40 % RH). This finding indicates that some T3Es might be associated with the increased growth of *Xe* in *N. benthamiana* and pepper under higher humidity conditions. .

XopN is a key contributor to the water-soaking phenotype in Xe-infected tobacco and pepper plants

Since the mutant *Xe* Δ *HrcV* strain was unable to trigger water-soaking symptoms in either tobacco or pepper under any experimental conditions (Figure 3-1 B and D), we speculate that some T3E(s) must contribute to the development of a watery environment in the apoplast. Here, we attempted to investigate whether the T3E *XopN* in *Xe* could contribute to the water-soaking symptoms in both *N. benthamiana* and pepper leaves infected by *Xe* bacteria. Our previous work showed that the mutant *Xe* strain *Xe* Δ *XopQ* could infect *N. benthamiana* plants (Chapter 2). In this study, we further deleted either *XopN*, *XopX* or *Xe4428* (*Xe* *avrRxo1*, a homologue of *Xoc* *avrRxo1*), in the *Xe* Δ *XopQ* background. These isogenic strains were inoculated on *N. benthamiana* plants. The infected plants were maintained under different RH conditions. As shown in Figure 3-2A, when *XopN* was deleted from *Xe*, the water-soaking phenotype was dramatically reduced; in contrast, the deletion of *XopX* or *Xe-AvrRxo1* did not significantly compromise the water-soaking phenotype. We also performed a growth curve assay to monitor the bacterial growth on both pepper and *N. benthamiana* plants grown under 40% RH or 90% RH. As shown in Figure 3-2 B and C, under 40% RH, the *Xe* Δ *XopQ* Δ *XopN* strain grows to a reduced population level as compared to the *Xe* Δ *XopQ* strain, which suggests *XopN* has a significant virulent function. However, under 90% RH, *Xe* Δ *XopQ* Δ *XopN* and *Xe* Δ *XopQ* grew to a similar sized population level on both *N. benthamiana* and pepper plants. The mutant, *Xe* Δ *HrcC* grew to a similar population level under either 40% or 90% RH on either *N. benthamiana* or pepper plants.

To test if the XopN triggered water-soaking phenotype is related to increased water content in the apoplast, we directly measured the apoplast water content in *N. benthamiana* leaves infected with *Xe* strains with or without XopN. As shown in Figure 3-2D, the apoplast water in *N. benthamiana* leaves infected with *Xe* Δ *XopQ* reached 11.6 ± 2.2 mg/cm², which is significantly higher than the leaves infected with *Xe* Δ *XopQ* Δ *XopN* (4.4 ± 0.8 mg/cm²). In control plants, there is no significant difference in the total relative water content of *N. benthamiana* leaves infected with the two *Xe* strains (Figure 3-2E).

In addition, we performed an *Agrobacterium*-mediated transient assay to express XopN, XopX, *Xe* avrRxo1, and XopQ in *N. benthamiana*. The overexpression of XopN resulted in a water-soaking like cell-death in *N. benthamiana* and pepper at 2 days post-inoculation (dpi) (Figure 3-3), while the overexpression of XopX, XopQ or *Xe* AvrRxo1 resulted in dry and yellowish cell death (Figure 3-3). Interestingly, this particular phenotype can only be induced by the expression of XopN in the cytosol but not in the nucleus (Supplemental Figure S3-1). Taken together, our results demonstrate that XopN, expressed and delivered either by *Xe* or *Agrobacterium tumefaciens* into plant cells, is able to elicit water-soaking symptoms.

Different water-soaking phenotypes in the presence or absence of XopN is not caused by the variation in levels of bacterial populations in the infected plant leaves

XopN has a significant virulent function as the *Xe* strain carrying *XopN* would grow to a higher bacterial population as compared to plant leaves infected by the *Xe* strain when *XopN* was deleted. Therefore, we hypothesized that *Xe* Δ *XopN* mutants elicited a reduced water-soaking phenotype than the *Xe* strains carrying *XopN*, because the *Xe* Δ *XopN* mutants proliferate to a reduced bacterial population level in comparison to *Xe* strains expressing *XopN*. To test this possibility, the starting inoculum of the *Xe* Δ *XopQ* Δ *XopN* mutant was adjusted to 2×10^8 CFU/ml, while *Xe* Δ *XopQ* was adjusted to 1×10^8 CFU/ml. After infiltrating the bacterial inoculums into pepper and *N. benthamiana* leaves, the bacterial populations were measured at 4 dpi. Because the starting inoculum of *Xe* Δ *XopQ* Δ *XopN* is 2-fold higher than that of

*Xe*Δ*XopQ*, the two bacterial populations at 4 dpi reached a similar level (Figure 3-4 A and B). However, *Xe*Δ*XopQ* that carries *XopN* still triggered a more obvious water-soaking phenotype than that of *Xe*Δ*XopQ*Δ*XopN* in both *N. benthamiana* and pepper plants (Figure 3-4 C and D). This result negates the possibility that water-soaking triggered by *XopN* resulted from an increased bacterial population in the infected leaves.

Expression of XopN could increase stomatal conductance

For plant leaves infected with *Xe*, the bacterial cells propagate in the apoplast, which is directly connected to the external environment through the stomata. We, therefore, also measured if *XopN* could regulate the stomatal aperture and subsequently impact the exchange of water between the apoplast and the open air. In this study, we employed a portable photosynthesis system LI-COR-6400XT to measure the stomatal conductance of *N. benthamiana* leaves infiltrated by *Xe* mutant strains, *Xe*Δ*XopQ*, *Xe*Δ*XopQ*Δ*XopX*, *Xe*Δ*XopQ*Δ*AvrBs2*, and *Xe*Δ*XopQ*Δ*XopN*. As illustrated in Figure 3-5, the plant leaves infiltrated with *Xe*Δ*XopQ*Δ*XopN* have the lowest stomatal conductance rate (mol H₂O m⁻² s⁻¹), suggesting the infected leaves have a reduced stomata aperture. While the leaves infected with *Xe*Δ*XopQ*, *Xe*Δ*XopQ*Δ*XopX*, and *Xe*Δ*XopQ*Δ*AvrBs2* have similar stomatal conductance rates, which are all higher than that of *Xe*Δ*XopQ*Δ*XopN*. The higher stomatal conductance rate also reflects a relatively higher apoplast water potential [17, 18]. Therefore, this result is consistent with our previous observation that *XopN*, but not *XopX* or *AvrBs2*, could increase water content in the apoplast, which might subsequently increase the stomatal conductance rate.

Expression of XopN enhanced the growth of a nonpathogenic Xe strain on tobacco and pepper leaves

Since *XopN* could induce a water-soaking phenotype, and an increased water content in the apoplast, we also investigated whether the expression of *XopN* could promote the growth of the co-colonized bacterial cells. We first co-inoculated an *Agrobacterium tumefaciens* strain

expressing XopN along with *Xe*Δ*HrcV* on *N. benthamiana* (Figure 3-6A). Expression of XopN along with the inoculation of *Xe*Δ*HrcV* triggered a much stronger water-soaking phenotype than the expression of XopN alone, while *Xe*Δ*HrcV* alone or MgCl₂ could not trigger any water-soaking phenotype (Figure 3-6A).

We also evaluated the impact of XopN on the *in planta* growth of *Xe*Δ*HrcV*. In this experiment, we first infiltrated either *Xe*Δ*XopQ* or *Xe*Δ*XopQ*Δ*XopN* (4x10⁸cfu/ml⁻¹) into the whole leaves of *N. benthamiana* and pepper plants. At 48 hrs post-inoculation (hpi), the pre-infected leaves were spray-inoculated with the mutant strain *Xe*Δ*HrcV* (*Km_r*) (1x10⁵ CFU/ml⁻¹). Another 48 hours later, the bacterial populations of *Xe*Δ*HrcV* (*Km_r*) were measured by plating the recovered bacteria on culture media with or without the supplementation of kanamycin. Only the nonpathogenic *Xe*Δ*HrcV* (*Km_r*) strain carrying a kanamycin resistance gene allows growth on the media supplemented with kanamycin. As shown in Figure 3-6 B and C, inoculated leaves co-infected with *Xe*Δ*HrcV* (*Km_r*) and *Xe*Δ*XopQ* grew to higher population levels than leaves co-infected with *Xe*Δ*XopQ*Δ*XopN*. As controls, we also measured the bacterial populations of *Xe*Δ*XopQ* or *Xe*Δ*XopQ*Δ*XopN* in the inoculated plant leaves at 0 hpi and 48 hpi (before the spray inoculation with *Xe*Δ*HrcV* (*Km_r*), where no significant growth difference was detected between the two strains on either *N. benthamiana* or pepper plants. Therefore, we speculate that the pre-inoculation of *Xe*Δ*XopQ* (carrying XopN) created a favorable environment for enhancing *Xe*Δ*HrcV* (*Km_r*) colonization on tobacco and pepper plants. In contrast, the nonpathogenic strain *Xe*Δ*HrcV* (*Km_r*) has a relatively lower growth rate on either *N. benthamiana* or pepper plants pre-inoculated by *Xe*Δ*XopQ*Δ*XopN* that is lacking XopN.

XopN interacts with *NbVOZ1* and *NbVOZ2* and regulates the expression of *NPR1* in *N. benthamiana*

To investigate whether XopN could regulate the expression of plant defense-related genes, we employed real-time PCR to monitor the expression levels of the pathogenesis-related (PR)

genes *NbPR1* and the SAR regulator *NbNPR1*. The *N. benthamiana* plants were sprayed with either MgCl₂ (mock) or either of the *Xe* mutant strains (*Xe*Δ*XopQ* or *Xe*Δ*XopQ*Δ*XopN*). The inoculated leaf tissue was collected at 24 hours post-inoculation. The expression of *NbNPR1* and *NbPR1* were detected by using gene-specific primers (Supplemental information Table S1). Interestingly, inoculation with *Xe*Δ*XopQ*Δ*XopN* induced about 50 to 100 fold higher expression levels of *NbNPR1* and *NbPR1* than inoculation with *Xe*Δ*XopQ* (Figure 3-7 A). Therefore, the expression of *XopN* may repress the expression of *NPR1* and *PR1* in *N. benthamiana*.

A previous report suggests that *Xoo*-*XopN* from the rice pathogen *Xanthomonas oryzae* pv. *oryzae* (*Xoo*) interacts with a rice plant transcription factor, OsVOZ2 *in vivo* [19]. Therefore, we attempted to test if *Xe*-*XopN* could interact with the VOZ protein in *N. benthamiana* plant cells. As illustrated in Figure 3-7 B and C, we confirmed that *XopN* indeed interacts with both *NbVOZ1* and *NbVOZ2* via our results of the split-luciferase assay (Figure 3-7 B) and co-IP assay (Figure 3-7 C). In addition, the co-expression of *NbVOZ1* or *NbVOZ2* with *Xe*-*XopN* could localize *Xe*-*XopN*-YFP to the nucleus, while the expression of *Xe*-*XopN*-YFP alone predominately localizes in the cytosol of transformed plant cells (Supplemental Figure S3-2). Since the *VOZ1* and *VOZ2* encoding transcription factors are conserved in all plant species, we hypothesized that *XopN* might regulate the expression of *NbNPR1* and *NbPR1* by interacting with the *NbVOZ* transcription factor. To test this hypothesis, we cloned the *NbNPR1* promoter in front of a GUS (β-glucuronidase) reporter gene. The *NbNPR1* promoter:GUS was co-expressed with either *NbVOZ1*, *NbVOZ2* or GFP by using an *Agrobacterium*-mediated transient assay. Surprisingly, *NbVOZ1* or *NbVOZ2* co-expressed with the *NbNPR1* promoter:GUS fusion resulted in a stronger GUS staining signal than that of co-expression with the *GFP* gene. We also attempted to co-express *Xe*-*XopN* with the *NbNPR1* promoter:GUS in combination with *NbVOZ* on *N. benthamiana* plant leaves. However, no conclusive data was obtained (data not shown).

To our knowledge, this is the first report that the expression of *NPR1* could be regulated by

the VOZ transcription factor. However, further studies are needed to determine the molecular interactions between XopN, VOZ, and NPR1, which may also help us understand if NPR1 or other targets of VOZ could contribute to the water-soaking phenotype triggered by *Xe*-XopN.

Discussion

The Bacterial spot disease caused by *Xanthomonas euvesicatoria* (*Xe*) can be easily identified due to the appearance of dark, irregular, water-soaked areas on the leaf. While a number of studies have indicated that an aqueous environment is essential for bacterial proliferation, it remains unclear which component of *Xe* contributes to the development of water-soaked symptoms in infected pepper and tomato plants. In this study, we identified that the T3E *Xe*-XopN has a key role in promoting the water-soaking phenotype in *Xe* infected plant leaves.

The virulence function of XopN has been previously characterized. For example, *Xoo*-XopN expressed in *Xanthomonas oryzae* pv. *oryzae* (*Xoo*), a xylem pathogen causing bacterial blight in rice, can suppress LipA-induced callose deposition [19, 20]. The XopN expressed by *Xanthomonas euvesicatoria* can interact with host defense-related proteins including the atypical receptor-like kinase named TARK1 and a 14-3-3 protein to suppress the PAMPs (pathogen-associated molecular patterns) involved in plant triggered immunity (PTI) upon *Xe* colonization in tomato. *Xe*-XopN and *Xoo*-XopN may share conserved functions to suppress PTI in different plant species [21, 22]. In this study, we characterized a new virulence function of XopN, that promotes the establishment of a water-enriched apoplast and enhanced colonization and proliferation of *Xe* bacterial cells in leaf tissue. However, are there any connections between the previously characterized virulence function and the XopN-mediated water-soaking phenotype? Is that possible that PTI-related events such as callose deposition can block water from being transported from the plant cell to the apoplast space? Answers to these questions will help gain a deep understanding of effector-trigger susceptibility.

Several residues of *Xe*-XopN have been reported to be essential for the full virulent function

of *Xe*-XopN. Specifically, *Xe*-XopN interacts with the tomato 14-3-3 isoform TFT1 in a phosphorylation manner at S688 along with two leucine residues (L64, L65) [21]. Moreover, mutations of these key residues in XopN prevents its binding to TFT1 in plant extracts [21]. When expressed in *Xe*, these XopN mutants also have reduced virulent function [21]. The residues L64 and L65 are required for XopN to bind to the Atypical Receptor-Like Kinase1 (TARK1) in tomato. In our preliminary data (data not shown), the mutation of S688 along with L64 and L65 did not alter the ability of XopN to trigger water-soaking phenotype. Therefore, the XopN triggered water-soaking phenotype may be independent of TFT1 and TARK1.

Although *Xe*-XopN is the primary component regulating the development of the water-soaking phenotype triggered by *Xe*, deletion of *XopN* did not completely abolish the water-soaking phenotype (Figure 3-2A). As shown in supplemental Figure S3-3A, we also demonstrated that the deletion of the type II secretion system (T2SS) in *Xe* reduced the water-soaking phenotype triggered by *Xe*, while the deletion of both XopN and the T2S almost completely blocked the water-soaking symptom. In Gram-negative bacteria various enzymes like the lipolytic enzyme are generally secreted via T2S [23]. It was proposed that the T2SS could enhance the establishment of T3S (Type Three Secretion System) during the *Xe* infection [24]. Thus, T2SS per se might not have the role of controlling the water-soaking phenotype, but by contrast, its function might be to help other T3Es including XopN to be translocated into plant cells. We also identified that the deletion of *glpF*, a glycerol transporter gene in *Xe*, partially compromised the water-soaking phenotype when the mutant strain was inoculated on *N. benthamiana* (Figure S3-3B). The *glpF* has been reported to participate in the synthesis of exopolysaccharides in *Xe*, where the exopolysaccharide produced by *Xe* may also contribute to the development of the water-soaking phenotype [5, 25]. However, the exact function of *glpF* and how it contributes to the water-soaking symptom is still in need of further investigation.

Apart from its contribution to the induction of the water-soaking phenotype, XopN was found

to be able to suppress the expression of NPR1 and PR1 in *N. benthamiana*. As NPR1 functions as a master regulator of the salicylic acid (SA)-signaling pathway and is a key component of plant basal immunity, it will be intriguing to investigate further whether or not XopN can suppress the SA-mediated SAR by down-regulating the expression of NPR1. To test this possibility, we also generated transgenic *N. benthamiana* plants to induce the expression of XopN (data not shown). These transgenic plants will allow us to further characterize the molecular functions of XopN in the future.

Previous research on the NPR1-mediated signal transduction pathway mainly focuses on how NPR1 regulates its downstream signaling events. For example, NPR1 induces the expression of the SA-dependent defense gene and disease resistance via its interaction with the transcription factors TCP and TGA in the nucleus. Several post-translational modifications of NPR1 proteins, including those that effect phosphorylation, S-nitrosylation and sumoylation, are essential for the regulation of NPR1 [26, 27]. However, few studies elucidate the regulation expression of NPR1 by upstream components. A recent study revealed the presence of W-box sequences in the promoter of the AtNPR1 genes. The expression of AtNPR1 can be regulated by WRKY6 and WRKY18 in a SA-dependent way [28-31]. SA also promotes the formation of a protein complex that includes NPR1, CDK8 (CYCLIN-DEPENDENT KINASE8) and WRKY18 in *Arabidopsis* plant cells. The complex can bind to the W-box in the NPR1 promoter region and regulate AtNPR1 expression [29].

In this study, we identified another transcription factor *NbVOZ* that might be targeted by XopN to regulate the transcriptional capacity of *NbNPR1*. *VOZ* is a plant transcription factor family with two members, *VOZ1* and *VOZ2*, that are conserved in diverse plant species [32-36]. Interestingly, a *VOZ* family member in rice, *OsVOZ2*, was identified as a target of *Xoo*-XopN in rice plant cells [19]. Consistently, *Xe*-XopN can interact with two members of *NbVOZ*, *NbVOZ1* and *NbVOZ2*, in *N. benthamiana* plant cells (Figure 3-7 B and C), which may also

regulate the transcriptional activity of *NbNPR1* in a GUS-reporter assay (Figure 3-7 D). In the future, electrophoretic mobility shift assay and a chromatin immunoprecipitation (ChIP)-PCR will be performed to validate whether *NbVOZ1* and *NbVOZ2*, can bind to the promoter of *NbNPR1*. Transgenic *N. benthamiana* plants with the overexpression of *NbVOZ1* and *NbVOZ2*, and mutant *N. benthamiana* plants carrying *VOZ1/VOZ2* deletions, will be also generated for evaluating the function of *NbVOZ1/NbVOZ2* in response to the *Xe* infection.

Methods and materials

Plant material and growth conditions

Seeds from *N. benthamiana* and pepper (*Capsicum annuum*, *Ca*) were germinated in soil at room temperature under 8h/16h light/dark cycle at 25°C/20°C. After germination, plants were grown under 14h/10h light/dark cycle at 25°C/20°C. For the experiments described herein, 6-week-old tobacco and pepper plants were used.

Bacteria growth

Escherichia coli (*E. coli*) *DH5 α* and *Rho5* were grown on Luria agar medium at 37°C. *Agrobacterium tumefaciens* (*A. tumefaciens*) strain *GV2260* and *Xe* were grown on a Luria agar medium and an NYGA medium at 28°C. The concentrations of antibiotic selections in this study were as follows: 50 μ g/ml kanamycin (Km), 100 μ g/ml Spectinomycin (Sp), and 30 μ g/ml gentamycin (Gm). *Xe* and *A. tumefaciens* strain *GV2260* were intrinsically both resistant to rifampicin (Rif) with a concentration of 100 μ g/ml.

Phytopathogen strains and mutant strains generated by the marker-exchange approach

Xe and its various mutants were utilized for the investigation in this study. The T3Es were knocked out from *Xe* genome one-by-one. The general procedure we used included two steps: (a) marker exchange to remove the gene, and (b) application of flippase to remove kanamycin, which is the marker introduced during the last step in order to identify the mutant strain [37].

Upstream and downstream sequences flanking XopN were amplified using the genome DNA of *Xe* as the template. In terms of the primers we utilized, *Xe*-XopN upstream was amplified with primers “*Xe*-XopN upstream SwaI For” and “*Xe*-XopN downstream SwaI Rev,” while *Xe*-XopN downstream was amplified with primers “*Xe*-XopN upstream pmeI For” and “*Xe*-XopN downstream pmeI Rev”. The upstream sequence of XopN was cloned to the PCR8 vector using the Gibson assembly kit (New England Biolabs), while the downstream sequence of XopN was cloned to the construct from the final step, again via Gibson assembly. Finally, the construct was named as PCR8-XopN upstream-Km_r-XopN downstream, which we then subcloned to vector PLVC18L by LR Gateway cloning (Invitrogen) to generate pLVC18L-XopN upstream-Km_r-XopN downstream-SacB/R.

The plasmid DNA was transfected to *Rho5* for further conjugation. Note that *Rho5* already carries the helper plasmid DNA for conjugation. *Xe* and *Rho5* carrying the construct were co-cultured for 4 hours in a liquid medium with diaminopimelic acid. After conjugation, the mix of bacteria was placed on the medium without supplementation of antibiotic to co-culture for another 48 hours. The *Xe*Δ*XopN* mutant was selected from the NYGA medium supplemented with Rifamycin and Kanamycin.

In order to remove another T3E gene from *Xe*Δ*XopN* profile, we needed to remove the selection marker introduced to *Xe* during the final step. A plasmid DNA pEDV6-flippase-Gentamycin–SacB/R can recognize the flanking sequence of Kanamycin and cut off the Kanamycin gene using the flippase. After conjugating the above-described plasmid DNA to *Xe*Δ*XopN* (Km_r), we then screen the *Xe* clone carrying the vector based on the selection of gentamycin, after which we determined whether kanamycin had been removed, given that it is sensitive to this antibiotic. Since the SacB/R gene is toxic when combined with sucrose, the supplementation of sucrose in the medium was used to eliminate the pEDV6 construct. The *Xe* clone sensitive to both gentamycin and kanamycin can be used to knock out the other T3Es.

In general, the description provided above represents the typical procedure for producing *Xe* mutant strains impaired by multiple T3Es. For this investigation, we prepared the following 11

Xe mutants using this approach: *Xe*Δ*XopQ*, *Xe*Δ*HrcV*, *Xe*Δ*HrcV* (*Kmr*), *Xe*Δ*XopQ*Δ/*XopN*, *Xe*Δ*XopQ*Δ*XopX*, *Xe*Δ*XopQ*Δ*avrBS2*, *Xe*Δ*XopQ*Δ*avrRxo1*, *Xe*Δ*XopQ*Δ*glpF*, *Xe*Δ*XopQ*Δ*T2SS*, *Xe*Δ*XopQ*Δ*T2SS*Δ*XopN*, and *Xe*Δ*XopQ*Δ*glpF*Δ*T2SS*. All primers used for marker exchange in this chapter can be found in the supplemental table S3-1.

Gene cloning, site-directed mutagenesis, and plasmid construction

The ORF of *XopN* and the ORFs of *NbVOZ1*, *NB*, and *VOZ2* were cloned to two destination vectors, pEarley101 and pEarley102 vectors, both carrying a 35S promoter. These two vectors, pEarley101 and pEarley102, displayed HA-tag and 3Flag-tag at C terminals, respectively. The *Xe-XopN* ORF was amplified from the genome DNA of *Xe* using primers “*Xe-XopN* ORF For” and “*Xe-XopN* ORF Rev”, and cloned into the pDonr207 vector (donor vector) using BP Gateway cloning (Invitrogen). The same procedure was followed for cloning the ORFs of *NbVOZ1* and *NbVOZ2* to the pDonr207 vector. The sequences of primers are listed in the supplementary table S3-1. The above donor vectors were subcloned to pEarley101 or pEarley102, in *GV2260* using modified LR Gateway cloning kit as described [38].

Bacterial growth curve assay

The bacterial proliferation in inoculated *N. benthamiana* and *C. annuum* plants was assessed via standard growth curve assays [39, 40]. Different humidity settings were achieved by covering a acrylamide fiberglass box, in which a humidifier and a humidity/temperature Data Logger (Lascar) were placed. The humidity and temperature were recorded over the period of disease assay.

Two inoculation methods (infiltration and spray) were used in this study. The bacteria were cultivated on a medium supplemented with appropriate antibiotics at 28 °C for two days; the bacterial cells were then suspended in 10 mM MgCl₂ and diluted to 1X10⁵ CFU/ml⁻¹. The bacterial inoculum was infiltrated into the backside of the plant leaf using a blunt-end needleless syringe. For the subsequent inoculation, *Xe*Δ*HrcV* with Kanamycin resistance was

spray-inoculated to *N. benthamiana* leaves pre-treated by *Xe* Δ *XopQ* and *Xe* Δ *XopQ* Δ *XopN*. The bacterial cells were then collected and suspended in 10mM MgCl₂ with 0.02% Silwet L77 and diluted to OD₆₀₀ 0.1. The plants were covered and kept at 100% moisture levels for one day prior to inoculation. The inoculated plants were maintained under 14 h light/10 h dark at room temperature for 6 days; leaf discs (990 mm²) were randomly sampled from the inoculated leaves at Day 0 and Day 6 for growth curve assays. The sampled leaf discs were grounded in 990 μ L of 10 mM MgCl₂, and vortexed for one minute before dilution and plating on respective media supplemented with proper antibiotics. The plates were cultivated at 28°C until the bacteria colonies could be counted. These bacteria colony numbers were then used to calculate the bacteria proliferation ratio (Log₁₀ CFU/cm²). All growth curves represent three biological repeats with replicates.

Agrobacterium-mediated transient assay, western blot, and co-immunoprecipitation

The agrobacteria infiltration, plant protein isolation, and co-IP were performed as described by Krasileva KV et al. (2010) [41]. Agrobacterium strains carrying different constructs were adjusted to OD₆₀₀ 0.4 and infiltrated to the mesophyll tissue using blunt-end syringes without needles. Leaf disks (1 cm²) were collected at 2 dpi and ground in a 100 μ L 1X Laemmli SDS-PAGE buffer. Then, 25 μ L protein extract samples were loaded into 10% SDS-PAGE gel. The protein samples were blotted to PVDF membrane and hybridized with the appropriate antibody [anti-HA-HRP (1: 2,000), anti-T7-3Flag (1: 2,000)]. The western blot signal was detected by using an ECL kit (Thermo Scientific, USA). After western blotting detection, the PVDF membrane was stained with 0.5 % Ponceau S solution to detect the Rubisco protein as the equal loading control. For co-IP, the Flag-tagged fusion protein was immunoprecipitated with anti-3Flag and the co-IP samples were detected with anti-HA-HRP. Prior to immunoprecipitation, 25 μ L of samples were saved as the input control. The immunoprecipitated proteins and input controls were loaded on 10% SDS-PAGE gel, blotted with a nitrocellulose membrane, and probed with either anti-Flag followed by a secondary

antibody or anti-HA-HRP.

RNA isolation, RT-PCR and real-time PCR

For RT-PCR, total RNA was isolated from *N. benthamiana* leaf tissues using TRIzol Reagent (Invitrogen) according to the manufacturer's instructions. DNA contamination was eliminated by treating total RNA with UltraPure DNase I (Invitrogen). The integrity and quantity of total RNA were ascertained by running it through 0.8% agarose gel using a NanoDrop ND-1000 spectrophotometer (NanoDrop Technologies). Then, cDNA synthesis was performed using the SuperScript III First-Strand System for RT-PCR kit (Invitrogen) with an oligo-dT primer based on the manufacturer's instructions. Real-time PCR was carried out with a specimen of cDNA diluted 20-times using the Qiagen SYBR Green PCR kit in accordance with the manufacturer's protocol. Gene-specific primers for real-time PCR were synthesized by IDT (Integrated DNA Technologies) and referred to as "NbActin real-time PCR For," "NbActin real-time PCR Rev," etc.

GUS Assay-Construction of Reporter Plasmids and Transgenic Plants

The promoter region of NbNPR1 was amplified via PCR using *N. benthamiana* genome DNA as the template. We then cloned it to pDonor207 vector, which was subsequently introduced to the plasmid DNA pKgwfs7.0 carrying a GUS gene [42]. The final construct is referred to as pKgwfs7.0-NbNPR1promoter:GUS. After being transfected to *GV2260*, it was used for the GUS reporter assay. NbVOZ1 and NbVOZ2 driven by the 35S promoter were then used to determine if they could regulate the transcriptional activity of the NbNPR1 promoter. Two combinations were utilized: 1) 35S:NbVOZ1 and NbNPR1promoter:GUS, and 2) 35S:NbVOZ1 and NbNPR1promoter:GUS. Another combination, 35S:GFP and NbNPR1promoter:GUS, served as the control. *N. benthamiana* leaves were infiltrated with *GV2260* cultures within OD600 0.4 (0.2 + 0.2).

According to the methods described by Jefferson et al. (1987) [43, 44], after incubation for 48

hours, we determined the GUS enzyme activity in the tested plants by staining with X-glucuronide (Life Technologies/GibcoBRL) as a substrate. After destaining with 70% ethanol overnight, we were able to evaluate the GUS assay capacity using Image J.

Split Luciferase constructs generation and assay

The ORFs of NbVOZ1, NbVOZ2, and XopN in donor vectors generated above were cloned to luciferase expression vectors via LR cloning. Specifically, NbVOZ1 and NbVOZ2 were cloned to the vector harboring N-terminal luciferase (NLUC), while XopN was cloned to the vector harboring C-terminal luciferase (CLUC); all were then transfected into *Agrobacterium GV2260*. Two combinations were utilized: 1) NLUC-NbVOZ1 and CLUC-XopN, and 2) NLUC-NbVOZ2 and CLUC-XopN. A positive control consists of NLUC-Rar1 and CLUC-Sgt1 along with a negative control consists of two empty vectors that were also used to validate the appropriateness of this approach. *N. benthamiana* leaves were infiltrated with *GV2260* cultures within OD600 0.4 (0.2 + 0.2). After incubation for 48 hours, luciferin (0.25 g/L) was infiltrated to the same spot carrying the *Agrobacterium* and incubated for an additional 10 min. Prior to detecting the luciferase signal, the *N. benthamiana* leaves were placed in the dark for 10 min owing to quenching auto-fluorescence signals. Chemical fluorescence signals were detected using the CCD camera of the Gel Doc™ XR+ System (Bio-Rad).

Stomatal conductance

A portable photosynthesis system (LI-6400T, Li-Cor Inc., USA) with a 6400-02B light source (blue and red diode) was used to measure the following photosynthetic gas exchange parameters of the *N. benthamiana* leaves *in vivo*: net photosynthetic rate (P_n), intercellular CO₂ concentration (C_i), transpiration rate (E), and stomatal conductance (G_s). Before the measurement, *N. benthamiana* leaves were infiltrated by four isogenic *Xe* strains including *Xe*Δ*XopQ*, *Xe*Δ*XopQ*Δ*XopX*, *Xe*Δ*XopQ*Δ*AvrBs2*, and *Xe*Δ*XopQ*Δ*XopN*. After the measurement, the data of E and G_s were utilized for further analysis. Measurements were

obtained under an artificial irradiance of $1000 \mu\text{mol (photons) m}^{-2} \text{s}^{-1}$ at a temperature of 25°C using the fifth completely expanded leaf from the top of each plant. CO_2 concentration and ambient water-vapor pressure were maintained at $385 \mu\text{mol mol}^{-1}$ and $1.30 \pm 0.15 \text{ kPa}$, respectively.

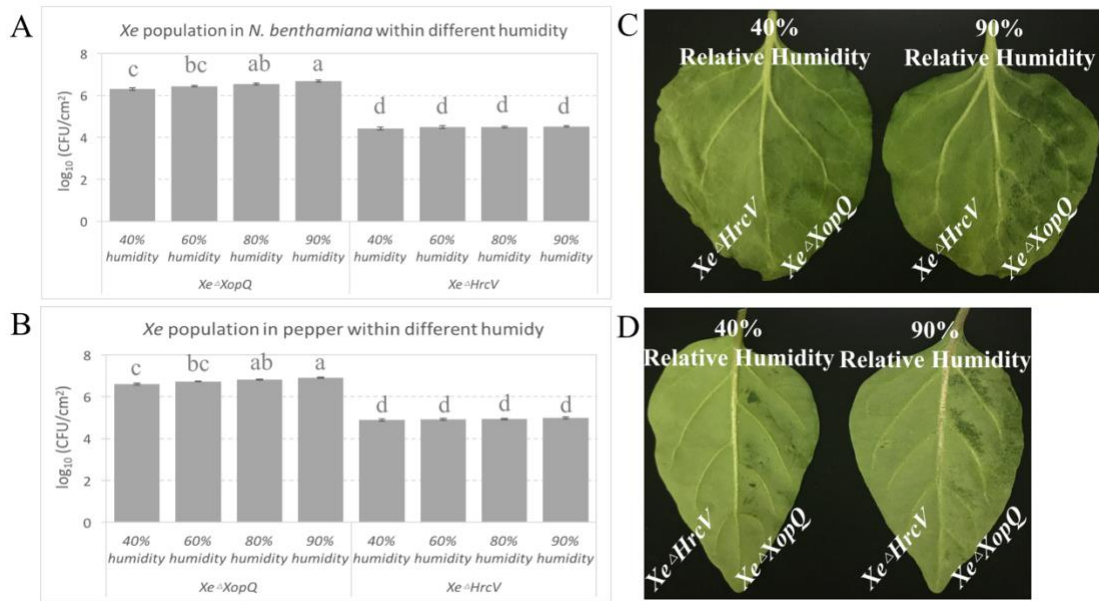


Figure 3- 1 The amplification of *Xe* increases with elevated humidity in both tobacco and pepper.

Bacterial populations of *Xe* Δ *XopQ* and *Xe* Δ *HrcV* grown on (A) and pepper (C) leaves under 40% humidity including (RH) , 60% RH, 80% RH and 90% RH. The populations were measured at 6 days post-inoculation (dpi) with a starting inoculum of 1×10^5 cfu ml⁻¹. Two-way ANOVA with Tukey's test (significance set at $P \leq 0.05$) was performed. Significant differences are indicated by different letters. n = 3 technical replicates; data are shown as mean \pm s.e. The phenotypes of *Xe* infection, under 40% RH and 90% RH, of *N. benthamiana* (B) and pepper (D) leaves that were inoculated by *Xe* Δ *XopQ* and *Xe* Δ *HrcV*, respectively. The left half of the leaf was inoculated by *Xe* Δ *HrcV*, while right half was inoculated by *Xe* Δ *XopQ*. The pictures of visualized symptom were taken 6 dpi with a starting inoculum of 1×10^5 cfu ml⁻¹. Experiments were repeated three times with similar results.

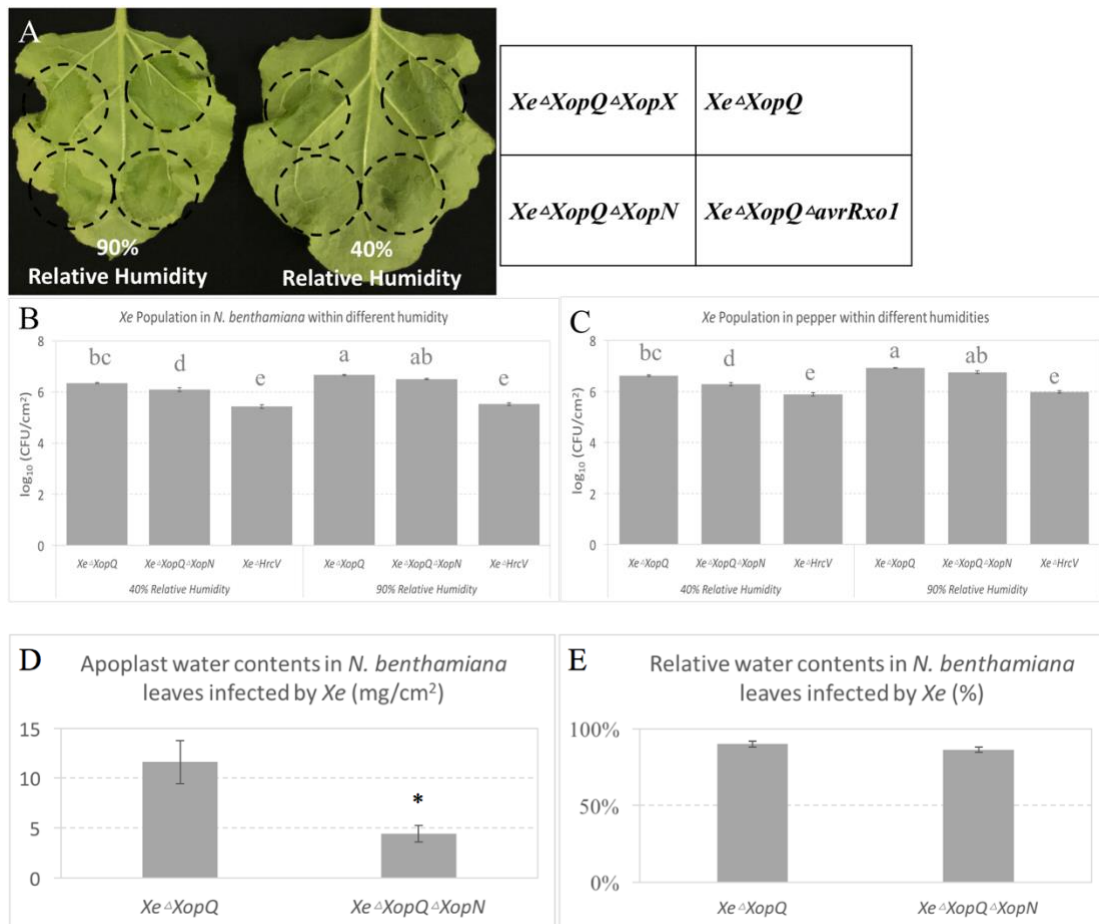


Figure 3- 2 *XopN* is required for developing of the water-soaking phenotype in the *Xe* infected tobacco and pepper plants , but this function can be impacted by high humidity.

Four *Xe* isogenic strains including *Xe* Δ *XopQ*, *Xe* Δ *XopQ* Δ *XopX*, *Xe* Δ *XopQ* Δ *avrRxoI*, and *Xe* Δ *XopQ* Δ *XopN* within a concentration OD600 at 0.4 were inoculated to wild type *N. benthamiana* (A). Pictures were obtained at 2 days post-inoculation. In planta growth of three *Xe* strains including *Xe* Δ *XopQ*, *Xe* Δ *XopQ*, and *Xe* Δ *HrcV* measured at Day 6 with a starting inoculum of 10⁴ CFU/mL after infiltration of leaves of *N. benthamiana* (B) and pepper (C) under normal humidity and 90% relative humidity. Two-way ANOVA with Tukey's test (significance set at $P \leq 0.05$) was performed. $n = 3$ biological replicates; data are shown as mean \pm s.e. Different letters indicate statistically significant differences. Leaf relative water content and apoplastic water content were measured in *N. benthamiana* leaves inoculated by

*Xe*Δ*XopQ* and *Xe*Δ*XopQ*Δ*XopN* as shown in (D) and (E), respectively. Star indicates statistically significant differences. Experiments were repeated three times with similar results.



Figure 3- 3 Transient expression of XopN induces water-soaking symptoms in both tobacco and pepper.

N. benthamiana and pepper leaves were inoculated by *Agrobacterium* harboring *Xe-XopN*, *Xe-XopX*, *Xe-XopQ* and *Xe-avrRxo1* driven by 35S promoter at a concentration at OD600 0.4. Pictures were obtained 2 days post-inoculation. Experiments were repeated three times with similar results.

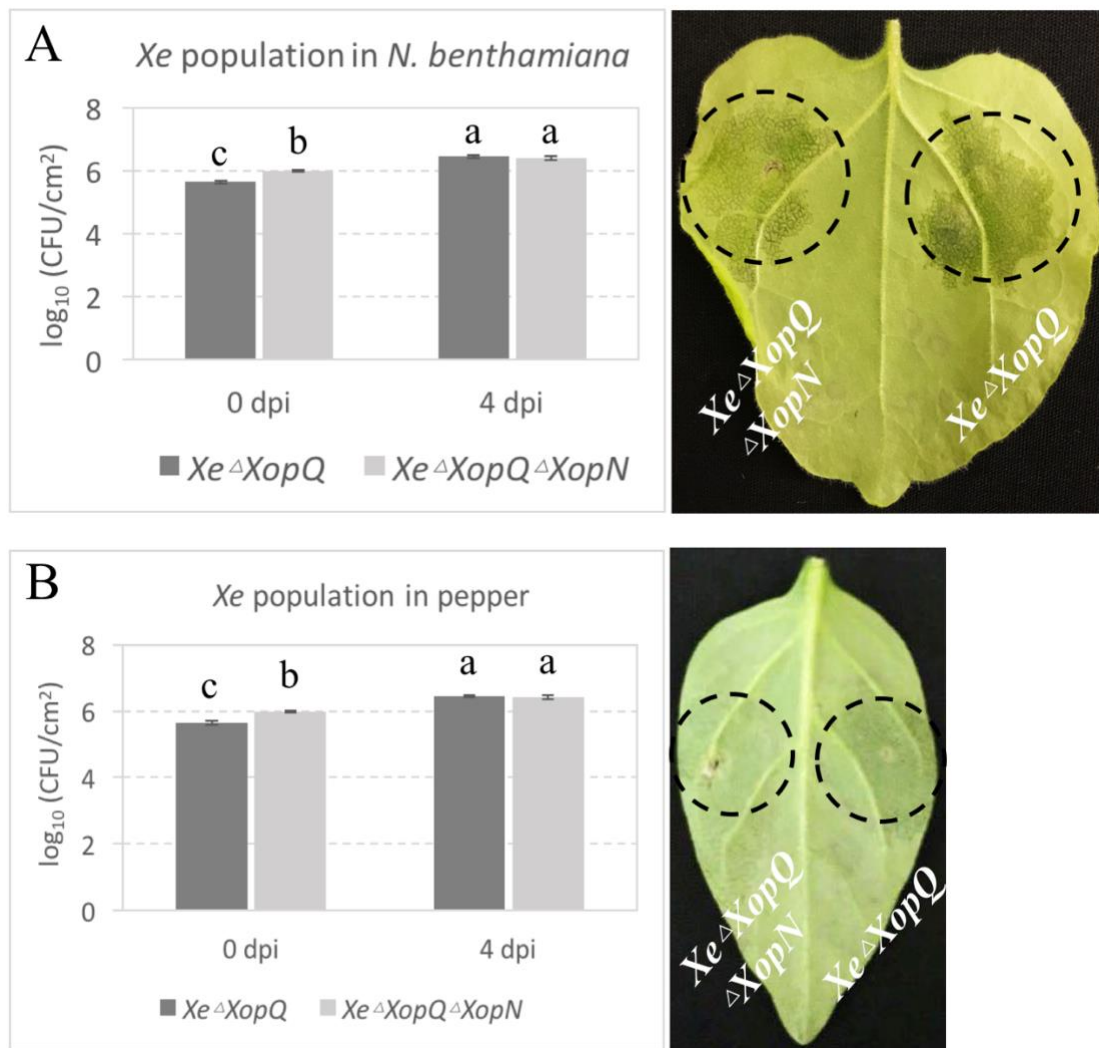


Figure 3- 4 Different water-soaking phenotypes in presence or absence of XopN is not caused by the variation of bacterial populations in the infected plant leaves.

In planta growth of *Xe* Δ *XopQ* and *Xe* Δ *XopQ* Δ *XopN* measured at 4 Day post infiltration to leaves of *N. benthamiana* (A) and pepper (C). The concentrations of starting inoculum of *Xe* Δ *XopQ* and *Xe* Δ *XopQ* Δ *XopN* were, respectively, 1×10^8 cfu ml⁻¹ and 2×10^8 cfu ml⁻¹. Visualized water-soaking phenotypes infected by *Xe* strains are shown in (B), *N. benthamiana*, and (D), pepper, respectively. On both leaves, the left spot indicates the inoculation of *Xe* Δ *XopQ* Δ *XopN*, while the right spot denotes the inoculation of *Xe* Δ *XopQ*. Experiments were repeated three times with similar results.

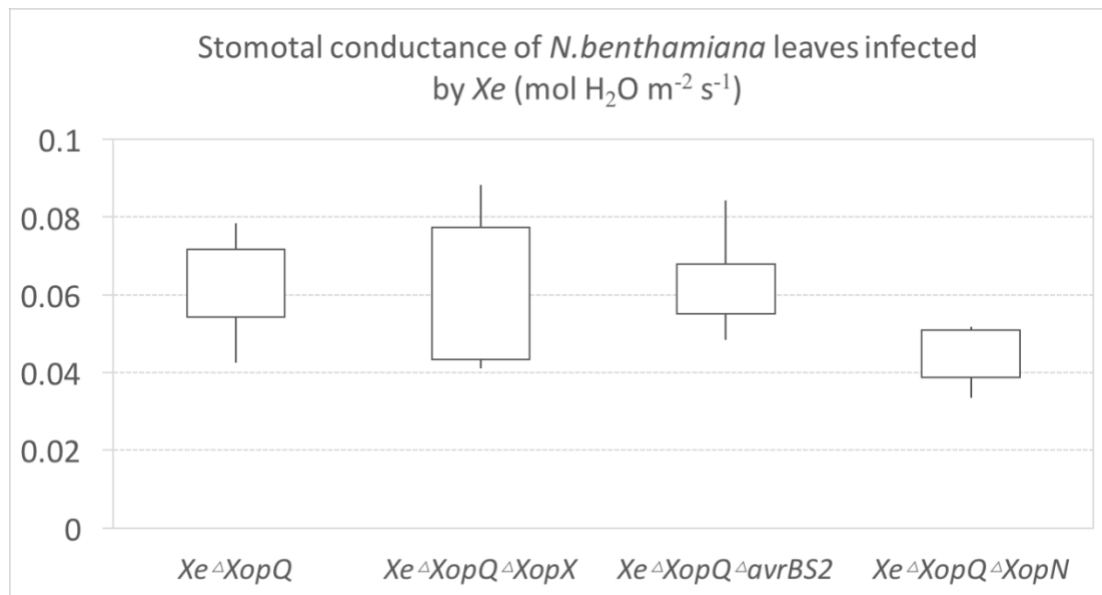


Figure 3- 5 XopN may up regulate stomatal aperture.

Stomatal conductance of *N. benthamiana* leaves were measured after inoculation by four *Xanthomonas* isogenic strains including *Xe*Δ*XopQ*, *Xe*Δ*XopQ*Δ*XopX*, *Xe*Δ*XopQ*Δ*avrBS2*, *Xe*Δ*XopQ*Δ*XopN*. The measurements were conducted 2 days post-inoculation and the starting inoculum concentration was 1×10^5 cfu ml⁻¹. The data are presented in a box plot. Experiments were repeated three times with similar results.

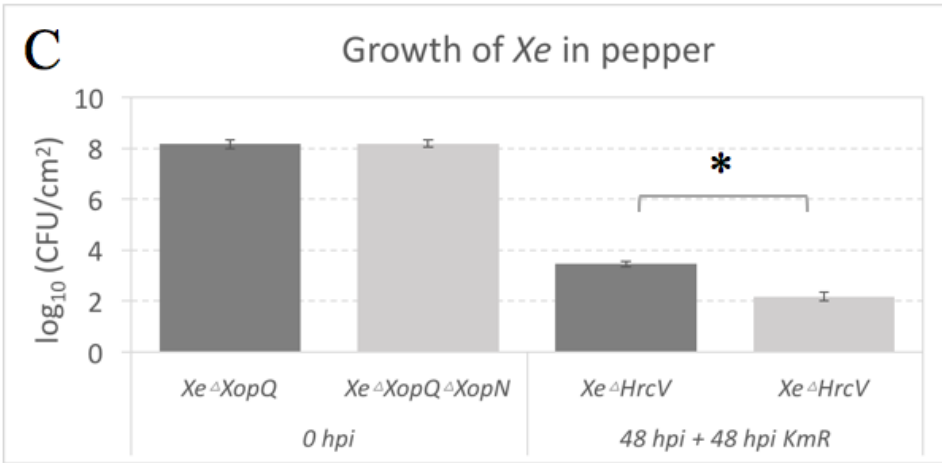
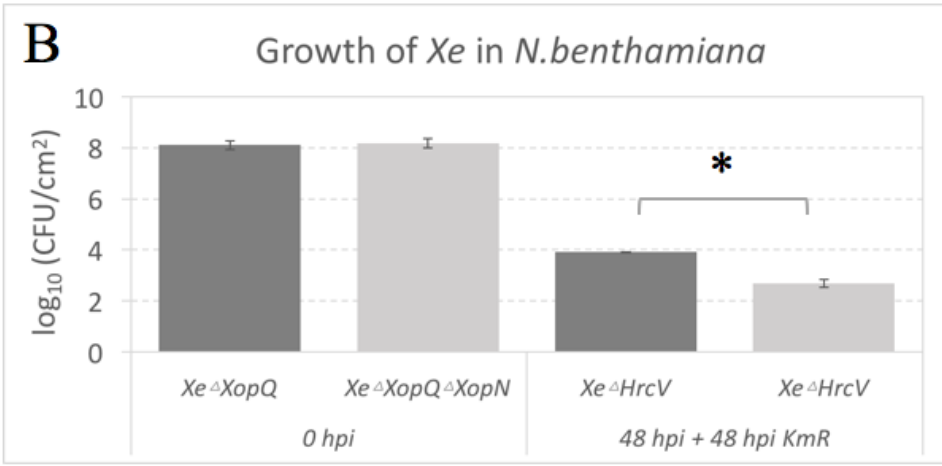
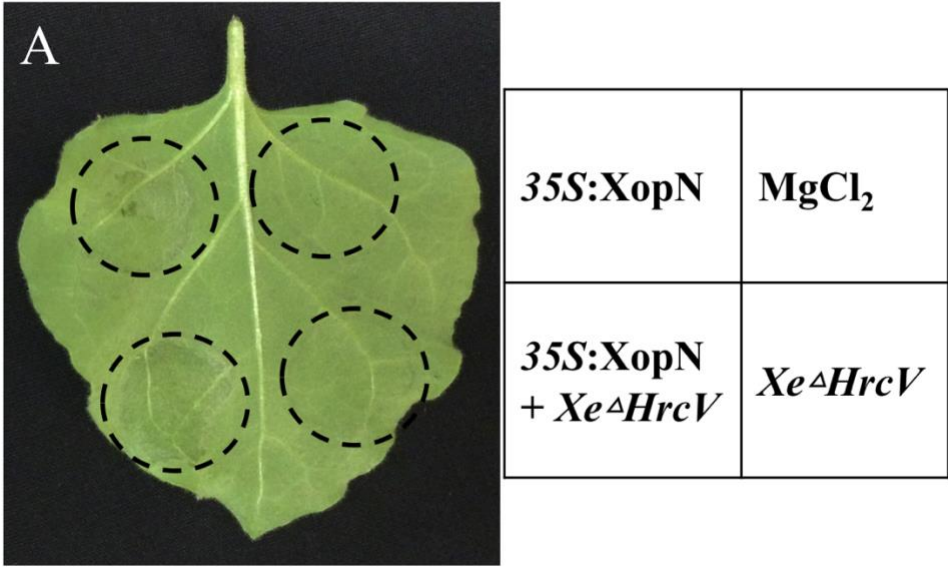


Figure 3- 6 A nonpathogenic *Xe* strain, *Xe* Δ *HrcV*, can trigger weak water soaking with

the co-expression of XopN and can be introduced by water soaking induced by XopN.

(A) *N. benthamiana* leaf was inoculated by MgCl₂, *Xe*-XopN (Agrobacteria), *Xe*Δ*HrcV*, a combination of *Xe*-XopN (Agrobacteria) and *Xe*Δ*HrcV* with a concentration of OD600 at 0.4 (single inoculation), or a concentration of OD600 at 0.4 (0.2 + 0.2, co-inoculation). The image was taken 2 days post-inoculation. For (B) and (C), the inoculation of *Xe*Δ*HrcV* followed the inoculation of *Xe*Δ*XopQ* and *Xe*Δ*XopQ*Δ*XopN* 48 hours later. The population of *Xe*Δ*HrcV* mutant strain with kanamycin-resistance was obtained at another 48 hours post-inoculation with a starting inoculum at 1×10^5 cfu ml⁻¹ in *N. benthamiana* (B) and pepper (C). Two-way ANOVA with Tukey's test (significance set at $P \leq 0.05$) was performed. Significant differences are indicated by asterisk. n = 3 biological replicates; data are shown as mean ± s.e. Experiments were replicated three times with similar results.

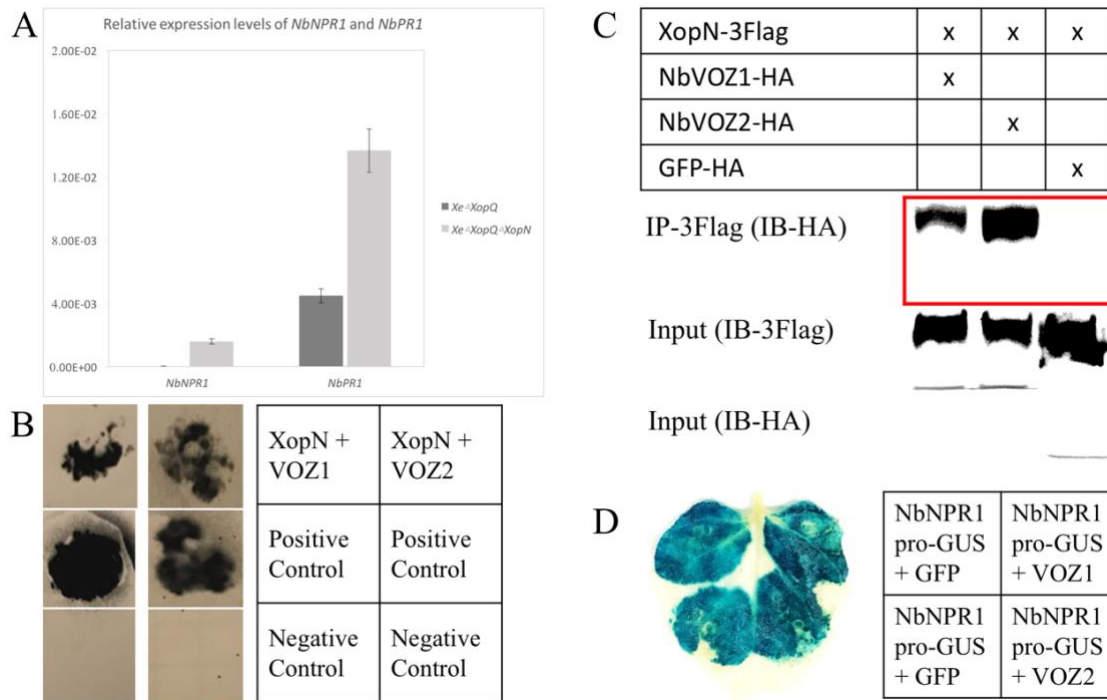


Figure 3- 7 XopN can regulate *NbNPR1* expression through its interaction with *NbVOZ1* and *NbVOZ2*.

(A) The relative expression levels of *NbNPR1* and *NbPR1* in leaves infected by *XeΔXopQ* and *XeΔXopQΔXopN* 24 hours post-inoculation with an inoculum concentration of 1×10^5 cfu ml⁻¹. (B) Split luciferase results for XopN with *NbVOZ1* or *NbVOZ2*. A combination of GUS-LucN and LucC-GUS was used as the negative control; a combination of RAR1-LucN and LucC-SGT1 was used as the positive control. (C) Co-immunoprecipitation of XopN fused with a 3×Flag tag and *NbVOZ1* or *NbVOZ2* fused with a HA tag in *N. benthamiana* leaves. The proteins pulled down by anti-3Flag beads were detected using western blotting with a-HA-HRP primary antibody. Two Western blots of the input protein extract (prior to precipitation) are shown in the middle and bottom. (D) Semi-quantitative evaluation of the impact of *NbVOZ1* and *NbVOZ2* on the activity of *NbNPR1* promoter fused with a GUS reporter. The co-inoculation of *Agrobacteria* carrying *NbNPR1* promoter:GUS along with *Agrobacteria* carrying *NbVOZ1*, *NbVOZ2*, or GFP with a concentration of OD600 at 0.4 (0.2 + 0.2). The staining was conducted 2 days post-inoculation and the picture was taken after destaining.

Supplementary information

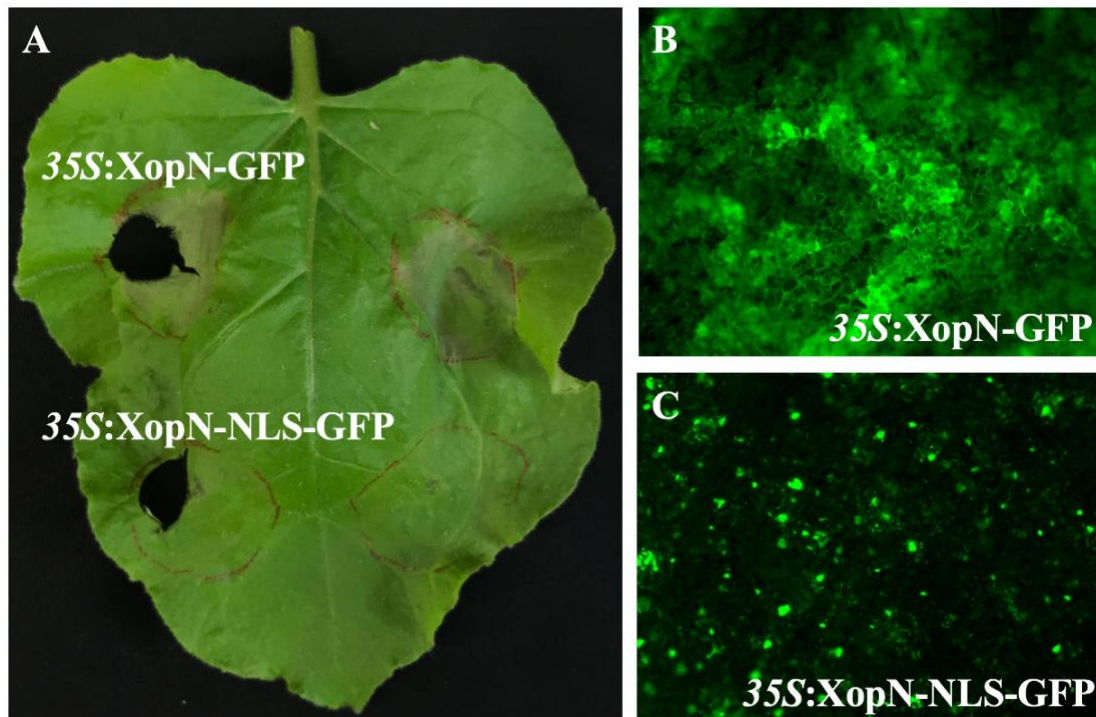


Figure S3- 1 Transient expression of XopN can trigger water-soaking cell death only localized at cytosol.

(A) *Agrobacterium* strain *GV2260* carrying *35S:XopN-GFP* and *35S:XopN-NLS-GFP* (Nuclear Localization Signal, NLS) at OD₆₀₀ 0.4 were inoculated to *N. benthamiana*. The fluorescent signals of *35S:XopN-GFP* and *35S:XopN-NLS-GFP* displayed their cellular localizations as shown respectively in (B) and (C). The image of the leaf in (A) was taken at 48 hours post-inoculation simultaneously with the observation of fluorescent signals. Experiments were repeated three times with similar results.

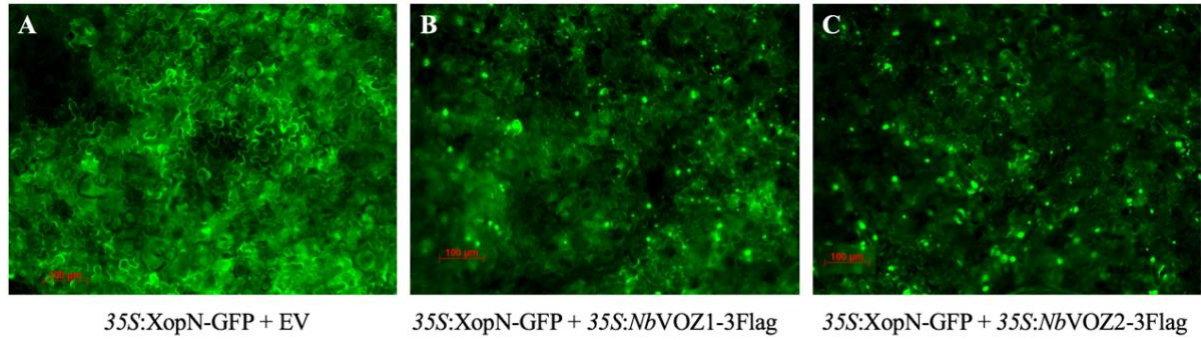


Figure S3- 2 The localization of XopN can be changed upon co-expression with *NbVOZ1* and *NbVOZ2*.

Co-expression of 3 sets of proteins including 35S:XopN-GFP with empty vector (A), 35S:XopN-GFP with 35S:*NbVOZ1*-3Flag (B), and 35S:XopN-GFP with 35S:*NbVOZ2*-3Flag (C) at OD600 0.8 (0.4 + 0.4) were inoculated to *N. benthamiana*. The fluorescent signals were observed at 48 hours post-inoculation. Experiments were repeated three times with similar results.

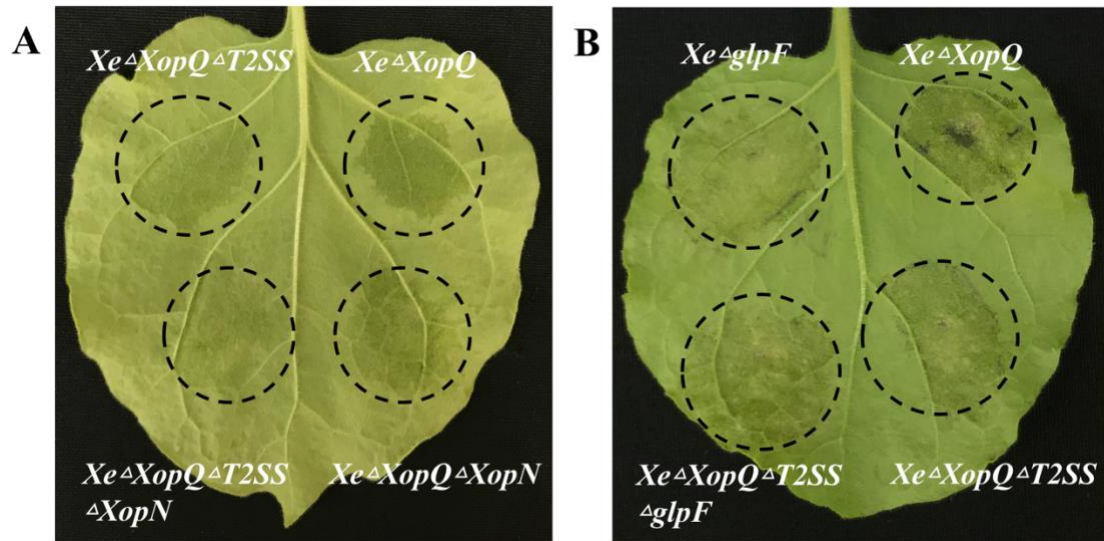


Figure S3- 3 Type 2 secretion system (T2SS) and glycerol uptake facilitator (glpF) are also involved in instigating water-soaking symptoms.

(A) Four *Xe* isogenic strains, including *Xe*Δ*XopQ*, *Xe*Δ*T2SS*Δ*XopQ*, *Xe*Δ*XopQ*Δ/*XopN* and *Xe*Δ*T2SS*Δ*XopQ*Δ*XopN* within a concentration OD600 at 0.4 were inoculated to wild-type *N. benthamiana*. (B) Four *Xe* isogenic strains including *Xe*Δ*XopQ*, *Xe*Δ*glpF*Δ*XopQ*, *Xe*Δ*XopQ*Δ*T2SS* and *Xe*Δ*T2SS*Δ*XopQ*Δ*glpF* within a concentration OD600 at 0.4 were inoculated to wild-type *N. benthamiana*. Pictures were obtained at 2 days post-inoculation. Experiments were repeated three times with similar results.

Table S3- 1 Sequences of primers utilized in this chapter

Name	Sequences
<i>Xe</i> -XopN ORF For	aaaagcaggcttgcataatgaagtcacccgcacccgtcgattc
<i>Xe</i> -XopN ORF Rev	caagaaaagctgggtagaattccaccaggcttgagtgttgc
<i>Xe</i> -avrRxo1 ORF For	caccggatccatggcatcgcgccattcggtg
<i>Xe</i> -avrRxo1 ORF Rev	gagctcgtcgattatcttatcagccaaat
<i>NbVOZ1</i> ORF For	aaaaagcaggcttgcataatgaagtcacccgcacccgtcgattc
<i>NbVOZ1</i> ORF Rev	agaaaagctgggtagaattccaccaggcttgagtgttgc
<i>NbVOZ2</i> ORF For	aaaaagcaggcttg atgaggaagggttcgaagagg
<i>NbVOZ2</i> ORF Rev	agaaaagctgggtacgttatgaagtagccatccagatc
<i>NbNPR1</i> promoter For	gggacaagttttacaaaaagcaggcttggttacacatgacatgtgca
<i>NbNPR1</i> promoter Rev	ggggaccactttgtacaagaagctgggtaacgcagtcaccactattatccat
<i>Xe</i> -XopN upstream SwaI For	gcaggctccgaattcgccctattttacgacagcctccctggcgct
<i>Xe</i> -XopN upstream SwaI Rev	aagcttaattggatccatttcatcgggacatctctgacgt
<i>Xe</i> -XopN upstream PmeI For	atggctaattcccatgtcgtttcaagcactggtgtgaggtgat
<i>Xe</i> -XopN upstream PmeI Rev	actagtcgacttaattaagtttgcgatgcgcgttcgaattc
<i>Xe</i> -avrRxo1 upstream SwaI For	gcaggctccgaattcgccctattttatgacaccgacgtgtgtgcgact
<i>Xe</i> -avrRxo1 upstream SwaI Rev	aagcttaattggatccatttaccgaaattcctctgcaccta
<i>Xe</i> -avrRxo1 upstream PmeI For	atggctaattcccatgtcgtttcagccaggctggtgcattacaatg
<i>Xe</i> -avrRxo1 upstream PmeI Rev	actagtcgacttaattaagtttatgtaccactttgattggaga
<i>Xe</i> -HrcV upstream SwaI For	gcaggctccgaattcgccctattttaacatcggacgatcgacagcct
<i>Xe</i> -HrcV upstream SwaI Rev	aagcttaattggatccatttgcagtggtggcgatcctgat
<i>Xe</i> -HrcV upstream PmeI For	atggctaattcccatgtcgtttcagccatcgttctgcagacgc
<i>Xe</i> -HrcV upstream PmeI Rev	actagtcgacttaattaagtttgactcaacgagcggatcagc
<i>Xe</i> -T2SS upstream SwaI For	gcaggctccgaattcgccctattttgccagaacgcacatcggtgacgt
<i>Xe</i> -T2SS upstream SwaI Rev	aagcttaattggatccatttaattaaggttgagattgagat
<i>Xe</i> -T2SS upstream PmeI For	atggctaattcccatgtcgtttgagacggaattcttgcgat
<i>Xe</i> -T2SS upstream PmeI Rev	actagtcgacttaattaagtttgatagcagcggcagcggcgtga
<i>Xe</i> -glpF upstream SwaI For	gcaggctccgaattcgccctattttaccagctggaagtggcaccga
<i>Xe</i> -glpF upstream SwaI Rev	aagcttaattggatccatttctgggtcgtacaggtgtacatc
<i>Xe</i> -glpF upstream PmeI For	atggctaattcccatgtcgtttggtgctgcgccaagccaacaa
<i>Xe</i> -glpF upstream PmeI Rev	a actagtcgacttaattaagtttcggcataggcttgcgagtcgct
<i>Xe</i> -AvrBS2 upstream SwaI For	gcaggctccgaattcgccctattttctgctgacgtcggccctc
<i>Xe</i> -AvrBS2 upstream SwaI Rev	aagcttaattggatccatttgcagctcgaaacgcggcg
<i>Xe</i> -AvrBS2 upstream PmeI For	atggctaattcccatgtcgtttgcaatttcaggccagtcctcat

<i>Xe-AvrBS2</i> upstream PmeI Rev	actagtcgacttaattaagttacgcgccggcgctatcgccggcac
<i>NbActin</i> real-time PCR For	tgaagatcctcacagagegtgg
<i>NbActin</i> real-time PCR Rev	ttgtatgtggctctcgtggattc
<i>NbNPR1</i> real-time PCR For	atggataatagtaggactgcgtt
<i>NbNPR1</i> real-time PCR Rev	aatgtcatgaggcaaggctttatc
<i>NbPRI</i> real-time PCR For	gctctgttctccctcgaag
<i>NbPRI</i> real-time PCR Rev	gcctcttagttgtctgcgtagct

References

1. Xin, X.F., et al., *Bacteria establish an aqueous living space in plants crucial for virulence*. Nature, 2016. 539(7630): p. 524-529.
2. Velasquez, A.C., C.D.M. Castroverde, and S.Y. He, *Plant-Pathogen Warfare under Changing Climate Conditions*. Curr Biol, 2018. 28(10): p. R619-R634.
3. Cheng, Y.T., L. Zhang, and S.Y. He, *Plant-Microbe Interactions Facing Environmental Challenge*. Cell Host Microbe, 2019. 26(2): p. 183-192.
4. Aung, K., Y. Jiang, and S.Y. He, *The role of water in plant-microbe interactions*. Plant J, 2018. 93(4): p. 771-780.
5. Elbanoby, F.E. and K. Rudolph, *Induction of Water-Soaking in Plant-Leaves by Extracellular Polysaccharides from Phytopathogenic Pseudomonads and Xanthomonads*. Physiological Plant Pathology, 1979. 15(3): p. 341-&.
6. Lozano-Duran, R., et al., *The bacterial effector HopMI suppresses PAMP-triggered oxidative burst and stomatal immunity*. New Phytol, 2014. 202(1): p. 259-69.
7. Ham, J.H., et al., *Multiple activities of the plant pathogen type III effector proteins WtsE and AvrE require WxxxE motifs*. Mol Plant Microbe Interact, 2009. 22(6): p. 703-12.
8. Ham, J.H., et al., *WtsE, an AvrE-family type III effector protein of Pantoea stewartii subsp. stewartii, causes cell death in non-host plants*. Mol Plant Pathol, 2008. 9(5): p. 633-43.
9. Jones, J.B., et al., *Reclassification of the xanthomonads associated with bacterial spot disease of tomato and pepper*. Syst Appl Microbiol, 2004. 27(6): p. 755-62.
10. Spoel, S.H., et al., *Proteasome-mediated turnover of the transcription coactivator NPR1 plays dual roles in regulating plant immunity*. Cell, 2009. 137(5): p. 860-72.
11. Shah, J., F. Tsui, and D.F. Klessig, *Characterization of a salicylic acid-insensitive mutant (sai1) of Arabidopsis thaliana, identified in a selective screen utilizing the SA-inducible expression of the tms2 gene*. Molecular Plant-Microbe Interactions, 1997. 10(1): p. 69-78.
12. Cao, H., et al., *Characterization of an Arabidopsis Mutant That Is Nonresponsive to Inducers of Systemic Acquired-Resistance*. Plant Cell, 1994. 6(11): p. 1583-1592.
13. Ryals, J.A., et al., *Systemic acquired resistance*. Plant Cell, 1996. 8(10): p. 1809-1819.
14. Tsuda, K. and I.E. Somssich, *Transcriptional networks in plant immunity*. New Phytol, 2015. 206(3): p. 932-47.
15. Cao, H., et al., *The Arabidopsis NPR1 gene that controls systemic acquired resistance encodes a novel protein containing ankyrin repeats*. Cell, 1997. 88(1): p. 57-63.
16. Durrant, W.E. and X. Dong, *Systemic acquired resistance*. Annu Rev Phytopathol, 2004. 42: p. 185-209.
17. Ewers, B.E., D.S. Mackay, and S. Samanta, *Interannual consistency in canopy stomatal conductance control of leaf water potential across seven tree species*. Tree Physiol, 2007. 27(1): p. 11-24.
18. Hartung, W., J.W. Radin, and D.L. Hendrix, *Abscisic Acid Movement into the Apoplastic solution of Water-Stressed Cotton Leaves: Role of Apoplastic pH*. Plant Physiol, 1988. 86(3): p. 908-13.

19. Cheong, H., et al., *Xanthomonas oryzae* pv. *oryzae* type III effector *XopN* targets *OsVOZ2* and a putative thiamine synthase as a virulence factor in rice. *PLoS One*, 2013. 8(9): p. e73346.
20. Sinha, D., et al., *Cell wall degrading enzyme induced rice innate immune responses are suppressed by the type 3 secretion system effectors XopN, XopQ, XopX and XopZ of Xanthomonas oryzae* pv. *oryzae*. *PLoS One*, 2013. 8(9): p. e75867.
21. Taylor, K.W., et al., *Tomato TFT1 is required for PAMP-triggered immunity and mutations that prevent T3E XopN from binding to TFT1 attenuate Xanthomonas virulence*. *PLoS Pathog*, 2012. 8(6): p. e1002768.
22. Kim, J.G., et al., *Xanthomonas T3E XopN Suppresses PAMP-Triggered Immunity and Interacts with a Tomato Atypical Receptor-Like Kinase and TFT1*. *Plant Cell*, 2009. 21(4): p. 1305-23.
23. Rosenau, F. and K. Jaeger, *Bacterial lipases from Pseudomonas: regulation of gene expression and mechanisms of secretion*. *Biochimie*, 2000. 82(11): p. 1023-32.
24. Tamir-Ariel, D., et al., *A secreted lipolytic enzyme from Xanthomonas campestris* pv. *vesicatoria* is expressed in planta and contributes to its virulence. *Mol Plant Pathol*, 2012. 13(6): p. 556-67.
25. Zhou, F., et al., *Lyciumbarbarum Polysaccharide (LBP): A Novel Prebiotics Candidate for Bifidobacterium and Lactobacillus*. *Front Microbiol*, 2018. 9: p. 1034.
26. Saleh, A., et al., *Posttranslational Modifications of the Master Transcriptional Regulator NPR1 Enable Dynamic but Tight Control of Plant Immune Responses*. *Cell Host Microbe*, 2015. 18(2): p. 169-82.
27. Gatz, C., *From pioneers to team players: TGA transcription factors provide a molecular link between different stress pathways*. *Mol Plant Microbe Interact*, 2013. 26(2): p. 151-9.
28. Chai, J.Y., et al., *Mitogen-activated protein kinase 6 regulates NPR1 gene expression and activation during leaf senescence induced by salicylic acid*. *Journal of Experimental Botany*, 2014. 65(22): p. 6513-6528.
29. Chen, J., et al., *NPR1 Promotes Its Own and Target Gene Expression in Plant Defense by Recruiting CDK8*. *Plant Physiol*, 2019. 181(1): p. 289-304.
30. Yu, D., C. Chen, and Z. Chen, *Evidence for an important role of WRKY DNA binding proteins in the regulation of NPR1 gene expression*. *Plant Cell*, 2001. 13(7): p. 1527-40.
31. Wang, D., N. Amornsiripanitch, and X. Dong, *A genomic approach to identify regulatory nodes in the transcriptional network of systemic acquired resistance in plants*. *PLoS Pathog*, 2006. 2(11): p. e123.
32. Selote, D., et al., *The E3 ligase BRUTUS facilitates degradation of VOZ1/2 transcription factors*. *Plant Cell Environ*, 2018. 41(10): p. 2463-2474.
33. Prasad, K.V.S.K., D.H. Xing, and A.S.N. Reddy, *Vascular Plant One-Zinc-Finger (VOZ) Transcription Factors Are Positive Regulators of Salt Tolerance in Arabidopsis*. *International Journal of Molecular Sciences*, 2018. 19(12).
34. Nakai, Y., et al., *Overexpression of VOZ2 confers biotic stress tolerance but decreases abiotic stress resistance in Arabidopsis*. *Plant Signal Behav*, 2013. 8(3): p. e23358.
35. Koguchi, M., et al., *Vascular plant one-zinc-finger protein 2 is localized both to the nucleus*

- and stress granules under heat stress in Arabidopsis*. Plant Signal Behav, 2017. 12(3): p. e1295907.
36. Celesnik, H., et al., *Arabidopsis thaliana VOZ (Vascular plant One-Zinc finger) transcription factors are required for proper regulation of flowering time*. Biology Open, 2013. 2(4): p. 424-431.
37. Lee, S.W. and P.C. Ronald, *Marker-exchange mutagenesis and complementation strategies for the Gram-negative bacteria Xanthomonas oryzae pv. oryzae*. Methods Mol Biol, 2007. 354: p. 11-8.
38. Traore, S.M. and B. Zhao, *A novel Gateway(R)-compatible binary vector allows direct selection of recombinant clones in Agrobacterium tumefaciens*. Plant Methods, 2011. 7(1): p. 42.
39. Melotto, M., et al., *Plant stomata function in innate immunity against bacterial invasion*. Cell, 2006. 126(5): p. 969-80.
40. Katagiri, F., R. Thilmony, and S.Y. He, *The Arabidopsis thaliana-pseudomonas syringae interaction*. Arabidopsis Book, 2002. 1: p. e0039.
41. Krasileva, K.V., D. Dahlbeck, and B.J. Staskawicz, *Activation of an Arabidopsis resistance protein is specified by the in planta association of its leucine-rich repeat domain with the cognate oomycete effector*. Plant Cell, 2010. 22(7): p. 2444-58.
42. Karimi, M., D. Inze, and A. Depicker, *GATEWAY vectors for Agrobacterium-mediated plant transformation*. Trends Plant Sci, 2002. 7(5): p. 193-5.
43. Jefferson, R.A., T.A. Kavanagh, and M.W. Bevan, *Gus Fusions - Beta-Glucuronidase as a Sensitive and Versatile Gene Fusion Marker in Higher-Plants*. Embo Journal, 1987. 6(13): p. 3901-3907.
44. Jefferson, R.A., T.A. Kavanagh, and M.W. Bevan, *Beta-Glucuronidase (Gus) as a Sensitive and Versatile Gene Fusion Marker in Plants*. Journal of Cellular Biochemistry, 1987: p. 57-57.

Chapter 4 *Xanthomonas euvesicatoria* Gene Xe4429 Encodes an Antitoxin and also Functions as a Transcription Repressor

Summary

Xanthomonas euvesicatoria (*Xe*) is the causal agent of bacterial spot (BS) disease in pepper and tomato. We identified a *Xe* type three-secretion effector (T3E), Xe4428, which is a homologue of *Xanthomonas oryzae* pv. *oryzicola* (*Xoc*) T3E AvrRxo1 that functions as a NAD kinase. Xe4428 is required for the full virulence of *Xe* to infect pepper plants. Overexpression of AvrRxo1 or Xe4428 alone in bacterial or plant cells is toxic. We previously demonstrated that AvrRxo1-ORF2 functions as an antitoxin capable of binding to AvrRxo1 to suppress its toxicity. However, the detailed biochemical and biological functions of AvrRxo1-ORF2 remain unclear. In this study, we identified Xe4429 as the homologue of AvrRxo1-ORF2, which interacts with Xe4428 to suppress its toxicity in *Xe* bacterial cells. We also revealed that Xe4429 could bind to the promoter region of *Xe4428* and regulates its transcription. Therefore, we conclude that Xe4429 functions as an antitoxin and a transcription repressor in the *Xe* bacterial cells.

Introduction

Rice bacterial leaf streak (BLS) disease, caused by *Xanthomonas oryzae* pv. *oryzicola* (*Xoc*) is one of the most important bacterial diseases in rice fields. Thus far, no major resistance genes have ever been identified from any rice germplasm. A maize resistant gene *Rxo1* was isolated that can specifically recognize an effector gene *avrRxo1* to trigger disease resistance to BLS in transgenic rice plants [1-3]. The *Rxo1* gene encodes a typical NB-LRR type disease resistant protein, while the *avrRxo1* gene encodes a type III effector (T3E) protein [3].

In the genome of *Xoc*, *avrRxo1-orf1* is adjacent to another gene, *avrRxo1-orf2*, which encodes an atypical molecular chaperone of AvrRxo1-ORF1 [4, 5]. Overexpression of AvrRxo1-ORF1 in yeast, *E. coli*, and *N. benthamiana* plant cells is toxic, where the toxicity can be blocked by

the co-expression of AvrRxo1-ORF2 [4]. AvrRxo1-ORF1 and ORF2 can be co-crystallized, which showed AvrRxo1-ORF2 physically binds to AvrRxo1-ORF1, thereby serving as an antitoxin to eliminate the toxicity of AvrRxo1-ORF1 [4]. AvrRxo1-ORF1 has an ATP binding domain and a kinase domain, which can phosphorylate NAD, a central metabolite and signaling molecule in biosystems, to form 3'-NADP in both bacterial and yeast cells [5]. *Agrobacterium*-mediated transient expression of AvrRxo1 in *N. benthamiana* or infected rice leaves with *Xoc* carrying *avrRxo1* could trigger the accumulation of 3'-NADP, implying that AvrRxo1 is capable of manipulating the primary metabolic pathway *in planta*.

A point mutation on aspartic acid D193A in putative substrate-binding site of AvrRxo1 could inhibit its toxicity to bacterial, yeast, and plant cells, suppress its ability to trigger Rxo1-mediated disease resistance, and impair the capacity of suppression of the flg22-triggered ROS accumulation [5]. Another point mutation on the threonine T167N in the ATP-binding motif could also suppress the toxicity of AvrRxo1, but not completely abolish its NAD enzyme activity and the full virulence function [5-7]. An *AvrRxo1* homologue, *Xe4428*, was identified in the genome of *Xanthomonas euvesicatoria* (*Xe*), which is the causal agent of bacterial spot (BS) disease in pepper plants. *Xe4428* is adjacent to *Xe4429*, which is a homologue of *Xoc-AvrRxo1-orf2*. However, the detailed biological and biochemical functions of *Xe4428* and *Xe4429* has never been characterized.

In this study, we confirmed that *Xe4428* is a functional homologue of AvrRxo1, which can trigger the *Rxo1*-mediated defense responses in *N. benthamiana*. Therefore, we re-named *Xe4428* as *Xe-AvrRxo1*. *Xe-AvrRxo1* also has a virulence function that can promote the *Xe* bacterial proliferation on both pepper and *N. benthamiana* plants. We then revealed that *Xe4429* encodes an antitoxin that can suppress the toxicity of *Xe-AvrRxo1*. In addition, we identified that *Xe4429* can bind to the promoter region of *Xe-AvrRxo1* to suppress its expression in *Xe* bacterial cells. Hence, *Xe4429* functions as an antitoxin and a bacterial transcription repressor.

Results and discussions

Xe4428 is a homologue of Xoc-avrRxo1 that can trigger the Rxo1-mediated defense response in N. benthamiana plants

Xoc-avrRxo1 has been previously shown to be able to trigger the Rxo1-mediated disease resistance in rice and *N. benthamiana* plants. Here, we investigated whether Rxo1 could also recognize *Xe-avrRxo1* to trigger a defense response in *N. benthamiana* plants. As shown in Figure 4-1A and Figure S4-1, *Agrobacterium*-mediated transient expression of *Rxo1* and *Xe-avrRxo1* triggered strong cell death in *N. benthamiana*, tomato and pepper leaves. As a control, the mutant of Rxo1, Rxo1-D291E, and the mutant of *Xe-avrRxo1*, *Xe-avrRxo1*-D193T, failed to trigger cell death in *N. benthamiana*, tomato, and pepper leaves (Figure 4-1A and Figure S4-1). The inoculated *N. benthamiana* leaf was stained with DAB to detect the accumulation of H₂O₂. As shown in Figure 4-1B, the co-expression of *Rxo1* and *Xe-avrRxo1* resulted in an increased accumulation of H₂O₂.

We also monitored the expression of defense-related genes by RT-qPCR. As shown in Figure 4-1C, the expression level of NbNPR1 and NbPR4 with the co-infiltration of *Rxo1* and *Xe-avrRxo1* increased dramatically, while the expression of NbPR10 is significantly downregulated in comparison with the controls. Therefore, we confirmed that *Xe-avrRxo1* is a functional homologue of Xoc-AvrRxo1 that can trigger Rxo1-mediated defense response in *N. benthamiana* plants, which may involve the salicylic acid-associated signaling pathway.

Xe4428 possesses a significant virulence function that can enhance Xe proliferation via inducing stomatal opening in both pepper and tobacco plants

Our previous result showed the deletion of *Xe* effector XopQ would alter the host specificity of *Xe*, which allows it to infect *N. benthamiana* plants. In order to characterize the virulence function of *Xe-avrRxo1*, we generated isogenic *Xe* mutant strains that carry a deletion of XopQ alone or the double deletion of both *Xe-XopQ* and *Xe-avrRxo1*. The isogenic *Xe* strains

(*XeΔXopQ* and *XeΔXopQΔXe-avrRxo1*) were able to infect *N.benthamiana*, pepper, and tomato plants. However, inoculated *XeΔXopQΔXe-avrRxo1* strain grows to significantly lower population levels than that of *XeΔXopQ* on both *N.benthamiana* and pepper plants (Figure 4-2). Therefore, we conclude that *Xe-avrRxo1* possesses a significant virulence function that can promote bacterial proliferation on the inoculated plants.

Our previous result suggests that the expression of *Xoc-avrRxo1* could increase the stomatal aperture in *Arabidopsis*. Therefore, we attempted to test whether *Xe-avrRxo1* also has a similar role in regulating stomatal aperture. In this study, we choose to measure the stomatal conductance of pepper leaves infiltrated by wild-type *Xe* and mutant strain *XeΔavrRxo1* using a portable photosynthesis system (LI-COR 6400XT). As illustrated in Figure 4-3, upon infection with *XeΔavrRxo1*, the pepper leaves have reduced CO₂ conductance in stomatal cells in comparison to the pepper leaves inoculated with wild type *Xe* strain. This result indicates that pepper leaves inoculated with wild type *Xe* might have increased stomata aperture that resulted in a higher rate of CO₂ conductance than that of the mutant *XeΔavrRxo1* strain. Therefore, we speculate that *Xe-avrRxo1* also has the role of increasing the stomatal aperture, which still needs to be further validated by directly observing the stomatal aperture size under a microscope.

Expression of Xe-avrRxo1 is toxic to Xe and E. coli, and the toxicity can be blocked by the co-expression of Xe4429

To confirm if *Xe-avrRxo1* (designated as *Xe-avrRxo1* ORF1) is toxic to bacterial cells, and if *Xe4429* (designated as *Xe-avrRxo1*-ORF2) can block the toxicity of *Xe4428*, we employed an arabinosis-inducible expression system to express wild type *Xe-avrRxo1* or mutant *Xe-avrRxo1*-D193T with or without the *Xe4429* (*Xe-avrRxo1*-ORF2) in *E. coli* and *Xe* cells. As shown in Figure 4-4A, the expression of *Xe-avrRxo1* but not *Xe-avrRxo1*-D193T, or *Xe-avrRxo1* plus *Xe4429* (*Xe-avrRxo1*-ORF2) could inhibit the bacterial growth. As the control, when the bacterial strains were grown in LB medium without the supplement of arabinose, all

bacterial strains, except the strain carrying *Xe-avrRxo1* alone, have a similar growth rate. We speculate that a leaking expression of *Xe-avrRxo1* might reduce the bacterial growth rate. Nevertheless, we conclude that *Xe-avrRxo1* also possesses toxicity to *E. coli*, and the co-expression with *Xe4429* (*Xe-avrRxo1*-ORF2) could block its toxicity. The point mutation in the putative substrate-binding site D193T also abolished the toxicity of *Xe-avrRxo1*.

The same set of expression constructs were also transformed into a mutant *Xe* strain where both *Xe-avrRxo1* and *Xe4429* (*XeΔavrRxo1ΔXe4429*) were deleted. The transformed *Xe* strains were used for a growth curve assay. As shown in Figure 4-4B, inducible expression of wild type *Xe-avrRxo1*, but not the *Xe avrRxo1*-D193T, could strongly inhibit the bacterial cell proliferation. Interestingly, the co-expression of *Xe-avrRxo1* with *Xe4429* (*Xe-avrRxo1*-ORF2) still had a much slower growth rate than the other controls (Figure 4-4B). We speculate that the expressed *Xe-AvrRxo1* protein might not completely bind with *Xe4429* (*Xe avrRxo1*-ORF2). We originally cloned the open reading frames of *Xe-avrRxo1* and *Xe4429*, each in a single DNA fragment. The DNA fragment containing two gene open reading frames was subcloned behind the arabinose inducible promoter. Therefore, we speculate that *Xe-avrRxo1* has a higher expression rate than that of *Xe4429*, resulting in more *Xe-AvrRxo1* proteins than *Xe4429* proteins. The free *Xe-avrRxo1* proteins without binding of *Xe4428* would be toxic to *Xe* cells. However, if we know the wild type *Xe* strain also expresses *Xe avrRxo1* and *Xe4429* from a single operon, where *Xe-avrRxo1* is located in front of *Xe4429*, then why we did not see *Xe-avrRxo1* have any toxicity to the wild type *Xe* cells? Previous reports about the toxin-antitoxin pairs suggest that some antitoxins also function as the transcriptional repressor, where it can bind to the promoter sequence of the toxin gene [8, 9].

To test if *Xe4429* (*Xe-avrRxo1*-ORF2) also has a similar function, we amplified out the *Xe* genomic DNA fragment that contains the native promoter and the open reading frames of *Xe-avrRxo1* and *Xe4429*. The DNA fragment was cloned to a broad-host spectrum vector pVSP61 [10] to generate a complementary construct p*Xe avrRxo1*-ORF1:ORF2. We also performed site-directed mutagenesis to introduce a point mutation D193T into p*Xe avrRxo1*-ORF1:ORF2,

which resulted in p*Xe*-avrRxo1-ORF1-D193T:ORF2. The two complementary constructs were transformed into mutant *Xe* Δ avrRxo1 Δ Xe4429 strain. The wild type *Xe*, *Xe* Δ avrRxo1 Δ Xe4429, *Xe* Δ avrRxo1 Δ Xe4429 (p*Xe* avrRxo1-ORF1:ORF2), and *Xe* Δ avrRxo1 Δ Xe4429 (p*Xe* avrRxo1-ORF1-D193T:ORF2) strains were used for growth curve assay. As shown in Figure 4-4C, all strains have an almost identical growth rate. As a control, we also confirmed that the arabinose supplement did not alter the growth rate of these *Xe* strains. Therefore, we conclude that when *Xe*-avrRxo1 and Xe4429 (*Xe*-avrRxo1 ORF2) are co-expressed by the native promoter in *Xe*, the toxicity of *Xe*-avrRxo1 could be completely blocked by Xe4429.

Purified ORF2 (Xe4429) protein binds to the promoter of Xe4428 in electrophoretic mobility shift assay

As previously described, we speculate that Xe4429 could bind to the promoter region of *Xe*-avrRxo1 and repress the transcription of *Xe*-avrRxo1, which would result in a tight regulation of *Xe*-avrRxo1. To test this hypothesis, we purified either Xe4429 protein alone or *Xe*-AvrRxo1:Xe4429 protein complex for an electrophoretic mobility shift assay (EMSA). The purified proteins were incubated with a DNA fragment containing the promoter of *Xe*-avrRxo1 before they were separated in agarose gel. As shown in Figure 4-5, the mobility of the DNA fragment containing the *Xe*-avrRxo1 promoter region altered in the DNA electrophoresis gel when it was mixed with purified Xe4429 (*Xe*-avrRxo1-ORF2) recombinant protein. The shifting DNA band could be inhibited by supplementing large amounts of unlabeled competitor DNA that contains the promoter of *Xe*-avrRxo1. In contrast, *Xe*-avrRxo1: Xe4429 protein complex did not alter the mobility of the DNA fragment. Therefore, our EMSA suggests Xe4429, which is the homologue of *Xoc*-avrRxo1-ORF2 binds to the promoter region of *Xe*-avrRxo1 *in vitro*.

Xe4429 functions as a transcriptional repressor in Xe cells that were grown on nutrient broth medium but not in the plant leaf tissue

Since Xe4429 is able to bind to the promoter of *Xe-avrRxo1* (Figure 4-5), we also attempt to investigate if Xe4429 can regulate the expression of *Xe-avrRxo1* in *Xe* bacterial cells. To this end, we first cloned the native promoter of *Xe-avrRxo1* and fused it with the Nanoluc gene [11]. This DNA fragment was further cloned into a pBMTBX vector that carries either Xe4429 alone, or *Xe-avrRxo1*: Xe4429, or a GFP gene as a control. As a control, we also cloned the Nanoluc gene into the pBMTBX vector. Detailed schemes of tested constructs are illustrated in Figure 4-5A. These expression constructs were transformed into the mutant *XeΔXe-avrRxo1ΔXe4429* strain, and grown on the medium supplemented with or without 0.4 % arabinose (expression inducer). As shown in Figure 4-5B (panel 2), the expression of Xe4429 repressed the expression of *Xe-avrRxo1* promoter:Nanoluc. In contrast, the expression of GFP could not repress the expression of *Xe-avrRxo1* promoter:Nanoluc (Figure 4-5 (panel 4)). Interestingly, the expression of *Xe-avrRxo1*:Xe4429 complex also repressed the expression of *Xe-avrRxo1* promoter:Nanoluc (Figure 4-5 (panel 3)). This result is inconsistent with the EMSA result shown in Figure 4-4, where the *Xe-avrRxo1*: Xe4429 complex could not bind to the promoter of *Xe-avrRxo1*. We speculate that in the *Xe* cells, the *Xe-avrRxo1*: Xe4429 complex may have association and dissociation dynamics allowing some free Xe4429 that could bind to the promoter region of *Xe-avrRxo1*. An alternative explanation is that the association and dissociation dynamics also result in free *Xe-AvrRxo1* that could be toxic to *Xe* bacterial cells, and therefore, suppress the expression of Nanoluc. This possibility is indeed consistent with the growth curve data shown in Figure 4-4B, where the co-expression *Xe-avrRxo1* and Xe4429 controlled by the same arabinose inducible promoter still has some toxicity to *Xe* bacterial cells. We also investigated if Xe4429 could repress the expression *Xe-avrRxo1* when the *Xe* bacterial cells were grown in plant tissues. The *Xe* strains, as listed in Figure 4-5A, were infiltrated into pepper leaves, supplemented with either arabinose (expression inducer) or glucose (non-inducer as the control). Strong Nanoluc enzyme activities were observed in all *Xe* strains (Figure 4-6). Therefore, when the *Xe* bacterial cells were grown in the pepper leaf tissues, Xe4429 could not repress the expression of *Xe-avrRxo1*.

To summarize, in this study, we characterized the biological and biochemical functions of *Xe-avrRxo1* and *Xe4429*. Our results revealed that *Xe-avrRxo1* is a functional homologue of *Xoc-AvrRxo1*, while *Xe4429* encodes an antitoxin and also functions as a bacterial transcription repressor. Therefore, *Xe4429* can regulate the toxicity of *Xe-avrRxo1* by direct protein-protein interaction, and also by protein-DNA interaction to suppress the transcription of *Xe-avrRxo1*.

Methods and materials

Plant material and growth conditions

Seeds from *N.benthamiana*, pepper (*Capsicum annuum*, Ca), and tomato (*Solanum lycopersicum*, Sl, cultivar: Rio Grande) were germinated in soil at room temperature under 12h/12h light/dark cycle at 25°C/20°C. After germination, plants were grown under 14h/10h light/dark cycle at 25°C/20°C. The 6-week-old tobacco, pepper, and tomato plants were used for the experiments detailed herein.

Bacterial growth

Escherichia coli (*E. coli*) strains *DH5α* and *Rho5* were grown on Luria agar medium at 37 °C. *Agrobacterium tumefaciens* (*A. tumefaciens*) *GV2260* strain and *Xe* were grown on Luria agar medium and NYGA medium at 28 °C, respectively. *E. coli* and *Rho5* antibiotic selections used in this study were as follows: 50 µg/ml kanamycin, 100 µg/ml carbenicillin, 100 µg/ml spectinomycin, chloramphenicol 34 µg/ml, and 50 µg/ml gentamycin. *Xe* and *A. tumefaciens* antibiotic selection were 100 µg/ml rifampicin, and/or 50 µg/ml kanamycin.

Gene cloning, site-directed mutagenesis, plasmid construction, and Agrobacterium-mediated transient assay

Two ORFs of *Xe-avrRxo1* and its corresponding resistant gene, *Rxo1*, were ultimately cloned to the pEarley101 vector with a 35S promoter using identical procedures for each. The *Xe-avrRxo1* was amplified from the genomic DNA of *Xe* using primers “*Xe-avrRxo1* ORF For”

and “*Xe*-avrRxo1 ORF Rev,” while Rxo1 was amplified from the genomic DNA of maize using primers “Rxo1 ORF For” and “Rxo1 ORF Rev,” which were both subsequently cloned into the pDonr207 vector (donor vector) using BP Gateway cloning (Invitrogen). The sequences of the other primers used in this study are provided in Supplementary Table 4-1. The donor vectors noted above were subcloned to the pEarley101 vector in *GV2260* using modified LR Gateway cloning kit as previously described [12].

The vector of pDonr207-*Xe*-avrRxo1-ORF was used to generate its mutant, *Xe*-avrRxo1-D193T, using primers “*Xe*-avrRxo1-ORF-D193T For” and “*Xe*-avrRxo1-ORF-D193T Rev”; a similar approach was used for the mutant Rxo1-D291E. The various primer sequences are listed in Table S4-1. The vectors of pDonr207-*Xe*-avrRxo1-ORF-D193T and pDonr207-Rxo1-ORF-D291E were subcloned to the pEarley101 vector in *GV2260* using a modified LR Gateway cloning kit as noted above. Using blunt-end syringes, the leaf mesophyll tissues were infiltrated by *Agrobacterium* strains harboring different constructs within the concentration of OD600 0.4 [13].

RNA isolation, RT-PCR and real-time PCR

For RT-PCR, the total RNA was extracted from *N.benthamiana* leaves using TRIzol Reagent (Invitrogen, Carlsbad, CA) according to the manufacturer’s instructions. Any DNA residue was eliminated by treating with UltraPure DNase I (Invitrogen). The integrity and quantity of total RNA were determined by electrophoresis in 1% agarose gel and a NanoDrop ND-1000 spectrophotometer (NanoDrop Technologies, Wilmington, DE). cDNA synthesis was performed using the SuperScript III First-Strand RT-PCR Kit (Invitrogen) with an oligo-dT primer based on the manufacturer’s instructions. Real-time PCR was conducted with cDNA 20 times diluted and specific primers (Supplemental Table 4-1) using the Quantitect SYBR Green PCR kit (Qiagen) according to the manufacturer’s protocols.

Reactive oxygen species (ROS) detection

The reactive oxygen species were visualized in leaf tissues by staining with DAB (Sigma-Aldrich), as described previously [14, 15]. *N.benthamiana* leaves were detached and vacuum-infiltrated with the DAB solution. The leaf samples were then placed in a petri dish with the DAB solution for 4 hours at room temperature. Afterwards, the leaves were fixed with a solution containing 60% [vol/vol] ethanol, 20% [vol/vol] lactic acid, and 20% [vol/vol] glycerol. The fixed leaves were decolorized in a 2.5 g chloral hydrate per milliliter water solution overnight and were visualized using a white-light microscope.

Bacterial growth curve assay

Bacterial proliferation on the inoculated *N.benthamiana*, *C.annuum*, and *S.lycopersicum* plants was assessed via standard growth curve assays [16, 17]. During the spray inoculation, the bacterial strains were cultivated on their respective medium plate at 28 °C for two days, after which the bacterial cells were collected and suspended in 10 mM MgCl₂ with 0.02% Silwet L77 and diluted to OD₆₀₀ at 0.2. The plants were covered and maintained at 100% moisture levels for one day prior to inoculation. The bacterial inoculum was sprayed on the plant leaves using a spray bottle. The inoculated plants were covered, sealed, and maintained under 100% moisture overnight, and then cultivated under 14 h light/10 h dark at room temperature for an additional 5 days. Leaf discs (990 mm²) were randomly sampled from inoculated leaves on the fifth day for growth curve assay. The sampled leaf discs were ground in 588 µL of 10 mM MgCl₂, and vortexed evenly prior to dilution and plating on respective medium supplemented with proper antibiotics. The plates were cultivated at 28 °C until the bacteria colonies could be counted; these numbers were then used to calculate the bacteria proliferation ratio (Log₁₀ CFU/cm²). All growth curves underwent three biological repeats with technical replicates.

Monitoring the growth rates of E. coli and Xe strains expressing AvrRxo1 in enriched medium

The *Xe-AvrRxo1-ORF1*, *Xe-AvrRxo1-ORF1:ORF2*, *Xe-AvrRxo1-ORF1-D193T*, and nanoluc (negative control) were cloned into the Gateway-compatible vector, pBMTBX (from Addgene)

and expressed in *E. coli* strain *C41*. Strains were grown at 37°C in LB liquid medium supplemented with 100 µg/ml ampicillin. The bacterial culture was diluted to OD600 0.01, and the expression of the protein was induced by adding 0.4 mM arabinose. Bacterial cultures with a mock inducer, glucose, served as the control. Four *Xe* strains, (a) wild-type *Xe*, (b) *Xe*Δ*avrRxo1*, (c) *Xe*Δ*avrRxo1* (*pavrRxo1-wild type*), and (d) *Xe*Δ*avrRxo1* (*pavrRxo1-D193T*) were also grown in a NYG medium for evaluating their toxicity to *Xe*. The bacterial growth was monitored by a spectrometer.

Cloning, expression, and purification of AvrRxo1-ORF1:ORF2 and avrRxo1-ORF2

DNA fragments containing AvrRxo1-ORF1:ORF2 and AvrRxo1-ORF2 genes were amplified from the genomic DNA of *Xe* and cloned into a pENTR-D-TOPO vector (Invitrogen, Carlsbad, CA) [1]. They were then subcloned into a modified gateway compatible pGEX4T-1 destination vector via LR cloning (Invitrogen). A TEV protease cleavage site was introduced between the GST and the targeted protein for removal of the GST tag. The plasmids were transformed into *E. coli* *C41* cells (Lucigen, Middleton, WI) and grown overnight in 5 ml LB medium containing 100 mg/L ampicillin at 37°C. The culture was transferred into 1 liter LB medium containing ampicillin to reach a concentration of OD600 at 0.6. Then, 1 mM Isopropyl-1-thio-β-D-galactopyranoside (IPTG) was added to the bacterial culture and then incubated at 220 rpm at 28°C for another 8 hours. The bacterial cells were harvested and lysed by incubating with 1 µg/ml lysozyme on ice for 30 min, followed by sonication on ice. The lysate was centrifuged at 13,000 g for 15 min at 4°C and the supernatant was collected, which was then used for subsequent purification. Glutathione Sepharose 4B (GenScript, Piscataway, NJ) affinity resin and Q-sepharose ion-exchange column were used to purify the proteins of AvrRxo1-ORF1:ORF2 and AvrRxo1-ORF2. The purity of the proteins was evaluated by 12% SDS-PAGE. The protein concentration was determined by a protein assay kit (Bio-Rad) using bovine serum albumin as the standard [4].

Electrophoretic mobility shift assay (EMSA)

Electrophoretic mobility shift assay (EMSA) was performed as previously reported [18, 19]. The *Xe*-avrRxo1 promoter DNA was amplified from the pDonr207-*Xe*-avrRxo1 using FAM labeled “M13For” and “M13Rev” primers. The unlabeled competitor DNA of the *Xe*-avrRxo1 promoter was amplified with regular M13 For/Rev primers. In brief, the FAM-labeled DNA fragment of the *Xe*-avrRxo1 promoter was mixed with both avrRxo1-ORF1:ORF2 and avrRxo1-ORF2 protein, along with different amounts of the unlabeled competitor DNA fragment in a reaction buffer (10 mM Tris, 100 mM KCl, 1 mM EDTA, 0.1 mM DTT, 5 %v/v glycerol, 0.01 mg/mL BSA, pH 7.5) at room temperature for 20 min. The reactions were processed and separated on 1% agarose gel in the TAE buffer. The fluorescence signal was captured by a gel scanner, Typhoon FLA7000 equipped with a 635 nm laser filter (GE Healthcare, Piscataway, NJ).

Xe-avrRxo1 ORF2 transcription regulating trial

Based on the *Xe*Δ*avrRxo1* mutant background, an additional five *Xe* strains were generated. For this phase of the investigation, a pVSP61 backbone carrying a constitutive expression promoter served as the positive control; in contrast, pBMTBX-Nanoluc served as the blank or negative control [11]. The avrRxo1-ORF2, avrRxo1-ORF1:ORF2, and GFP were cloned to the same vector with the avrRxo1 promoter expressing Nanoluc. Accordingly, five constructs were then transformed to *Xe*Δ*avrRxo1*: (a) pBMTBX-Nanoluc, (b) pBMTBX-*Xe*4428-ORF2-*Xe*4428pro-Nanoluc, (c) pVSP61-*Xe*4428pro-Nanoluc, (d) pBMTBX-*Xe*4428-ORF1:ORF2-*Xe*4428pro-Nanoluc, and (e) pBMTBX-GFP-*Xe*4428pro-Nanoluc. The bacteria were cultured on the LB medium with the antibiotic and 0.4 mM arabinose. Note that bacterial cultures grown on a medium supplemented with 0.4 mM glucose served as controls. All bacteria were collected after incubation for 48 hours at 28°C. The bacteria was adjusted to OD600 0.1 with 10 mM MgCl₂, for following Nanoluc reporter assay *in vitro* as well as infiltration to pepper leaves. Additionally, 1 mM substrate was added to the bacterial cultures, or infiltrated to pepper leaves.

After incubation for 10 mins, chemical fluorescence signals were detected using the CCD camera of a Gel Doc™ XR+ System (Bio-Rad).

Stomatal conductance

A portable photosynthesis system LI-6400T (Li-Cor Inc., USA) with a 6400-02B light source (blue and red diode) was utilized to measure the following photosynthetic gas exchange parameters: net photosynthetic rate (P_n), transpiration rate (E), stomatal conductance (G_s), and the intercellular CO₂ concentration (C_i) of *pepper* leaves infiltrated by *Xe* and *Xe*Δ*avrRxo1* *in vivo* as reported [20]. G_s was used for further analysis. Measurements were obtained under an artificial irradiance of 1000 μmol (photons) m⁻² s⁻¹ at 25°C using a completely expanded leaf in the same position from each plant. The CO₂ concentration and ambient water vapor pressure were set at 385 μmol mol⁻¹ and 1.30 ± 0.15 kPa, respectively.

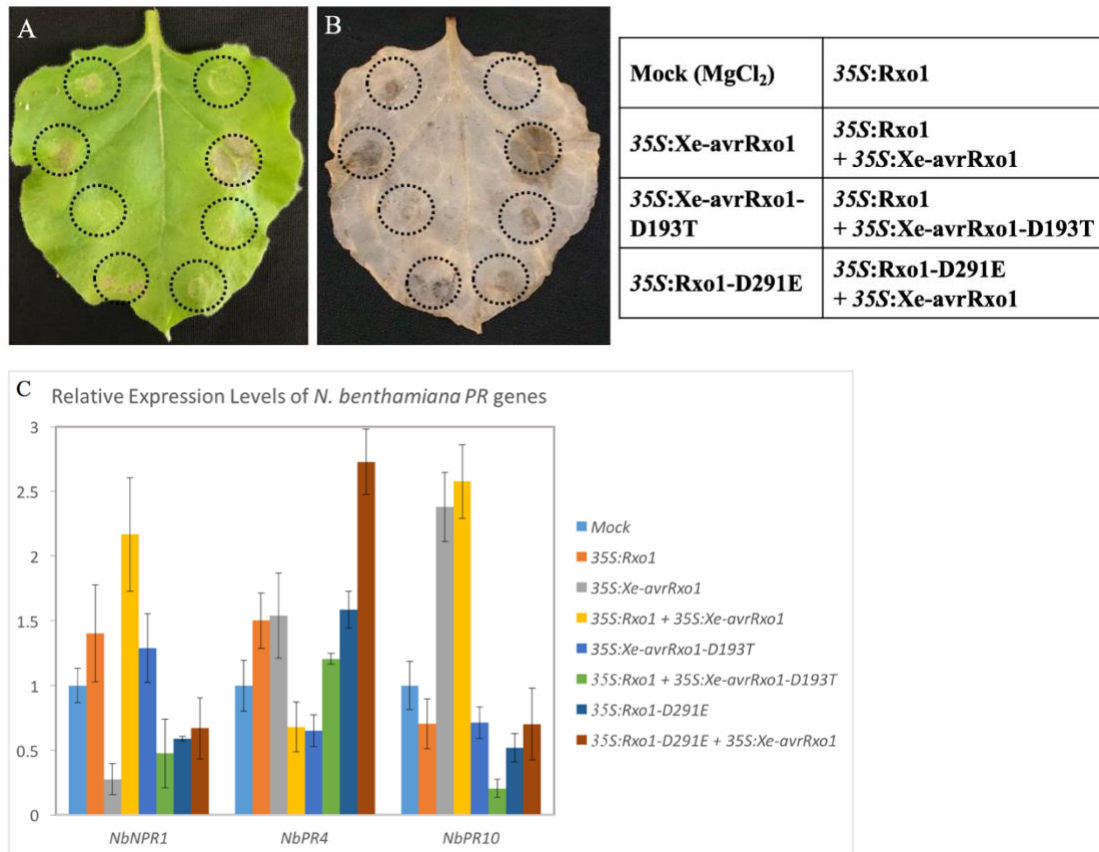


Figure 4- 1 *Xe4428* is a homologue of *Xoc-avrRxo1* that can trigger the *Rxo1*-mediated defense response in *N. benthamiana*.

(A) Transient assay in *N. benthamiana* leaf by *Agrobacterium*. The *agrobacterium* harboring the following constructs were used as inoculants: MgCl₂, 35S:Rxo1, 35S:Xe-avrRxo1, a combination of 35S:Rxo1 and 35S:avrRxo1, 35S:Xe-avrRxo1-D193T, a combination of 35S:Rxo1 and 35S:Xe-avrRxo1-D193T, 35S:Rxo1-D291E, and a combination of 35S:Rxo1-D291E and 35S:Xe-avrRxo1 within OD600 0.4 (single inoculation) or OD600 0.4 + 0.4 (co-inoculation). Picture was obtained 2 days post-inoculation. Experiments were replicated three times within similar results. (B) DAB staining of *N. benthamiana* leaf from (A). (C) The relative expression levels of *NbNPR1*, *NbPR4* and *NbPR10* in *N. benthamiana* leaves infected as above for 24 hours. Experiments were repeated three times with similar results and data are shown as mean ± s.e.

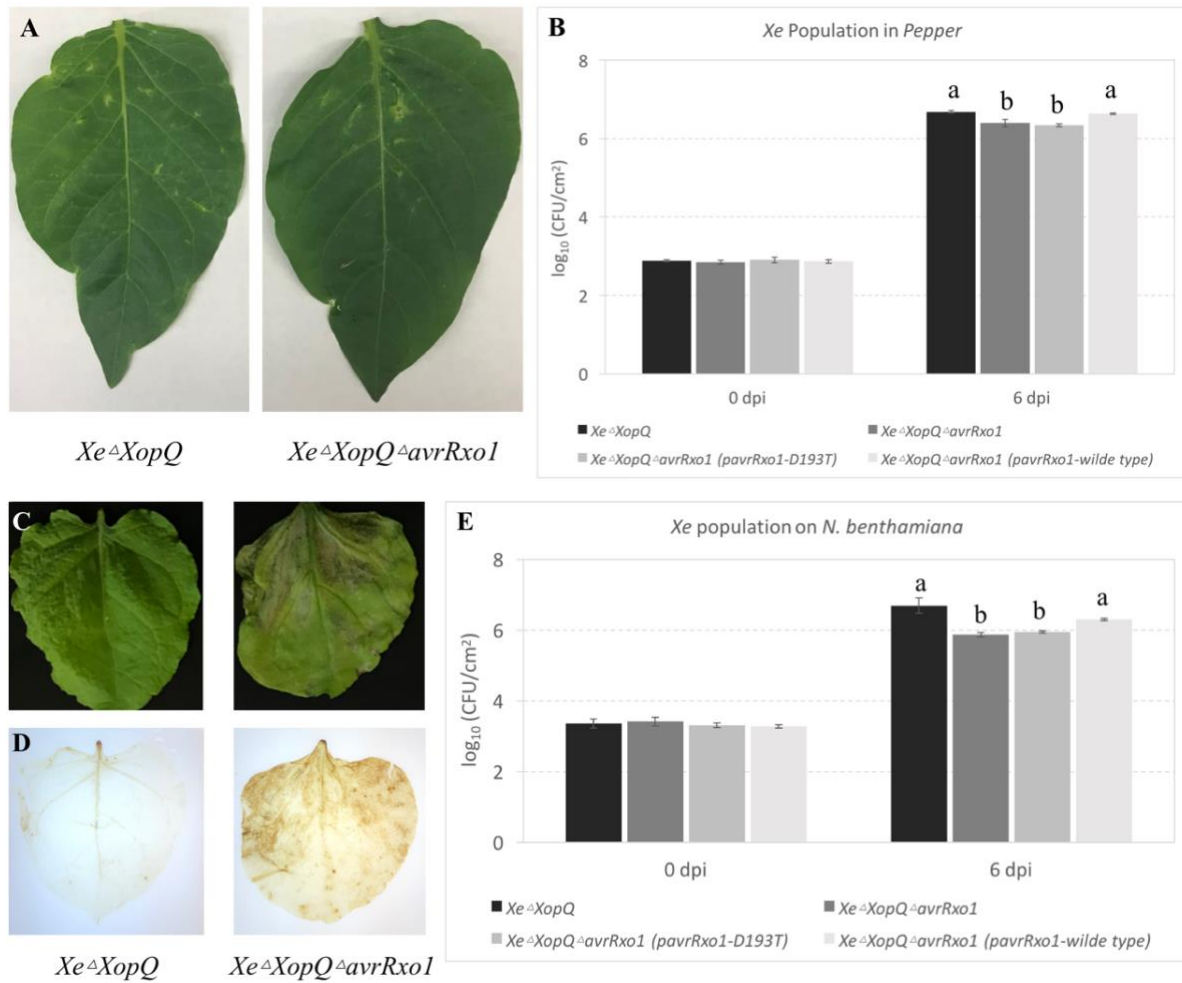


Figure 4- 2 *Xe4428* possesses a remarkable virulence function that can enhance *X. euvesicatoria* proliferation on both pepper and tobacco.

In planta growth of *Xe* Δ *XopQ*, *Xe* Δ *XopQ* Δ *avrRxo1*, *Xe* Δ *XopQ* Δ *avrRxo1* (*pavrRxo1*-D193T), and *Xe* Δ *XopQ* Δ *avrRxo1* (*pavrRxo1*-wild type) measured at Day 6 after infiltration in leaves of pepper (A and B) and *N. benthamiana* (C, D and E). The concentration of the starting inoculum of *Xe* strains was 1×10^5 cfu ml⁻¹. Visualized disease symptom phenotypes infected by *Xe* strains are shown in (A) pepper and (C) *N. benthamiana*. (D) DAB staining of *N. benthamiana* leaves from (C). Experiments were repeated three times with similar results and data are shown as mean \pm s.e.

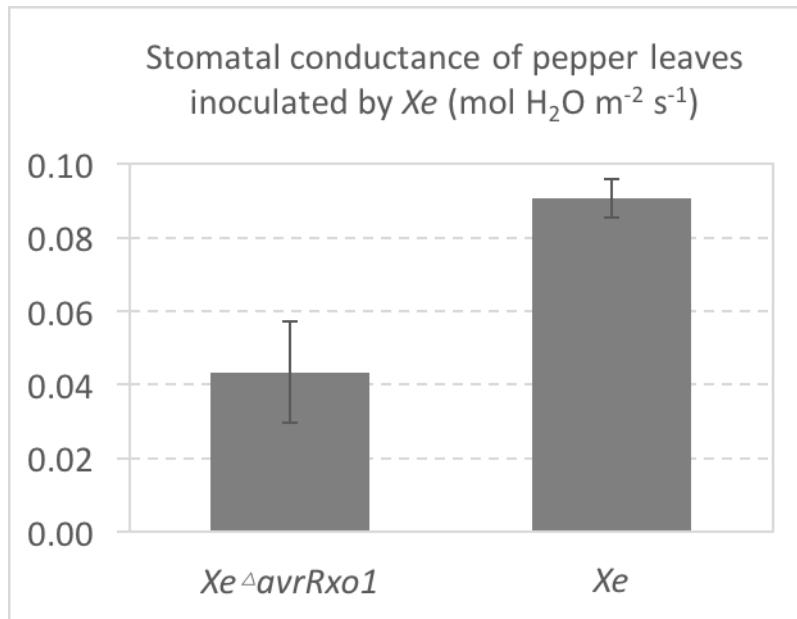


Figure 4- 3 Expression of *Xe-avrRxo1* in *Xe* could increase the stomatal conductance in pepper leaves.

Stomatal conductance of *pepper* leaves was measured by using a portable photosynthesis system (LI-COR 6400) at twodays post incoualction with the *Xe* isogenic strains, *Xe* and *Xe*Δ*avrRxo1*, respectively. The measurements were conducted at two days post-inoculation, and the starting inoculum concentration was adjusted to 1×10^5 cfu ml⁻¹. Experiments were replicated three times with similar results, and data are shown as mean \pm s.e.

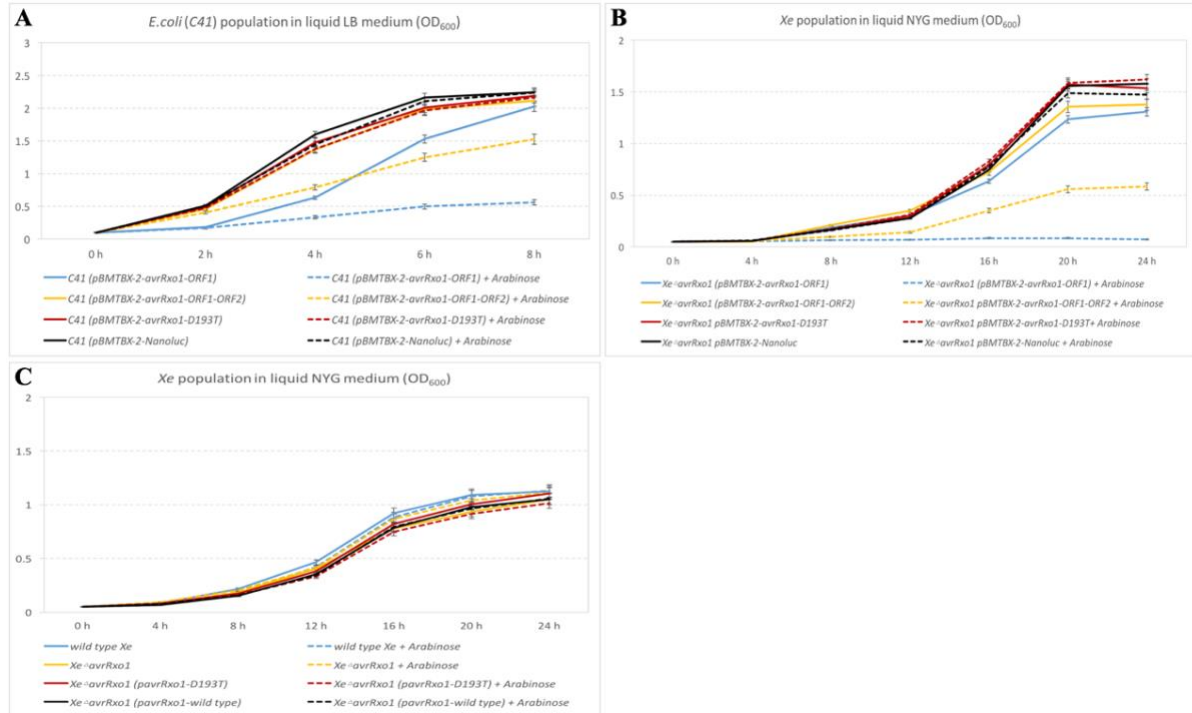


Figure 4- 4 Expression of *AvrRxo1-ORF1* (*Xe4428*) is toxic to *Xe* and *E. coli*, and its toxicity can be suppressed by *AvrRxo1-ORF2* (*Xe4429*).

Growth of four *E. coli* strains (A) and four *Xe* Δ *avrRxo1* strains (B) harboring pBMTBX-*Xe* *avrRxo1-ORF1*, pBMTBX-*Xe* *avrRxo1-ORF1-ORF2*, pBMTBX-*Xe* *avrRxo1-ORF1-D193T*, and pBMTBX-Nanoluc, respectively, with and without 0.4% arabinose (inducer) at 37°C and 28°C. Growth of four *Xe* strains (C) including wild type *Xe*, *Xe* Δ *avrRxo1*, *Xe* Δ *avrRxo1* (*pavrRxo1-D193T*), and *Xe* Δ *avrRxo1* (*pavrRxo1-wild type*) with and without 0.4 % arabinose (the expression inducer) at 28°C. Experiments were replicated three times with similar results and data are shown as mean \pm s.e.

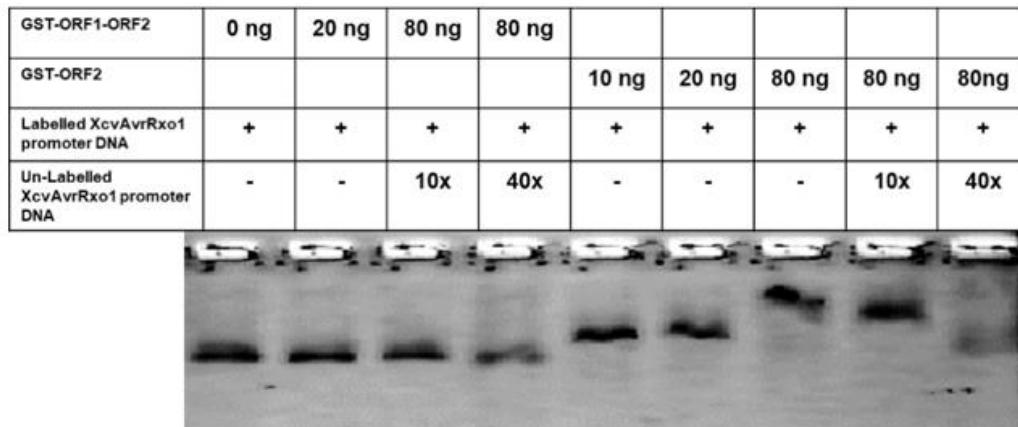
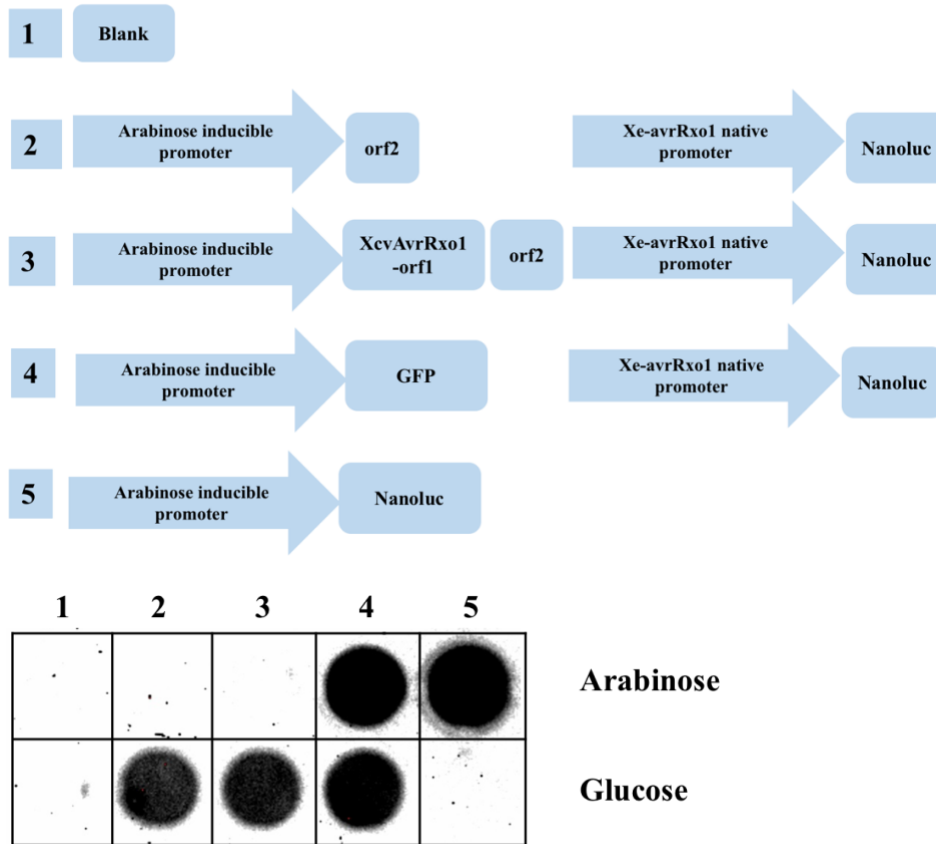


Figure 4- 5 Purified *Xe-avrRxo1*-ORF2 (Xe4429) protein binds to the promoter of *Xe-avrRxo1* (Xe4428).

Labelled *Xe-avrRxo1* promoter DNA and unlabeled *Xe-avrRxo1* promoter DNA combined with purified proteins, *Xe-avrRxo1*-ORF1-ORF2 and *Xe-avrRxo1*-ORF2, respectively, were processed via an electrophoretic mobility shift assay. Experiments were repeated three times with similar results.

Scheme of the construct for nanoluc activity assay



1. *Xe Δ avrRxo1-ORF1:ORF2*
2. *Xe Δ avrRxo1-ORF1:ORF2 (pBMTBX-Xcv4428-ORF2-Xcv4428pro-Nanoluc)*
3. *Xe Δ avrRxo1-ORF1:ORF2 (pBMTBX-Xcv4428-ORF1-ORF2-Xcv4428pro-Nanoluc)*
4. *Xe Δ avrRxo1-ORF1:ORF2 (pBMTBX-GFP-Xcv4428pro-Nanoluc)*
5. *Xe Δ avrRxo1-ORF1:ORF2 (pBMTBX-Nanoluc)*

Figure 4- 6 Nanoluc reporter assay to test the transcription activity driven by *Xe-avrRxo1* promoter *in vitro*.

(A) Scheme of the different constructs used for the nanoluc activity assay. (B) The following six *Xe* strains were grown on a nutrient broth medium containing arabinose or glucose (the control): 1) *Xe Δ avrRxo1*, 2) *Xe Δ avrRxo1 (pBMTBX-avrRxo1-ORF2-avrRxo1pro-Nanoluc)*,

3) *Xe* Δ *avrRxo1* (*pBMTBX-avrRxo1-ORF1-ORF2-avrRxo1pro-Nanoluc*), 4) *Xe* Δ *avrRxo1* (*pVSP61-avrRxo1pro-Nanoluc*), 5) *Xe* Δ *avrRxo1* (*pBMTBX-Nanoluc*), and 6) *Xe* Δ *avrRxo1* (*pBMTBX-GFP-avrRxo1pro-Nanoluc*). Experiments were repeated three times with similar results.

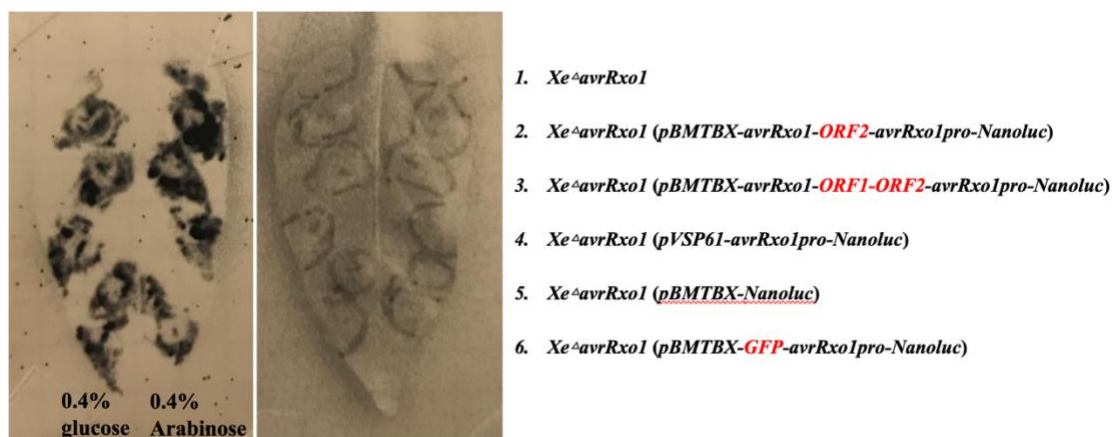


Figure 4- 7 Nanoluc reporter assay to test the transcription activity driven by *Xe-avrRxo1* promoter *in vivo*.

Six *Xe* strains (listed above) were infiltrated into pepper leaf with either 0.4% arabinose or 0.4% glucose (the negative control). Chemical fluorescence signals in the pepper leaf were detected using the CCD camera of a Gel Doc™ XR+ System (Bio-Rad). Experiments were conducted for three times within similar results.

Supplementary information

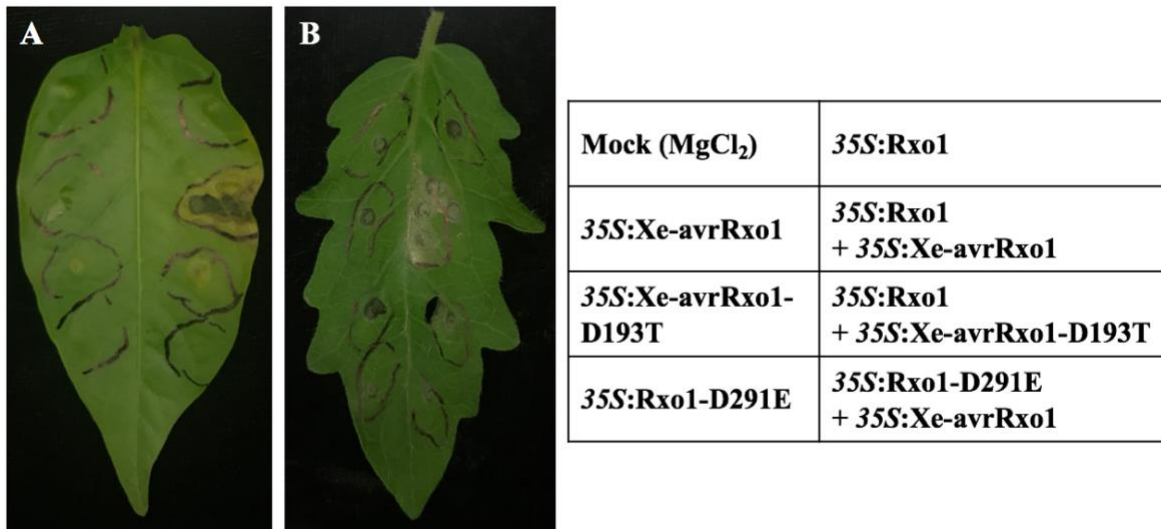


Figure S4- 1 *Xe4428* is a homologue of *Xoc-avrRxo1* that can trigger the *Rxo1*-mediated defense response in pepper and tomato.

Transient assay in leaves of pepper (*Capsicum annuum*, Ca, cultivar: Early Calwonder) and tomato (*Solanum lycopersicum*, Sl, cultivar: Money Maker) by *Agrobacteria*. The *agrobacteria* harboring the following constructs were used as inoculants: MgCl₂, 35S:Rxo1, 35S:Xe-avrRxo1, a combination of 35S:Rxo1 and 35S:avrRxo1, 35S:Xe-avrRxo1-D193T, a combination of 35S:Rxo1 and 35S:Xe-avrRxo1-D193T, 35S:Rxo1-D291E, and a combination of 35S:Rxo1-D291E and 35S:Xe-avrRxo1 with OD600 0.4 (single inoculation) or OD600 0.4 + 0.4 (co-inoculation). Picture was obtained 2 days post-inoculation. Experiments were replicated three times within similar results.

Table S4- 1 Sequences of primers utilized in this chapter

Name	Sequences
<i>Rxo1</i> For	ATGTATCCGTATGCACGtTCTGGTTCGCGAACTG
<i>Rxo1</i> Rev	CAGTTCGCGAACCAGAACGTGCATACGGATACAT
<i>Rxo1_D291E</i> For	TCTGATTATCCTGGATGaaGTGTGGATGGCCAAC
<i>Rxo1_D291E</i> Rev	GTTGGCCATCCACACTTCATCCAGGATAATCAGA
<i>Rxo1_D508V</i> For	ATGTATCCGTATGCACGtTCTGGTTCGCGAACTG
<i>Rxo1_D508V</i> Rev	CAGTTCGCGAACCAGAACGTGCATACGGATACAT
<i>Xe-avrRxo1</i> upstream Swal For	GCAGGCTCCGAATTCGCCCTTatttATGAGCACCGACGTGTTGTGCGACT
<i>Xe-avrRxo1</i> upstream Swal Rev	aagctTaatattggatccatttACGAAATTCCTCTGCACCTA
<i>Xe-avrRxo1</i> upstream PmeI For	atggctaattcccatgctGtttCAGCCAGGCTGGTGCATTTACAATG
<i>Xe-avrRxo1</i> upstream PmeI Rev	actagtcgaCttaattaagtttATGTATCCACTTTGATTGGAGA
<i>Xe-XopQ</i> upstream Swal For	GCAGGCTCCGAATTCGCCCTTatttCAGGGCGACGCAAGTGCCGTGAC
<i>Xe-XopQ</i> upstream Swal Rev	aagctTaatattggatccatttAACGGATTGCGGTGGGCTGCAT
<i>Xe-XopQ</i> upstream PmeI For	tggetaattcccatgctGtttACGAGGGGCAACGCGGGCGCTGA
<i>Xe-XopQ</i> upstream PmeI Rev	actagtcgaCttaattaagtttGTTTGCACGCTACGCCATCCTG
<i>Xe-avrRxo1-ORF1</i> For	caccGGATCCATGGCATCGCCGCCGATTCGGTG
<i>Xe-avrRxo1-ORF1</i> Rev	GAGCTCAATTAGCTCGCTGTGAGCAGCT
<i>Xe-avrRxo1-ORF2</i> For	AAACATATGAAAACTTTGAAAGGCGCAGA
<i>Xe-avrRxo1-ORF2</i> Rev	AAAGGATCCCTGCAGTTATGACCAAGAGGAAAGTGTCTCAA
<i>Xe-avrRxo1-promoter</i> For	caccTCTAGATTTGGTTCAGCTGATTCCACT
<i>Xe4428_D193T</i> For	GGTTGCATCAATCCAacaGTATTCAAGAGTTCGCT
<i>Xe4428_D193T</i> Rev	AGCGAACTCTTGAATActgtTGGATTGATGCAACC

References

1. Zhao, B., et al., *The avrRxo1 gene from the rice pathogen Xanthomonas oryzae pv. oryzicola confers a nonhost defense reaction on maize with resistance gene Rxo1*. Mol Plant Microbe Interact, 2004. 17(7): p. 771-9.
2. Zhao, B.Y., et al., *The Rxo1/ Rba1 locus of maize controls resistance reactions to pathogenic and non-host bacteria*. Theor Appl Genet, 2004. 109(1): p. 71-9.
3. Zhao, B., et al., *A maize resistance gene functions against bacterial streak disease in rice*. Proc Natl Acad Sci U S A, 2005. 102(43): p. 15383-8.
4. Han, Q., et al., *Crystal Structure of Xanthomonas AvrRxo1-ORF1, a Type III Effector with a Polynucleotide Kinase Domain, and Its Interactor AvrRxo1-ORF2*. Structure, 2015. 23(10): p. 1900-1909.
5. Shidore, T., et al., *The effector AvrRxo1 phosphorylates NAD in planta*. PLoS Pathog, 2017. 13(6): p. e1006442.
6. Horsefield, S., et al., *NAD(+) cleavage activity by animal and plant TIR domains in cell death pathways*. Science, 2019. 365(6455): p. 793-799.
7. Wan, L., et al., *TIR domains of plant immune receptors are NAD(+)-cleaving enzymes that promote cell death*. Science, 2019. 365(6455): p. 799-803.
8. Unterholzner, S.J., B. Poppenberger, and W. Rozhon, *Toxin-antitoxin systems: Biology, identification, and application*. Mob Genet Elements, 2013. 3(5): p. e26219.
9. Triplett, L.R., et al., *AvrRxo1 Is a Bifunctional Type III Secreted Effector and Toxin-Antitoxin System Component with Homologs in Diverse Environmental Contexts*. PLoS One, 2016. 11(7): p. e0158856.
10. Axtell, C.A. and G.A. Beattie, *Construction and characterization of a proU-gfp transcriptional fusion that measures water availability in a microbial habitat*. Appl Environ Microbiol, 2002. 68(9): p. 4604-12.
11. Zhang, D., et al., *The Use of a Novel NanoLuc -Based Reporter Phage for the Detection of Escherichia coli O157:H7*. Sci Rep, 2016. 6: p. 33235.
12. Traore, S.M. and B. Zhao, *A novel Gateway(R)-compatible binary vector allows direct selection of recombinant clones in Agrobacterium tumefaciens*. Plant Methods, 2011. 7(1): p. 42.
13. Krasileva, K.V., D. Dahlbeck, and B.J. Staskawicz, *Activation of an Arabidopsis resistance protein is specified by the in planta association of its leucine-rich repeat domain with the cognate oomycete effector*. Plant Cell, 2010. 22(7): p. 2444-58.
14. Bindschedler, L.V., et al., *Peroxidase-dependent apoplastic oxidative burst in Arabidopsis required for pathogen resistance*. Plant J, 2006. 47(6): p. 851-63.
15. Daudi, A., et al., *The apoplastic oxidative burst peroxidase in Arabidopsis is a major component of pattern-triggered immunity*. Plant Cell, 2012. 24(1): p. 275-87.
16. Melotto, M., et al., *Plant stomata function in innate immunity against bacterial invasion*. Cell, 2006. 126(5): p. 969-80.
17. Katagiri, F., R. Thilmony, and S.Y. He, *The Arabidopsis thaliana-pseudomonas syringae*

interaction. Arabidopsis Book, 2002. 1: p. e0039.

18. Van Eck, L., et al., *The transcriptional network of WRKY53 in cereals links oxidative responses to biotic and abiotic stress inputs*. Funct Integr Genomics, 2014. 14(2): p. 351-62.

19. Zatakia, H.M., et al., *ExpR coordinates the expression of symbiotically important, bundle-forming Flp pili with quorum sensing in Sinorhizobium meliloti*. Appl Environ Microbiol, 2014. 80(8): p. 2429-39.

20. Wang, Z., et al., *Effects of drought stress on photosynthesis and photosynthetic electron transport chain in young apple tree leaves*. Biol Open, 2018. 7(11).